Acylated 1H-1,2,4-Triazol-5-amines Targeting Human Coagulation Factor XIIa and Thrombin: Conventional and Microscale Synthesis, Anticoagulant Properties, and Mechanism of Action

Marvin Korff, Lukas Imberg, Jonas M. Will, Nico Bückreiß, Svetlana A. Kalinina, Benjamin M. Wenzel, Gregor A. Kastner, Constantin G. Daniliuc, Maximilian Barth, Ruzanna A. Ovsepyan, Kirill R. Butov, Hans-Ulrich Humpf, Matthias Lehr, Mikhail A. Panteleev, Antti Poso, Uwe Karst, Torsten Steinmetzer, Gerd Bendas, and Dmitrii V. Kalinin*

Cite This: https://dx.doi.org/10.1021/acs.jmedchem.0c01635

Read Online

ACCESS | Metrics & More | Article Recommendations | SI Supporting Information

ABSTRACT: We herein report the conventional and microscale parallel synthesis of selective inhibitors of human blood coagulation factor XIIa and thrombin exhibiting a 1,2,4-triazol-5-amine scaffold. Structural variations of this scaffold allowed identifying derivative **21i**, a potent 29 nM inhibitor of FXIIa, with improved selectivity over other tested serine proteases and also finding compound **21m** with 27 nM inhibitory activity toward thrombin. For the first time, acylated 1,2,4-triazol-5-amines were proved to have anticoagulant properties and the ability to affect thrombin- and cancer-cell-induced platelet aggregation. Performed mass spectrometric analysis and molecular modeling allowed us to discover previously unknown interactions between the synthesized inhibitors and the active site of FXIIa, which uncovered the mechanistic details of FXIIa inhibition. Synthesized compounds represent a promising starting point for the development of novel antithrombotic drugs or chemical tools for studying the role of FXIIa and thrombin in physiological and pathological processes.
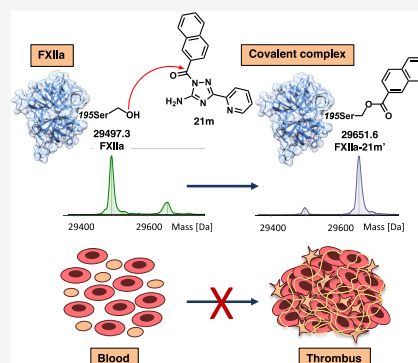
INTRODUCTION

The natural process of hemostasis is essential for the prevention of life-threatening extensive bleeding. Dysregulation of hemostasis, however, can lead to a dangerous pathology termed thrombosis, which is characterized by the undesired formation of a potentially deadly blood clot inside a vein or an artery. Deep venous and arterial thrombosis is associated with thromboembolism, which in turn triggers major cardiovascular disorders: myocardial infarction, ischemic stroke, and peripheral arterial ischemia.[1] Considering the high mortality rate and economic losses associated with thrombosis,[2,3] presently available measures in thrombosis prevention are insufficient and indicate the need for the development of novel antithrombotic drugs.

Apart from antiplatelet drugs, the current thrombosis therapy relies on anticoagulants, which, despite being life-saving medications, prevent blood coagulation in situations when the clotting is desired (e.g., trauma or surgery), thereby causing a life-threatening side effect of internal bleeding.[4,5] Besides the internal bleeding, clinically used anticoagulants exhibit a number of drawbacks. Heparins, for instance, can only be administered in the form of injection, have a short biological half-life, and might elicit heparin-induced thrombocytopenia.[6,7] Vitamin K antagonists (e.g., warfarin) display a narrow therapeutic window, interact with a number of drugs and foods, have slow onset/offset of action, and cause coumarin-induced hepatitis.[8] In contrast, direct oral anticoagulants (DOACs) such as direct thrombin inhibitors (e.g., dabigatran (**1**, Figure 1) and FXa inhibitors (e.g., rivaroxaban (**2**, Figure 1) demonstrate rapid onset/offset of action and predictable pharmacokinetics.[9,10] However, even these new drugs are reported to induce life-threatening bleeding.[11] Therefore, novel anticoagulants with a new mechanism of action are needed to control thrombosis without the risk of bleeding.

Among plasma coagulation factors, Hageman factor (FXII) is relatively less studied and considered as an emerging target for thrombosis prevention. Hageman factor is a serine protease circulating in the blood as an inactive zymogen, which upon contact with negatively charged surfaces (e.g., the collagen of damaged vessels, artificial surfaces such as glass) undergoes the activation (FXIIa formation). Formed FXIIa activates both FXI, triggering the intrinsic blood coagulation cascade, and plasma kallikrein, activating the kallikrein−kinin system.[12,13]

Infestin-4 (3)

FXIIa K_i = 0.1 nM
FXa K_i = 53 nM
Trypsin K_i = 11.3 nM

Dabigatran (1)

FIIa K_i = 4.5 nM
FXa K_i = 3.8 μM
FXIIa IC$_{50}$ > 33 μM
Trypsin K_i = 50 nM

Rivaroxaban (2)

FXa IC$_{50}$ = 0.4 nM
FIIa IC$_{50}$ > 20 μM
FXIIa IC$_{50}$ > 33 μM
Trypsin IC$_{50}$ > 20 μM

Arg-Cys-Phe$^{4\text{-FH}}$-Arg-Leu-Pro-Cys-Arg-Gln-Leu-Arg-Cys-norArg

FXII801 (4)

FXIIa K_i = 1.6 nM
FIIa K_i > 40 μM
FXa K_i > 40 μM
Trypsin K_i = 1.3 μM

(5)

FXIIa IC$_{50}$ = 5 μM
FIIa IC$_{50}$ > 100 μM
FXa IC$_{50}$ > 100 μM

(6)

FXIIa IC$_{50}$ = 190 nM
(covalent inhibition)
Trypsin = 52 nM

(7)

FXIIa IC$_{50}$ = 210 nM

Macromolecules   **Small molecules**

Figure 1. Exemplary macromolecular and small-molecule inhibitors of plasma coagulation factors with their inhibitory profile.

Figure 2. Molecular surface of human coagulation factor XIIa (A) and thrombin (B) near the active site (PDB: 6B74[28] and PDB: 1A4W[29]). The residues are depicted as gray stick models. Substrate-binding sites are labeled (S1−S4 and S1′). The catalytic residues (His57, Asp102, Ser195) are indicated in red. The arrows point to amino acids that form the "oxyanion hole" (Gly193 and Ser195). The surface is colored as follows: lipophilic regions are in orange, hydrophilic in blue, and neutral in white.

Recent studies showed a fundamental role of Hageman factor in arterial and venous thrombosis. FXII-knockout mice are protected from arterial and deep vein thrombosis as well as ischemic stroke.[14,15] Despite its essential role in thrombosis, the deficiency of FXII does not affect hemostasis in animals, and FXII-deficient patients demonstrate a normal hemostatic ability.[12,16] Therefore, FXIIa represents a new, potentially safe, and promising target for thrombosis prevention. Therapeutic application of FXIIa inhibitors should be especially effective in the prevention of contact-mediated thrombosis triggered by medical devices.[17] Devices such as vascular catheters, artificial heart valves, and dialysis membranes are reported to induce blood coagulation *via* FXII activation.[18] A selective inhibition

or depletion of FXII was in turn proved to prevent device-induced thrombosis in animal models,[19−21] whereas antico-agulants targeting, *e.g.*, FXa and thrombin showed limited ability to prevent medical-device-induced thrombosis.[22,23] Besides, as FXII serves as a connection point between coagulation and inflammation cascades, inhibitors of FXIIa, apart from being potential antithrombotics, could find their application in the treatment of disorders such as hereditary angioedema,[24] sepsis,[25] multiple sclerosis,[26] and Alzheimer's disease.[27] A recently published crystal structure of FXIIa gives an insight into the enzyme's active site.[28] It contains the catalytic triad formed by Asp102, His57, and Ser195 (Figure 2A), a typical "oxyanion hole" also found in related serine

Scheme 1. Synthesis of 3-Pyridyl-Substituted 1,2,4-Triazol-5-amines 7 and 10−13[a]

[a]Reagents and conditions: (a) aminoguanidine hydrochloride, neat, 190 °C, 5 h, **9a** 58%, **9b** 74%, **9c** 66%; (b) tetrahydrofuran (THF)/pyridine 1:1, 0 °C to r.t., 2−5 h, **10a** 42%, **7** 77%, **10c** 87%, **11c** 57%, **12a** 15%, **13c** 70%.

proteases, and distinctive substrate-binding sites (S1−S4 and S1′−S2′, Figure 2A), the structural features that could be exploited for the rational FXIIa inhibitor design.

On the other hand, despite the risk of bleeding side effects, the therapeutic application of inhibitors of the extrinsic blood coagulation pathway in some pathologies like cancer-associated thrombosis is practically unavoidable. Cancer-associated thrombosis, which develops *via* activation of primary and secondary hemostasis, affecting both intrinsic and extrinsic coagulation pathways, is the second leading cause of mortality of cancer patients.[30,31] Tissue factor (TF), which is expressed on the outer membranes of tumor cells, is suggested to be the main contributor to thrombin generation and fibrin formation in cancer patients.[32] It leaves little to no alternatives to the inhibitors of the extrinsic or common pathway (*e.g.*, thrombin inhibitors) in the prevention of cancer-associated thrombosis. Recent studies, however, suggest a significant role of contact system activation in the development of cancer-associated thrombosis (recently reviewed[33]). It has been found that tumor cells trigger contact-system activating FXII by releasing negatively charged molecules such as phosphatidylserine, glycosaminoglycans, polyphosphate, collagen, and nucleic acids.[33−36] For instance, breast and pancreatic cancer cells were shown to induce TF-independent thrombin generation *via* activation of FXII.[37] Moreover, it has been proven that prostate-cancer-associated thrombosis is driven to a significant extent by polyphosphate-activated FXII and that the inhibition of this activation is sufficient to protect mice from lethal pulmonary embolism without risk of causing bleeding.[38] The interplay between different factors of coagulation pathways in the cancer microenvironment is complex and not fully understood. Therefore, compounds that could selectively inhibit one of the pathways, as well as compounds capable of dual inhibition, are of interest as chemical tools to study this interplay. From this perspective, both selective and dual FXIIa and thrombin inhibitors might be of interest.

Historically, FXIIa was not recognized as a valuable drug target and, therefore, only few examples of FXIIa inhibitors are known. Among them, apart from the recently disclosed FXIIa-blocking antibody 3F7,[39] two macromolecular inhibitors, insect protein infestin-4[40] (**3**, FXIIa K_i = 0.1 nM, Figure 1) and peptide-like macrocycle FXII801[41] (**4**, FXIIa K_i = 1.6 nM, Figure 1), are known. Among few small molecules, coumarin **5**,[42] boronic acid **6**,[28] and also substituted aminotriazole **7**[43] are reported as FXIIa inhibitors (Figure 1). For our study, coumarin **5** and boronic acid **6** were disregarded as lead structures, since **5** is a relatively weak FXIIa inhibitor (IC$_{50}$ = 5 μM)[23] and **6** is a covalent inhibitor with a problematic selectivity profile (*e.g.*, **6** inhibits trypsin with IC$_{50}$ = 52 nM).[28,42] In contrast, acylated 1,2,4-triazol-5-amine **7** (Figure 1) with a FXIIa IC$_{50}$ value of 210 nM[43] represents a promising lead structure for the development of novel FXIIa inhibitors.

The therapeutic potential of substituted 1,2,4-triazol-5-amines remains largely underexplored, despite their synthetic accessibility. For the aforementioned acylated aminotriazole **7**, apart from the FXIIa inhibitory activity, no information is disclosed on its selectivity over related serine proteases, anticoagulant activity, toxicity profile, and interactions with the FXIIa active site.

Herein, we report the synthesis of 1,2,4-triazol-5-amine-based selective inhibitors of blood coagulation factor XIIa and thrombin. Performed biochemical experiments revealed anticoagulant properties of the synthesized inhibitors and their ability to affect thrombin and cancer-cell-induced platelet aggregation, whereas mass-spectrometry-based analyses uncovered mechanistic details of FXIIa inhibition. Experimentally obtained data were reinforced by computational simulations, which allowed to rationalize the interactions between synthesized inhibitors and the active sites of the coagulation factor XIIa and thrombin.
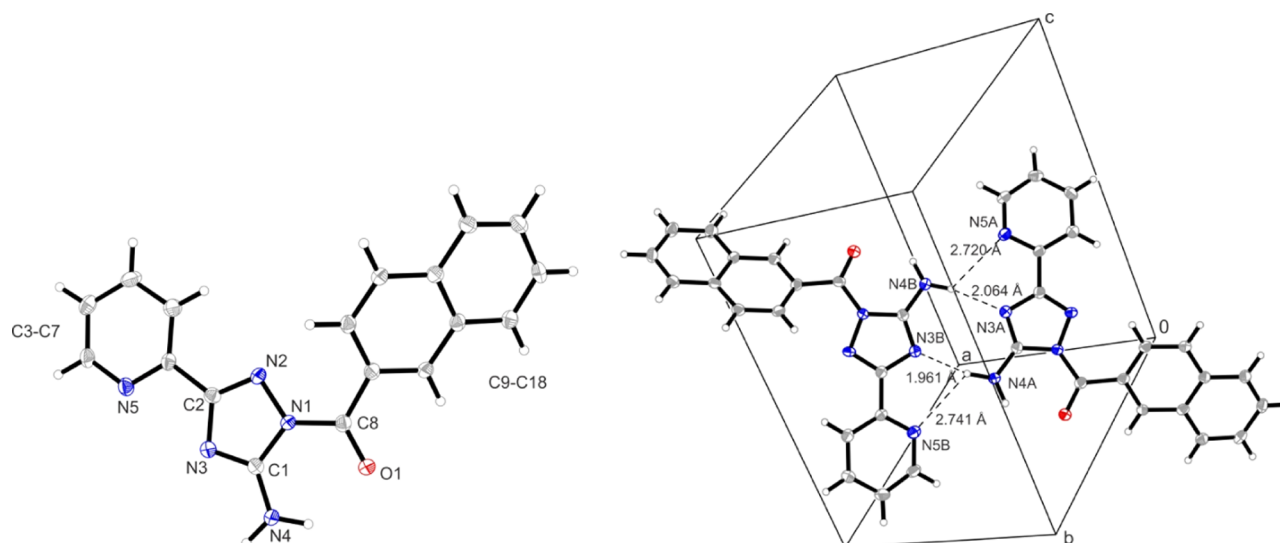
Figure 3. X-ray crystal structure of **21m** displaying the thermal ellipsoids at the 50% probability level (left). Formation of an asymmetrical dimeric unit (result of crystal packing) between the two crystallographically independent molecules (molecule "A" and "B") of compound **21m** involving strong and week N−H...N interactions (right).

Scheme 2. Synthesis of Benzoylated 3-Phenyl-1,2,4-triazol-5-amine 16[a]
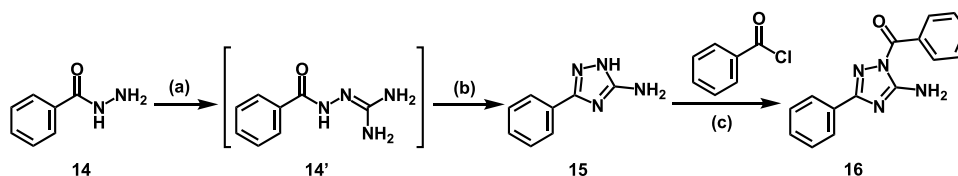
[a]Reagents and conditions: (a) S-methylisothiouronium sulfate, EtOH/H₂O 1:1, reflux, 16 h; (b) KOH (40%), reflux, 2 h, **15** 57%; (c) THF/pyridine 1:1, 0 °C to r.t., 3 h, **16** 92%.

RESULTS AND DISCUSSION

Conventional Synthesis of 1,2,4-Triazol-5-amines. The initial library of potential FXIIa inhibitors possessing the 1,2,4-triazol-5-amine scaffold was generated and screened for their biological activity to get the first insight into the structure−activity relationship (SAR) and to identify the most promising candidate for the further optimization. For this purpose, syntheses shown in Schemes 1−3 were performed.

At first, pyridinecarboxylic acids **8a−c** were fused with aminoguanidine hydrochloride at 190 °C, affording amidoguanidines, which without the isolation were cyclized into 3-pyridyl-substituted 1,2,4-triazol-5-amines **9a−c** (Scheme 1).[44] Aminotriazoles **9** exhibit annular tautomerism and exist in three main tautomeric forms **9**, **9′**, and **9″**, of which the tautomeric form **9** is prevalent (Scheme 1).[45,46] Tautomerism could complicate the subsequent acylation reactions due to the formation of several acylated products.[47] However, taking advantage of the observed low reactivity of the primary amino group of 1,2,4-triazol-5-amines **9a−c** and the equilibrium shift toward the tautomeric form **9**, in subsequent acylation and sulfonylation reactions employing temperature and addition rate control, exclusively N-1-substituted products **7** and **10−13** were successfully obtained. The regioselectivity of the mentioned reactions was unambiguously confirmed by X-ray crystallography (Figure 3).

As the cyclocondensation reaction between benzoic acid and aminoguanidine hydrochloride failed to produce corresponding 3-phenyl-1H-1,2,4-triazol-5-amine **15**, an alternative route for its synthesis was utilized (Scheme 2). According to the

reported procedure, hydrazide **14** was treated with S-methylisothiouronium sulfate accessing phenylamidoguanidine **14′**, cyclization of which resulted in aminotriazole **15**.[48] Finally, regioselective acylation of **15** allowed for the isolation of benzoylated 1,2,4-triazol-5-amine **16** possessing nonheteroaromatic phenyl moiety in position 3 of the triazole core.

Finally, acylated 1,2,4-triazole-3,5-diamines **20a−c** were synthesized (Scheme 3). For this, anilines **17a−c** were reacted

Scheme 3. Synthesis of Acylated 3-Arylamino-1,2,4-triazol-5-amines 14a−c[a]
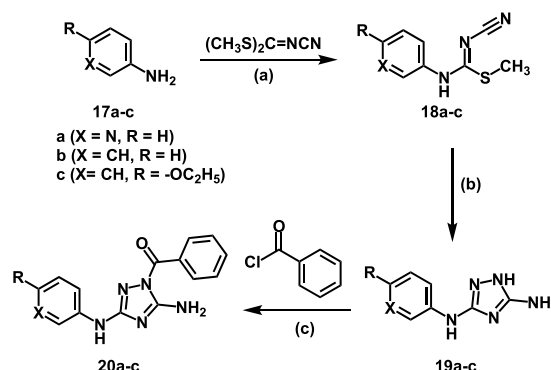
[a]Reagents and conditions: (a) i-PrOH, reflux, overnight, **18a** 47%, **18b** 46%, **18c** 91%; (b) NH₂NH₂·H₂O, EtOH, reflux, 2−16 h, **19a** 74%, **19b** 53%, **19c** 86%; (c) THF/pyridine 1:1, 0 °C to r.t., 2−18 h, **20a** 17%, **20b** 51%, **20c** 53%.

Table 1. Initial Screening of 1,2,4-Triazol-5-amines against Selected Serine Proteases

	R	R[1]	FXIIa	Thrombin	FXa	Trypsin
			1 hour IC$_{50}$ ± SD (nM)[a] Serine Protease			
15	phenyl	-H	>5000	>5000	>5000	>5000
9a	pyridin-2-yl	-H	>5000	>5000	>5000	>5000
9c	pyridin-4-yl	-H	>5000	>5000	>5000	>5000
16	phenyl	benzoyl	539 ± 45	1235 ± 24	>5000	>5000
10a	pyridin-2-yl	benzoyl	132 ± 10	235 ± 7	>5000	>5000
7	pyridin-3-yl	benzoyl	298 ± 28	865 ± 58	>5000	>5000
10c	pyridin-4-yl	benzoyl	106 ± 22	962 ± 21	>5000	>5000
13c	pyridin-4-yl	tosyl	>1000	>5000	>5000	>5000
12a	pyridin-2-yl	phenyl carbamate	617 ± 60	13020 ± 365	>5000	>5000
11c	pyridin-4-yl	cyclohexanoyl	>1000	>5000	>5000	>5000
20a	pyridin-3-yl-amino	benzoyl	>5000	>8000	>5000	>5000
20b	phenylamino	benzoyl	>1000	>5000	>5000	>5000
20c	4-ethoxyphenylamino	benzoyl	>1000	>5000	>5000	>5000
	Dabigatran (1)		>33000	6.4 ± 0.4	34% @ 1 μM	59% @ 5 μM
	Rivaroxaban (2)		>33000	55% @ 33 μM	0.7 ± 0.1	>5000
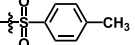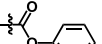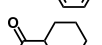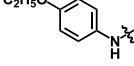
[a]Measurements were performed in triplicate; 1 h incubation time is specified as IC$_{50}$ values were time-dependent; substrate concentration $[S]_0 = 25$ μM; measured FXIIa $K_m = 167 ± 4$ μM for the Boc-Gln-Gly-Arg-AMC substrate; measured thrombin $K_m = 18 ± 1$ μM for the Boc-Val-Pro-Arg-AMC substrate. The K_i values could not be directly withdrawn from the Cheng–Prusoff equation in this case due to the enzyme–inhibitor covalent interaction (see the section "Mechanism of Inhibition").

with dimethyl N-cyanodithioimidocarbonate to form imidates **18a−c**, subsequent treatment of which with hydrazine hydrate afforded cyclization products **19a−c**.[47] The final acylation reaction with benzoyl chloride yielded compounds **20a−c**.

Inhibition of Serine Proteases. All synthesized 1,2,4-triazol-5-amines of the first round of conventional synthesis (Schemes 1−3) were assayed in vitro against relevant serine proteases of the blood coagulation cascade, FXIIa, thrombin, and FXa, as well as against trypsin using fluorogenic substrates according to previously reported procedures with minor variations.[41,43] Potent thrombin and FXa inhibitors dabigatran (**1**) and rivaroxaban (**2**), respectively, were used as positive controls. The IC$_{50}$ values were obtained in competition experiments, in which the enzyme was added to the mixture of the substrate and the inhibitor, followed by fluorescence measurements in the kinetic mode during 1 h (end-point readout was used). The results of in vitro enzymatic assays are summarized in Table 1.

As shown in Table 1, some of the synthesized 1,2,4-triazol-5-amines inhibit FXIIa in the nanomolar range with IC$_{50}$ values varying between 106 and 617 nM, simultaneously affecting the other key blood coagulation factor thrombin with IC$_{50}$ values

ranging between 235 nM and 13 μM. The substitution pattern of the 1,2,4-triazol-5-amine core significantly influenced the inhibitory profile of the synthesized compounds. Thus, 1,2,4-triazol-5-amines **15**, **9a**, **9c**, exhibiting a nonacylated annular secondary amino group, were completely inactive against the tested serine proteases. Acylation of the secondary amino group of the aminotriazoles with benzoyl chloride resulted in corresponding amides **16**, **10a**, and **10c**, which, in contrast, showed pronounced FXIIa and thrombin inhibitory properties (e.g., **10a**: IC$_{50}$ = 132 and 235 nM, respectively), signifying thereby the necessity of an acyl fragment for successful inhibition of FXIIa and thrombin. Not only the presence of an acyl moiety but also its structure appeared as an important factor determining the inhibitory properties of the synthesized aminotriazoles. Thus, in terms of FXIIa inhibition, benzoylated compounds, e.g., **10a** with FXIIa IC$_{50}$ = 132 nM, exhibited lower IC$_{50}$ values than their carbamate-based analogue **12a** (FXIIa IC$_{50}$ = 617 nM), which in turn was more active than compounds **11c** and **13c** possessing a cycloaliphatic acyl moiety and a sulfonamide residue on the secondary amino group, respectively (FXIIa IC$_{50}$ > 1 μM, for both). The same trend is apparent for the thrombin inhibition by the

aforementioned compounds. The structure of the acyl moiety also determined the inhibitor selectivity. For instance, being an FXIIa inhibitor of moderate potency, carbamate **12a** exhibited a 21-fold selectivity toward FXIIa over thrombin (Table 1). When considering the other structural alteration of the 1,2,4-triazol-5-amine scaffold, the introduction of an additional nitrogen atom bridge (1,2,4-triazole-3,5-diamines **20a–c**) resulted in no serine protease inhibitory properties (Table 1). Notably, none of the screened 1,2,4-triazol-5-amines, shown in Table 1, affected FXa or trypsin enzymatic activity, displaying thereby a clear preference toward FXIIa and thrombin inhibition.

Anticoagulant Activity of Series 1. Nine representative compounds of the synthesized 1,2,4-triazol-5-amines were examined for their anticoagulant properties in activated partial thromboplastin time (aPTT) and prothrombin time (PT) tests (Figure 4). These two tests allow us to distinguish whether the
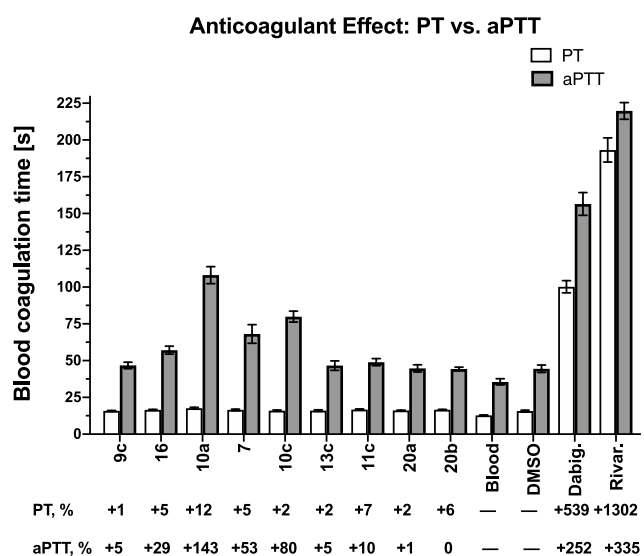
Figure 4. In vitro anticoagulant activity of selected 1,2,4-triazol-5-amines tested at 300 μM compared to that of dabigatran (**1**) and rivaroxaban (**2**) tested at 3 μM. The activated partial thromboplastin time (aPTT) and prothrombin time (PT) are shown in seconds. The percentage of aPTT and PT increase compared to the effect of dimethyl sulfoxide (DMSO) is shown under the diagram. Tests were performed at least in triplicate, and the average with standard deviation (SD) is given.

intrinsic (aPTT) or extrinsic (PT) pathway of blood coagulation is affected by the inhibitor. The experiments

were performed with the whole blood instead of plasma to modulate conditions resembling an in vivo situation when the whole matrix of blood is taken into consideration.

As can be seen in Figure 4, 1,2,4-triazol-5-amines influenced the whole blood coagulation in aPTT and PT tests to different extents. Specifically, synthesized compounds had almost no influence on the extrinsic coagulation cascade only slightly extending PT by 1–12% at 300 μM concentration. In contrast, at the same concentration, some of the compounds showed a stronger effect on the intrinsic coagulation pathway extending aPTT by up to 143% (aPTT for compound **10a** = 108 s vs aPTT (DMSO) = 44 s). Compounds' preference to inhibit the intrinsic but not the extrinsic coagulation cascade is noteworthy and promising since extrinsic cascade triggered by TF release is physiologically relevant, being a natural defense against bleeding, whereas intrinsic cascade initiated by FXIIa is implicated in thrombosis. In terms of SAR, aminotriazoles **10a**, **7**, and **10c**, possessing 2-, 3-, and 4-pyridyl moieties in position 3 of their 1,2,4-triazole scaffold showed the highest ability to prolong aPTT by 143, 53, and 80%, respectively. Pyridyl moiety replacement with a phenyl or aminoaryl residue resulted in anticoagulant activity reduction for compound **16** (aPTT +29%) or its complete loss for compounds **20a** and **20b**. This emphasizes the correlation between the superior ability of pyridyl-substituted derivatives to inhibit FXIIa and thrombin (**7**, **10a**, **10c**, Table 1) and, as a consequence, their anticoagulant properties (Figure 4). Compounds exhibiting no acyl moiety (**9c**), bearing a cycloaliphatic (**11c**) or sulfonamide residue (**13c**) on the annular nitrogen atom, showed practically no influence on the blood coagulation (Figure 4). This fact is also in agreement with no FXIIa or thrombin inhibitory properties of compounds **9c**, **11c**, and **13c** (Table 1).

Microscale Parallel Synthesis and Screening. From the screening of the initial series of synthesized compounds, acylated aminotriazole **10a** possessing the pyridin-2-yl moiety showed both FXIIa inhibitory properties and the highest ability to extend aPTT with only a little effect on PT. However, its FXIIa inhibitory potency, selectivity profile, and anticoagulant activity could be further improved. For this, considering the influence of the acyl moiety structure on the biological activity manifestation, one of the approaches would be to vary the acyl moiety of **10a** without changing its 1,2,4-triazol-5-amine core (**9a**). For this purpose, conventional acylation or amide coupling reactions could be performed, which, however, might be time-consuming and require multiple purification efforts of the final products with the use of column chromatography. Moreover, these reactions on typical laboratory scale require considerable amounts of starting materials and solvents to
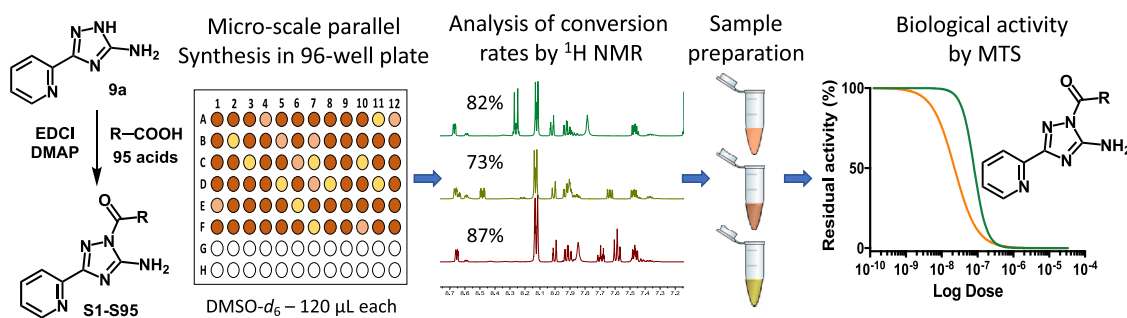
Figure 5. Schematic representation of the microscale parallel synthetic approach combined with medium-throughput screening (MTS) toward FXIIa and thrombin inhibitors.
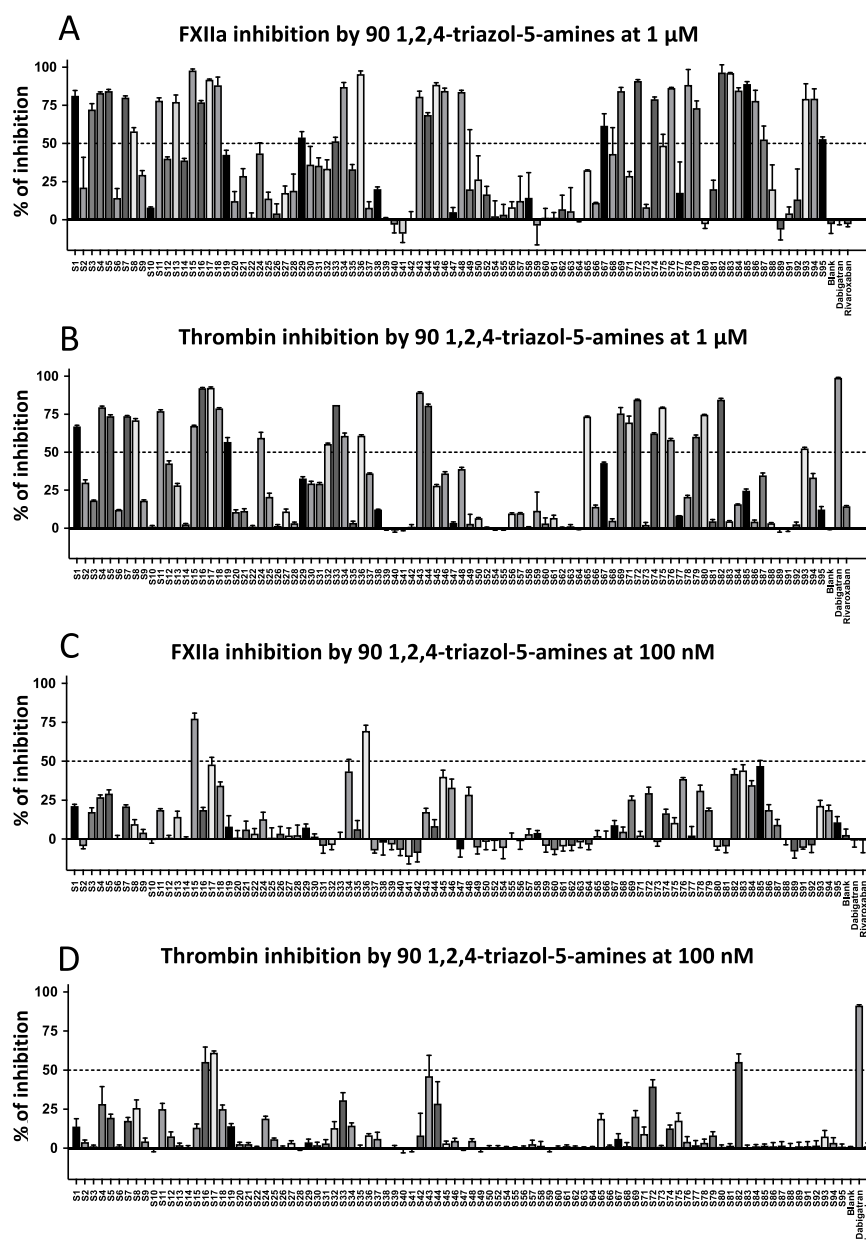
Figure 6. FXIIa and thrombin inhibition by 90 aminotriazoles obtained in microscale parallel synthesis at 1 μM (A and B) and at 100 nM (C and D). Tests were performed in triplicate, and the average with SD is given.

generate libraries of test compounds, which is associated with high expenses. Therefore, in this work, we utilized advantages of our in-house-developed microscale parallel synthetic methodology combined with medium-throughput screening (MTS) collectively, allowing us to access and test the biological activity of large series of compounds with minimum expenses.

The microscale parallel synthetic approach was realized as shown in Figure 5. At first, under the optimized conditions, in a 96-well plate, the microscale amide coupling reactions between 3-(pyridin-2-yl)-1H-1,2,4-triazol-5-amine **9a** and 95 structurally diverse carboxylic acids were performed in DMSO-d_6 (120 μL in each well) (Figure 5). The carboxylic acid component was represented by linear aliphatic, unsaturated, cycloaliphatic, aromatic, heteroaromatic, and amino acid-based carboxylic acids (Supporting Information). After the completion of the reactions, formed acylated aminotriazoles S1−

S95 were rapidly analyzed by ^{1}H NMR spectroscopy, allowing the determination of the conversion rate of each of the reactions (Figure 5 and Supporting Information) and the preparation of the samples of exact inhibitor concentration for the MTS. The generated library of 90 compounds was screened at 1 μM and 100 nM for the ability to inhibit FXIIa and thrombin (Figure 6).

Screening of aminotriazoles, generated in the microscale reactions, revealed 37 and 29 compounds as new FXIIa and thrombin inhibitors, respectively, the inhibitory activity of which exceeded 50% at 1 μM concentration (Figure 6A,B). This indicates about 30% hit-rate (active inhibitors) finding by the approach used. In general, when the annular nitrogen atom (1-N) of aminotriazole **9a** was acylated with linear aliphatic, unsaturated, cycloaliphatic carboxylic acids or amino acid-based derivatives, resulted compounds showed lower ability to inhibit both FXIIa and thrombin compared to aminotriazoles

Scheme 4. Synthesis of 3-Pyridyl-Substituted 1,2,4-Triazol-5-amines 21a–v[a]

21k: R = -Ph-3-CH$_3$
21l: R = -Pyrid-3-yl
21m: R = -2-Naphthyl
21n: R = -2-Furanyl
21o: R = -4-Tetrahydropyranyl
21p: R = -Ph-4-NH(CO)CF$_3$
21q: R = -Ph-4-NH(CO)Ph
21r: R = -Bn
21s: R = -Bn-2-I
21t: R = -Benzamidomethyl
21u: R = -Styryl
21v: R = -1,2,3,4-tetrahydro-1(S)-naphthyl

21a: R = -Ph-3,4-(CH$_3$)$_2$
21b: R = -Ph-4-OCH$_3$
21c: R = -Ph-4-C$_2$H$_5$
21d: R = -Ph-4-CF$_3$
21e: R = -Ph-2-NO$_2$
21f: R = -Ph-4-NO$_2$
21g: R = -Ph-4-F
21h: R = -Ph-4-Br
21i: R = -1-Naphthyl
21j: R = -Cyclohexyl
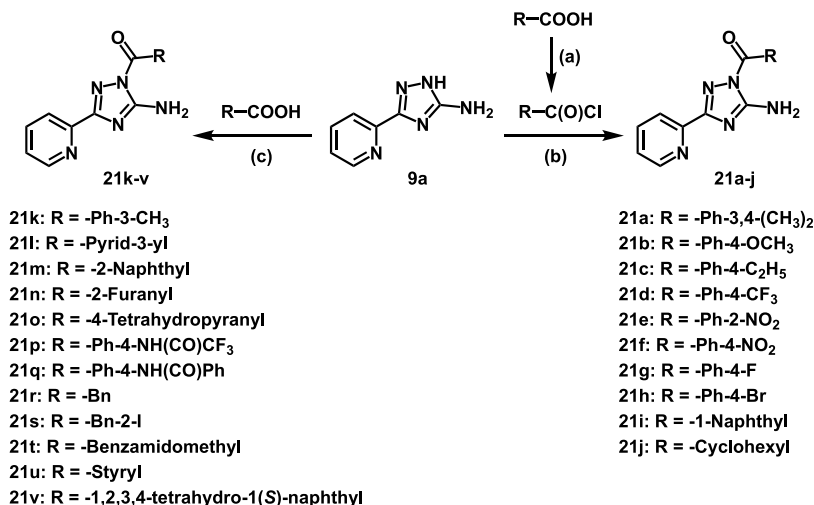
[a]Reagents and conditions: (a) oxalyl chloride, *N,N*-dimethylformamide (DMF, cat.), pyridine (dry), 0 °C to r.t., 1.5 h; (b) THF/pyridine 1:1, 0 °C to r.t., 2–18 h, **21a** 60%, **21b** 72%, **21c** 74%, **21d** 25%, **21e** 43%, **21f** 46%, **21g** 69%, **21h** 64%, **21i** 77%, **21j** 83%; (c) EDCI, DMAP, DMF (dry), 0 °C to r.t., 3–16 h, **21k** 65%, **21l** 26%, **21m** 55%, **21n** 78%, **21o** 77%, **21p** 70%, **21q** 89%, **21r** 5%, **21s** 61%, **21t** 66%, **21u** 75%, **21v** 75%.

bearing aromatic acyl fragments (Supporting Information). Heteroaromatic acyl moieties also showed a reduced tendency to inhibit the activity of tested serine proteases compared to their nonheteroaromatic analogues. In many cases, the inhibitory activity of synthesized compounds toward FXIIa and thrombin overlapped (Figure 6A,B). For some compounds, however, the tendency for selectivity can already be seen at 1 μM but is more apparent in the experiments with 100 nM inhibitor concentration (Figure 6C,D). Thus, aminotriazole with screening number S15 possessing the α-naphthoyl moiety showed noticeable 77% of FXIIa inhibition at 100 nM while inhibiting thrombin by 13% only. In contrast, its β-naphthoylated analogue S16 showed the inverted tendency, inhibiting FXIIa and thrombin at 100 nM by 19 and 55%, respectively (Figure 6C,D). Also, structurally related *S*-configured 1,2,3,4-tetrahydronaphthalene derivative S36 showed selectivity toward inhibition of FXIIa (70%) over thrombin (6%) along with 2-iodophenylacetic acid derivative S85 inhibiting FXIIa by 47% and thrombin by 2% only (Figure 6C,D). The full table of FXIIa and thrombin inhibition rates by 90 aminotriazoles is given in the Supporting Information.

Second Round of Conventional Synthesis. Based on the screening of compounds from the microscale parallel synthesis, 21 acylated derivatives of **9a** were selected for the conventional synthesis and their further biological activity evaluation. To verify the applicability of the utilized microscale parallel synthetic approach combined with MTS as a selector of active compounds, apart from the most promising and potentially active aminotriazoles, several derivatives showing low, moderate, and no inhibitory activity toward FXIIa and FIIa were also included into the set of compounds for the conventional synthesis.

Acylated 1,2,4-triazol-5-amines **21a–v** were accessed either via a direct regioselective acylation of the annular nitrogen atom (N-1) of **9a** with appropriate acid chlorides or via the amide coupling reactions between **9a** and the corresponding carboxylic acids (Scheme 4).

Inhibition of Serine Proteases by the Second Series of Compounds. All prepared 1,2,4-triazol-5-amines **21a–v** of the second round of conventional synthesis (Scheme 4) were

assayed in vitro for their ability to inhibit FXIIa, thrombin, FXa, and trypsin. The results of this evaluation are summarized in Table 2.

Despite exhibiting a common aminotriazole scaffold, each compound of series **21** displayed its unique inhibitory profile toward investigated serine proteases, which was determined by the acyl moiety structure (Table 2). When comparing the biological activity of compounds **21a–v** to that of aminotriazole **10a**, bearing an unsubstituted phenyl ring, its mono- (**21k**) and dimethylated (**21a**) analogues showed enhanced FXIIa and thrombin inhibitory properties, exhibiting IC$_{50}$ values against both enzymes below 100 nM (*e.g.*, for **21a** FXIIa IC$_{50}$ = 91 nM, thrombin IC$_{50}$ = 57 nM). However, the introduction of a somewhat bigger *para*-ethyl or *para*-methoxy substituent resulted in compounds **21c** and **21b**, respectively, with a slightly reduced inhibitory potency against both enzymes (Table 2). Also, a halogen atom introduction in the *para*-position of the phenyl ring (**21h–g**) led to a further decrease of compounds inhibitory properties toward FXIIa and thrombin. For example, fluorinated compound **21g** showed IC$_{50}$ values of 306 and 481 nM against FXIIa and thrombin, respectively. This effect, however, was not as pronounced as for the compounds **21d** and **21f** possessing *para*-trifluoromethyl- and *para*-nitro-substituted aromatic acyl moieties, respectively, which experienced a dramatic activity drop to a micromolar level (IC$_{50}$ = 3–5 μM and more toward FXIIa and thrombin).

Interestingly, it has been found that FXIIa tolerated the introduction of large substituents in the *para*-position of the aromatic ring better than thrombin. Thus, aminotriazoles **21p** and **21q**, possessing bulky 2,2,2-trifluoroacetamido- and benzamidobenzoic acid residues, showed FXIIa inhibition at the level of IC$_{50}$ = 142 and 109 nM, respectively, which is comparable to the inhibitory properties of compound **10a** bearing an unsubstituted aromatic acyl moiety (Table 2). However, in contrast to inhibitor **10a** with low selectivity profile, compounds **21p** and **21q** showed 24-fold and at least 18-fold selectivity, respectively, toward FXIIa over thrombin, which underwent only weak inhibition by **21p** (thrombin IC$_{50}$ = 3.4 μM) and **21q** (thrombin IC$_{50}$ > 2 μM). These two

Table 2. Inhibition Properties of 1,2,4-Triazol-5-amines 10a and 21a−v Toward Selected Blood Coagulation Factors and Trypsin
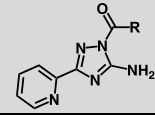
Cmpd. (MTS code)	R	Inhibition @1 µM (in MTS)[a]		1 hour IC$_{50}$ ± SD (nM)[a] Serine Protease			
	R	FXIIa	FIIa	FXIIa	FIIa	FXa	Trypsin
10a (S1)	phenyl	81%	67%	132 ± 10	235 ± 7	>5000	>5000
21k (S4)	2-CH₃-phenyl	83%	80%	93 ± 16	86 ± 4	>5000	>5000
21a (S17)	2,4-(CH₃)₂-phenyl	92%	93%	91 ± 9	57 ± 6	>5000	>5000
21b (S7)	4-OCH₃-phenyl	80%	71%	291 ± 9	329 ± 8	>5000	>5000
21c (S5)	4-C₂H₅-phenyl	85%	74%	162 ± 23	308 ± 12	>5000	>5000
21d (S6)	4-CF₃-phenyl	14%	12%	3207 ± 250	4572 ± 2692	>5000	>5000
21e (S68)	2-NO₂-phenyl	43%	5%	1560 ± 84	>5000	>5000	—
21f (S9)	4-NO₂-phenyl	29%	30%	5934 ± 1555	>5000	>5000	—
21h (S8)	4-Br-phenyl	58%	71%	793 ± 139	239 ± 33	>5000	>5000
21g (S74)	4-F-phenyl	79%	60%	306 ± 34	481 ± 18	>5000	>5000
21l (S19)	pyridyl	43%	57%	1606 ± 371	494 ± 42	>5000	>5000
21i (S15)	naphthyl	98%	67%	29 ± 5	375 ± 12	>5000	>5000
21m (S16)	naphthyl	77%	92%	138 ± 12	27 ± 2	48% @ 5 µM	>5000
21v (S36)	tetrahydronaphthyl (S)	96%	61%	134 ± 7	421 ± 2	>5000	>5000
21p (S78)	4-(NHC(O)CF₃)-phenyl	89%	21%	142 ± 24	3392 ± 136	>5000	>5000
21q (S45)	4-(NHC(O)Ph)-phenyl	89%	28%	109 ± 15	38% @ 2 µM	>5000	>5000
21n (S29)	furyl	54%	33%	968 ± 156	1768 ± 126	>5000	>5000
21r (S34)	benzyl	87%	61%	210 ± 22	509 ± 55	>5000	>5000
21s (S85)	2-I-benzyl	89%	25%	62 ± 22	1819 ± 155	>5000	—
21t (S38)	CH₂NHC(O)Ph	20%	12%	13200 ± 2499	>132000	>5000	>5000
21u (S2)	cinnamyl	21%	30%	9822 ± 2630	1562 ± 98	>5000	>5000
21j (S66)	cyclohexyl	11%	14%	>1000	>5000	>5000	>5000
21o (S64)	tetrahydropyranyl	1%	1%	12130 ± 5194	>5000	>5000	>5000
Blank[b]		- 3%	0%	—	—	—	—
Dabigatran (1)		- 1%	99%	>33000	6.4 ± 0.4	34% @ 1 µM	59% @ 5 µM
Rivaroxaban (2)		- 3%	15%	>33000	55% @ 33 µM	0.7 ± 0.1	>5000

[a]Measurements were performed in triplicate; 1 h incubation time is specified as IC$_{50}$ values were time-dependent; the substrate concentration $[S]_0$ = 25 µM; measured FXIIa K_m = 167 ± 4 µM for the Boc-Gln-Gly-Arg-AMC substrate; measured thrombin K_m = 18 ± 1 µM for the Boc-Val-Pro-Arg-AMC substrate. The K_i values could not be directly withdrawn from the Cheng−Prusoff equation in this case due to the enzyme−inhibitor covalent interaction (see the section "Mechanism of Inhibition"). [b]A microscale reaction with 0% of conversion was used as a blank.
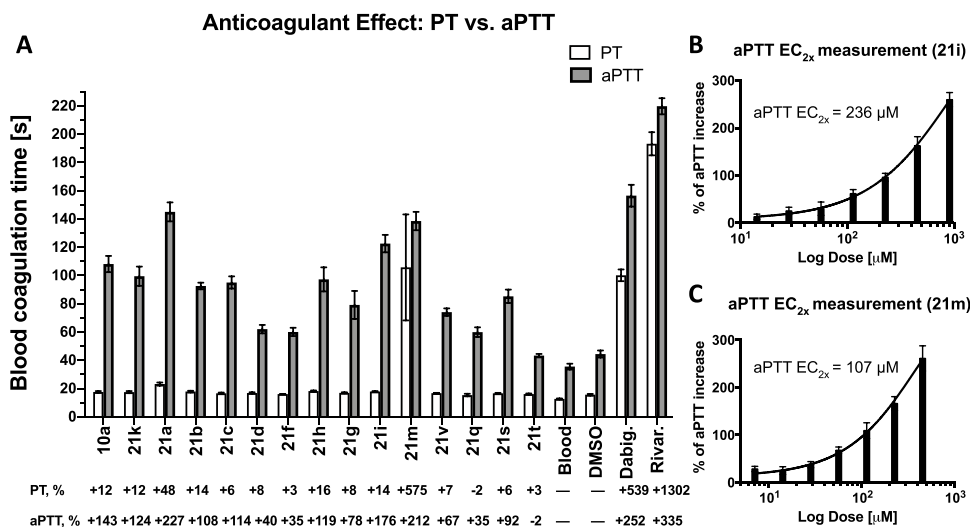
Figure 7. (A) In vitro anticoagulant activity of selected 1,2,4-triazol-5-amines tested at 300 μM compared to that of dabigatran (**1**) and rivaroxaban (**2**) tested at 3 μM. The activated partial thromboplastin time (aPTT) and prothrombin time (PT) are shown in seconds. The percentage increase of aPTT and PT compared to the effect of DMSO is shown under the diagram. (B and C) Measurement of aPTT EC_{2x} (concentration required to prolong aPTT twice) for **21i** (B) and **21m** (C). Tests were performed at least in triplicate, and the average with SD is given.

compounds might be used as a starting point for the development of FXIIa selective inhibitors.

Initially noticed during the MTS (Figure 6), the remarkable inhibitory profile of two naphthoyl derivatives **21i** and **21m** was now studied in detail (Table 2). Indeed, compound **21i** exhibiting the α-naphthoyl residue was found to be a potent 29 nM inhibitor of FXIIa with improved selectivity (nearly 13-fold) over thrombin (**21i**: thrombin IC_{50} = 375 nM). In contrast, its β-naphthoylated counterpart **21m** was proved to be a potent 27 nM inhibitor of thrombin with a reduced ability to affect FXIIa (IC_{50} = 138 nM).

When compared to the benzoic acid derivative **10a**, its more flexible phenylacetic acid-derived analogue **21r** inhibited FXIIa and thrombin with IC_{50} values of 210 and 509 nM, respectively, which indicates that the flexibility gain resulted in about twofold inhibitory activity loss toward both enzymes (Table 2). Upon the structure rigidification of compound **21r**, which resulted in chiral 1,2,3,4-tetrahydronaphthalene derivative **21v**, the inhibitory potency toward FXIIa was recovered (IC_{50} = 134 nM) and some selectivity over thrombin (IC_{50} = 421 nM) was gained. Also, the iodine atom introduction in the *ortho*-position of the aromatic ring of **21r** resulted in compound **21s**, which exhibited enhanced inhibitory activity toward FXIIa (IC_{50} = 62 nM) and 29-fold selectivity toward FXIIa over thrombin (IC_{50} = 1.8 μM).

Finally, aminotriazoles exhibiting furanyl (**21n**), pyridyl (**21l**), cyclohexyl (**21j**), tetrahydropyranyl (**21o**), styryl (**21u**), or benzamidomethyl (**21t**) residues showed low to no inhibitory properties toward FXIIa and thrombin, also confirming the results of MTS. Apart from compound **21m**, which showed 48% of FXa inhibition at 5 μM, none of the tested 1,2,4-triazol-5-amines was able to reach or show close to 50% of FXa or trypsin inhibition at 5 μM.

Anticoagulant Activity of Series 2. Of synthesized 1,2,4-triazol-5-amines **21a−v**, 14 representative compounds were tested for their anticoagulant properties in aPTT and PT tests. The outcome of this evaluation is given in Figure 7.

As can be seen in Figure 7A, anticoagulant properties of tested aminotriazoles varied significantly in both aPTT and PT tests. This activity fluctuation was linked to the compounds' selective or dual FXIIa and thrombin inhibition, which in turn was determined by the structure of tested compounds. Thus, α-naphthoylated compound **21i**, the most potent 29 nM inhibitor of FXIIa, affected the intrinsic blood coagulation, extending aPTT by 176%. The anticoagulant activity of **21i**, however, was lower than that of two other aminotriazoles **21a** and **21m** possessing 3,4-dimethylphenyl and β-naphthoyl residues, respectively, which prolonged aPTT even stronger by 227 and 212%, respectively. This might look like a discrepancy, considering a lower inhibitory activity of **21a** and **21m** toward FXIIa (91 and 138 nM, respectively) in comparison to **21i**. However, this contradiction is explained by the ability of **21a** and **21m** to strongly inhibit thrombin (57 and 27 nM, respectively), inhibition of which is also evident by prolonged PT for both compounds (48 and 575%, respectively). As the aPTT test is sensitive to inhibitors of both intrinsic and common coagulation pathways, for compounds **21a** and **21m**, the synergistic effect of FXIIa and thrombin inhibition is observed. It should, however, be noted that selective thrombin inhibition, *e.g.*, by dabigatran, could solely strongly prolong both PT and aPTT (Figure 7A).

Two most selective FXIIa inhibitors **21q** and **21s** (Table 2) showed almost no influence on the extrinsic blood coagulation (PT: 2 and 6%) while affecting the intrinsic coagulation pathway (aPTT was increased by 35 and 92%, respectively, Figure 7A). Compound **21t**, exhibiting no inhibitory properties toward FXIIa or thrombin (Table 2), as expected, failed to show anticoagulant activity, whereas more potent FXIIa and thrombin inhibitors such as **21b**, **21c**, and **21h** significantly prolonged aPTT by 108−114% (Figure 7A).

For aminotriazoles **21i** and **21m**, aPTT EC_{2x} (concentration required to prolong aPTT twice) was additionally measured. In this test, β-naphthoyl derivative **21m** showed about twice
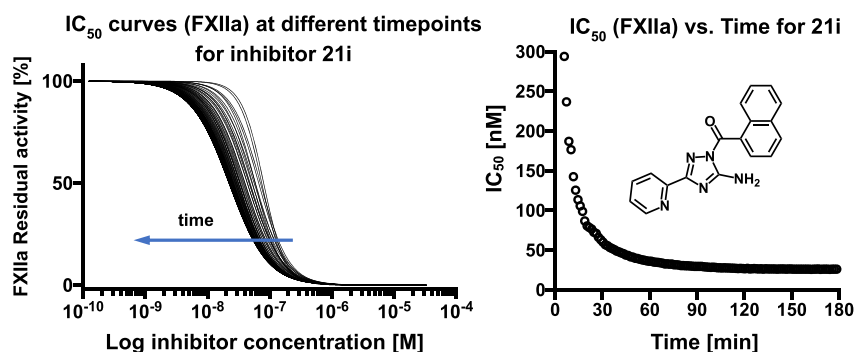
Figure 8. Time-dependent inhibition of FXIIa by aminotriazole **21i**. The enzyme (FXIIa, 2.5 nM) was added to a solution of a fluorogenic substrate (Boc-Gln-Gly-Arg-AMC, 25 μM) and inhibitor (ranged 0.5 nM–132 μM) in assay buffer, and fluorescence was read immediately in the kinetic mode for up to 180 min. Overtime, sigmoidal IC_{50} curves undergo a shift toward the lower values of log inhibitor concentrations (left). Measurement time plotted against calculated IC_{50} values of **21i** (right). This behavior suggests the covalent mechanism of FXIIa inhibition by **21i**.
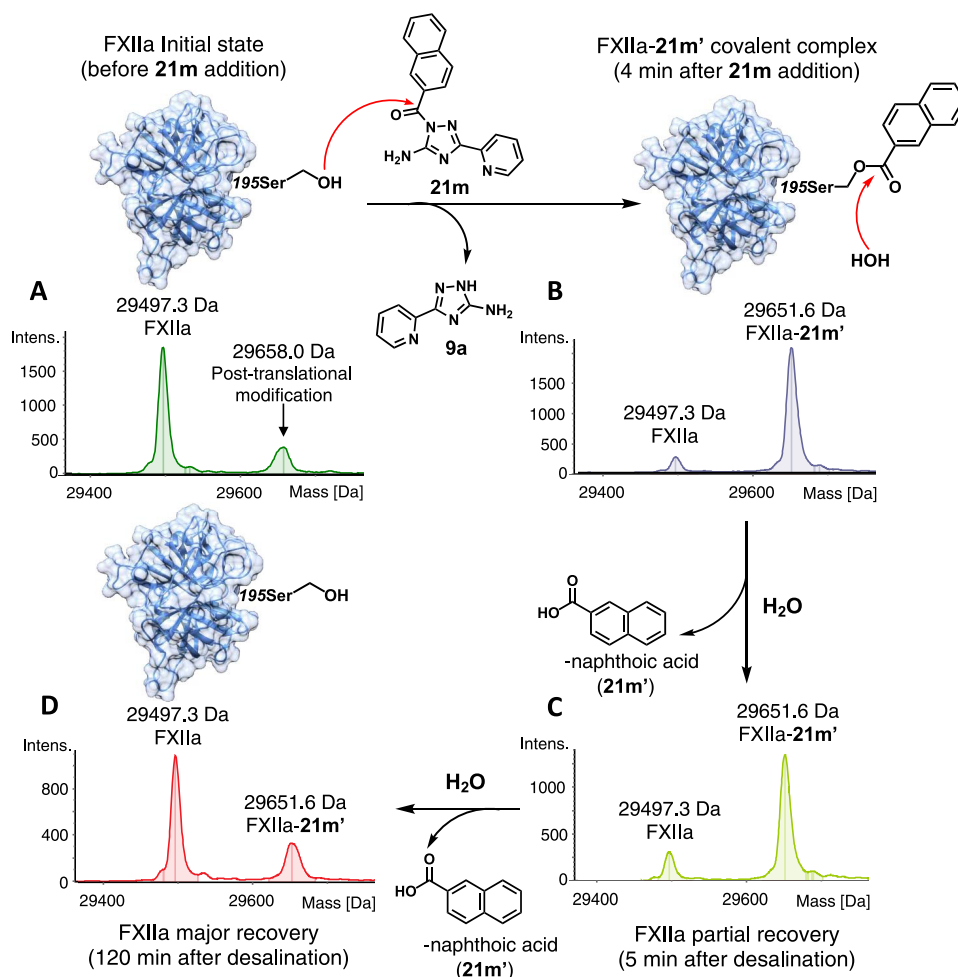
Figure 9. Covalent reversible inhibition of FXIIa by aminotriazole **21m** elucidated by mass spectrometry. Deconvoluted SEC/ESI-TOF mass spectra of intact FXIIa (A), FXIIa incubated (4 min) with **21m** (B), partially recovered FXIIa (C), and majorly recovered FXIIa (D). The main peaks are labeled with the corresponding deconvoluted masses. The schematic representation of FXIIa inhibition steps is also shown.

lower $EC_{2\times}$ of 107 μM compared to its α-naphthoyl-derived counterpart **21i**, $EC_{2\times}$ of which was 236 μM (Figure 7B,C).

Mechanism of Inhibition. While studying the inhibitory activity of synthesized 1,2,4-triazol-5-amines of both series 1 and 2 (Tables 1 and 2) toward FXIIa and thrombin, it has been observed that the IC_{50} values for each compound change over time significantly. For instance, the time-dependent behavior can be seen on the typical graph shown in Figure 8A for compound **21i** incubated with FXIIa. This graph clearly demonstrates distinct shifts of the IC_{50} sigmoidal curve during three hours of measurement. Time-dependent inhibition is even more apparent when measured IC_{50} values are plotted against time (Figure 8B). For the noncovalent reversible inhibitors such as dabigatran (**1**) and rivaroxaban (**2**), no time-dependent inhibition of thrombin and FXa, respectively, was observed in our experiments. These observations made us

K

suspect a covalent character of FXIIa and thrombin inhibition by the synthesized 1,2,4-triazol-5-amines.

To get insight into the mechanistic details of FXIIa inhibition, the advantages of size-exclusion chromatography (SEC) coupled with electrospray ionization mass spectrometry (ESI-MS) were utilized. In a typical experiment, FXIIa was incubated with the inhibitor of interest (molar ratio of 1:20), followed by chromatography and the enzyme–inhibitor complexes mass analysis. Also, the enzyme–inhibitor complex stability was examined in additional experiments to verify the possible reversibility of FXIIa covalent inhibition. The outcome of this evaluation and the proposed mechanism of FXIIa inhibition by the acylated 1,2,4-triazol-5-amines are summarized in Figure 9.

In the experiment, native FXIIa with a mass of 29497.3 Da (Figure 9A) changed its mass to 29651.6 Da after just 4 min of incubation with the inhibitor 21m (Figure 9B). This signal newly appeared on the mass spectrum was attributed to the FXIIa-21m' covalent complex (Figure 9B), which was presumably formed as a result of a nucleophilic attack of FXIIa catalytic Ser195 on the carbonyl carbon atom of 21m. The measured mass shift of Δm = 154.3 Da indicates that FXIIa acquired the β-naphthoic acid residue (21m') from the inhibitor 21m (Figure 9B). Subsequent removal of the excess of inhibitor 21m form the sample and the washing of the covalent complex (FXIIa-21m') with the excess of water allowed for the detection of at first partial (after 5 min, Figure 9C) and then major (after 120 min, Figure 9D) recovery of native FXIIa. The observed process of FXIIa recovery is consistent with the general catalytic mechanism of serine proteases, which proceeds via the hydrolysis step of the ester intermediate.

Additionally, the covalent mechanism of FXIIa inhibition was shown for five other acylated 1,2,4-triazol-5-amines (Figure 10). For instance, SEC/ESI-MS analysis of the 1,2,3,4-tetrahydronaphthalene derivative 21v and benzamido-benzoic acid derivative 21q revealed covalent complexes with masses of 29655.8 and 29720.5 Da, respectively, corresponding to the inhibitors' acyl moiety adducts (158.5 and 223.2 Da, respectively) to native FXIIa (Figure 10). Collectively, these findings suggest that synthesized acylated 1,2,4-triazol-5-amines are covalent reversible inhibitors of FXIIa and presumably of FIIa.

Binding Mode Study by Molecular Modeling. To rationalize the interactions between the synthesized inhibitors and blood coagulation factor XIIa and thrombin, molecular modeling studies were performed using available crystal structures of the enzymes.[28,49] The resultant binding modes for exemplary compounds are shown in Figure 11.

Tested inhibitors demonstrated a number of interactions with the active site of both FXIIa and thrombin sharing some similarities upon binding. Thus, the tetrahedral intermediate, the formation of which is suggested based on the performed mass spectrometry assay (vide supra), in each case was covalently bound to the oxygen atom of Ser195 (Figure 11A–D). Apart from that, the intermediate is additionally stabilized by two hydrogen bonds with the backbone amides of the "oxyanion hole" (Gly193 and Ser195, Figure 11A–D) of both FXIIa and thrombin, thereby mimicking the interactions of the natural tetrahedral intermediate, which is formed during the substrate cleavage. Further enzyme–inhibitor interactions are not universal for FXIIa and thrombin and depend on the
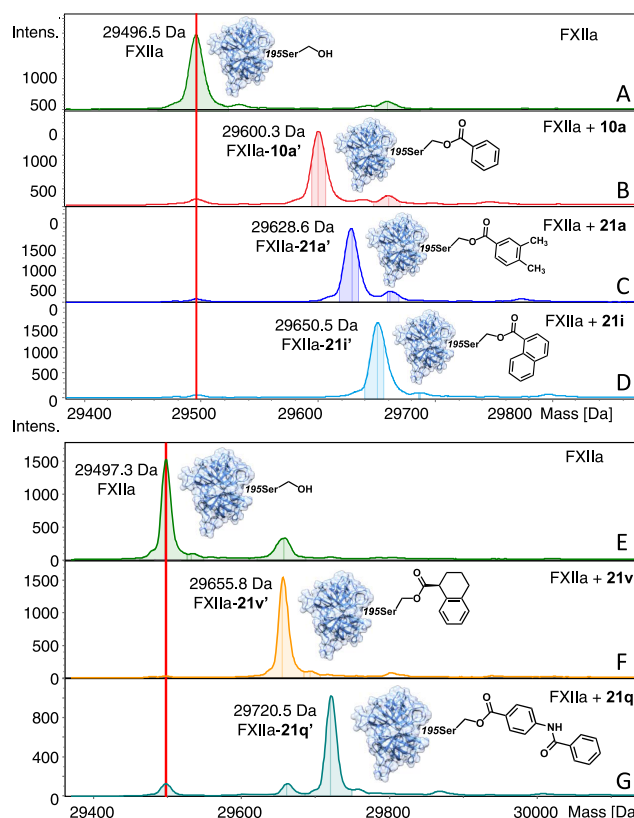
Figure 10. Deconvoluted SEC/ESI-TOF mass spectra of intact FXIIa (A, E) and five covalent complexes FXIIa-10a' (B), FXIIa-21a' (C), FXIIa-21i' (D), FXIIa-21v' (F), and FXIIa-21q' (G) formed after the FXIIa incubation with inhibitors 10a, 21a, 21i, 21v, and 21q, respectively. The peaks of interest are labeled with the corresponding deconvoluted masses. The schematic representation of FXIIa and FXIIa covalently bound to the acyl residues is also shown.

architecture of the active site of each enzyme and on the structural features of each inhibitor.

The specific 60-insertion loop (Tyr60A-Pro60B-Pro60C-Trp60D) of thrombin shapes its more narrow S2 pocket (especially due to Tyr60A and Trp60D) and also a more restricted S1' binding site (e.g., due to Lys60F insertion), preventing synthesized aminotriazoles from binding to the enzyme S1'–S4' binding sites (Figure 11B,D). Consequently, substituted aminotriazoles bind to the active site of thrombin in the way that their pyridyl moiety resides in S2 binding site partially protruding toward the amino acids of the S3 site (Figure 11B,D). Particularly, the pyridyl moiety of exemplary aminotriazole 10a undergoes hydrophobic interactions with Tyr60A, Trp60D, Leu99, and His57 of thrombin, whereas its primary amino group forms a hydrogen bond with Glu192 (Figure 11B). In thrombin, the aromatic part of the inhibitor's acyl moiety protrudes deeper into the selectivity pocket (S1) of the enzyme where it forms additional lipophilic interactions with, e.g., Cys191 and the backbone of Trp215. This fact might explain the lower tolerance of thrombin compared to that of FXIIa toward the introduction of bulky substituents in the para-position of the aromatic ring (e.g., low active thrombin inhibitors 21p and 21q, Table 2).

FXIIa is characterized by more spacious S1', S2, S3, and S4 sites compared to the corresponding sites of other serine proteases including thrombin.[50] This allows synthesized aminotriazoles to address unrestricted S1' site. Hence, we
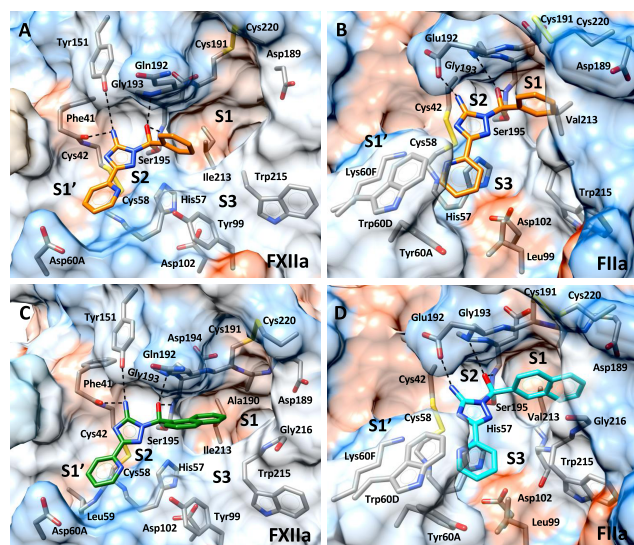
Figure 11. Calculated covalent binding conformation of inhibitor **10a** (orange stick model) in the active site of FXIIa (A) and thrombin (B). Predicted covalent binding conformations of α- and β-naphthoyl derivatives **21i** (green stick model, C) and **21m** (cyan stick model, D) in the active sites of FXIIa (C) and thrombin (D). The residues are depicted as gray stick models. Substrate-binding sites are labeled (S1−S3 and S1′). The surface is colored as follows: lipophilic regions are in orange, hydrophilic in blue, and neutral in white. PDB ID used: 6B77/FXIIa[28] and 6CYM/FIIa.[49]

observed that **10a** preferably binds to the amino acid residues of S2−S1′ binding sites of FXIIa (Figure 11A), which is in contrast to thrombin, where **10a** preferred to bind to S2−S3 sites (Figure 11B). In FXIIa, the pyridyl moiety of **10a** undergoes hydrophobic interactions not only with His57 but also with Cys58, whereas its aminotriazole aromatic ring, being also shifted toward S1′ site, interacts with Cys42 and Phe41 (Figure 11A). Upon binding to FXIIa, the aromatic fragment

of the acyl moiety of **10a** resides at the entrance of S1 selectivity pocket, forming lipophilic interactions only with Ser195, which should permit the bigger substituents' introduction both in the *para-* and *meta*-position of the aromatic ring to additionally address either S1 or S3 binding sites (Figure 11A).

Aminotriazoles possessing small acyl residues (*e.g.*, **10a**, **21a**, **21k**, Table 2) were found to interact efficiently with the active sites of both FXIIa and thrombin (Figure 11A,B), orienting their pyridyl residue toward either S1′ or S2 binding sites, respectively. That is why mentioned aminotriazoles experienced no selectivity, being equipotent inhibitors of FXIIa and thrombin. In contrast, compounds exhibiting structurally demanding acyl moieties showed a binding preference toward either FXIIa or thrombin. For instance, the selectivity profile is evidently driven by the structure of the acyl moiety of **21i** (29 nM inhibitor of FXIIa) and **21m** (27 nM inhibitor of thrombin) bearing spacious α- and β-naphthoyl residues, respectively (Table 2). Thus, the α-naphthoyl residue due to its geometry allows **21i** to adopt the energetically favorable conformation, facilitating compound's binding toward the direction of S2−S1′ binding site of FXIIa, whereas the β-naphthoyl substituent exhibiting less geometrical restriction is able to protrude deeper into the S1 pocket of thrombin orienting the rest of **21m** toward the S2−S3 pocket of thrombin (Figure 11C,D). Compared to the benzoyl moiety of **10a**, extended aromatic α- and β-naphthoyl residues of **21i** and **21m** acquire additional lipophilic interactions with, *e.g.*, Cys191, Ile213 (FXIIa, Figure 11C) and Val213, Asp189, Gly219, Gly266 (thrombin, Figure 11D). These additional interactions could explain lower IC$_{50}$ values of **21i** and **21m** toward FXIIa and thrombin compared to **10m** (Table 2).

Inhibition of Platelet Activation and Platelet Aggregation. As the search for new antithrombotic therapy of cancer-associated thrombosis is of high importance, the influence of the synthesized acylated 1,2,4-triazol-5-amines
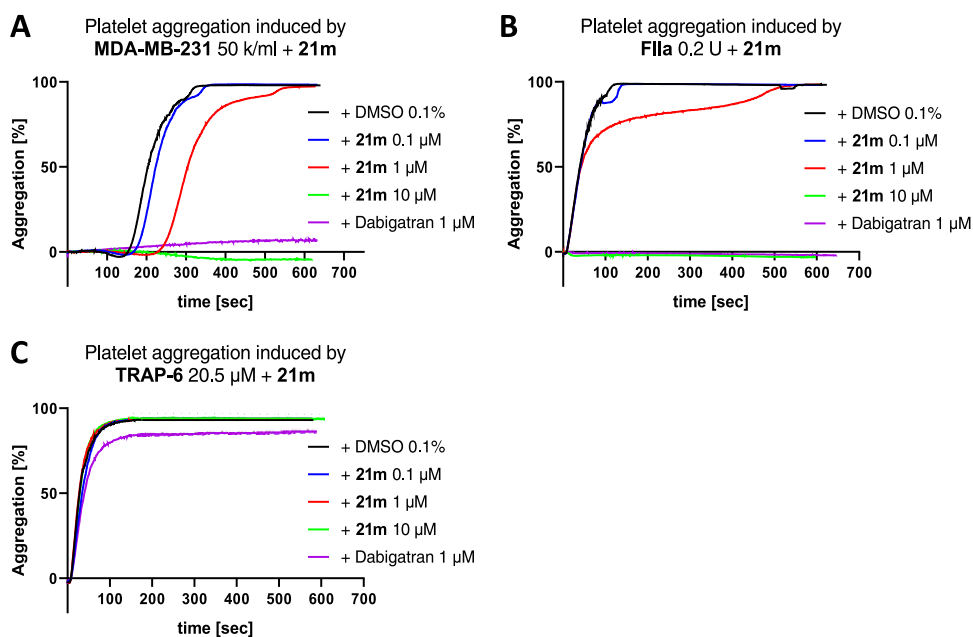
Figure 12. Platelet aggregation induced by MDA-MB-231 cancer cells (A), thrombin (B), or TRAP-6 (C) and measured by light transmission aggregometry in a coagulation-factor-free platelet buffer. In each case, platelets were preincubated with aminotriazole **21m** (0.1, 1, and 10 μM), dabigatran (1 μM), or DMSO (0.1%). Data are representative of three experiments (*n* = 3).

on the cancer-cell-induced platelet activation and aggregation was tested. Presumably, synthesized aminotriazoles might indirectly affect platelet activation via the inhibition of thrombin, which is formed upon plasma contact with TF expressed on the surface of cancer cells. The inhibition of FXIIa might also be beneficial in cancer-related thrombosis as cancer cells exhibit higher levels of the phospholipid phosphatidylserine on their outer membrane, which might contribute to FXII and platelet activation and thrombosis progression.[51−53] However, in coagulation-independent platelet activation tests due to the absence of clotting factors, the effect of FXIIa inhibition is expected to be minimal.

To estimate the ability of synthesized compounds to prevent platelet activation, two tests were performed. In the first test, the platelet aggregation was studied in a coagulation-factor-free buffer using light transmission aggregometry, where higher transmission indicates stronger platelet aggregation.[54] For this, in the presence and the absence of selected aminotriazoles 21i, 21m, and 21q, platelets were activated with a highly aggressive human breast cancer cell line MDA-MB-231, which expresses high levels of TF and strongly induces thrombin generation.[54] In a typical experiment, MDA-MB-231 cells induced fast (in about 400 s) and massive platelet aggregation (black curve, Figure 12A). Compounds 21i and 21q exhibiting preference toward FXIIa inhibition showed little to no influence on the breast-cancer-cell-induced platelet aggregation (Supporting Information). In contrast, being a 27 nM inhibitor of thrombin, compound 21m showed a dose-dependent ability to reduce platelet aggregation induced by MDA-MB-231 cancer cells (Figure 12A). At 100 nM, aminotriazole 21m showed practically no influence on MDA-MB-231-induced platelet aggregation (blue curve, Figure 12A). When, however, the test concentration was elevated to 1 μM, the evident shift of platelet aggregation curve (red curve) was observed, implying partial inhibition of platelet aggregation by 21m. A further concentration increase to 10 μM allowed for the complete prevention of MDA-MB-231-induced platelet aggregation by 21m during the observed time period (green line, Figure 12A).

To verify that aminotriazole 21m influenced cancer-cell-induced platelet aggregation via the thrombin inhibition, additional tests with platelets activated by thrombin (Figure 12B) and by thrombin receptor activating peptide-6 (TRAP-6, Figure 12C) were performed. Thrombin is a highly potent platelet activator, which binds to and cleaves the amino-terminal exodomain of the protease-activated receptors (PAR-1 and PAR-4) on the platelet surface. This cleavage unmasks a new receptor amino-terminus, which binds intramolecularly, thereby activating the receptor.[55,56] TRAP-6 is a peptide fragment of PAR-1 (residues 42−47) that directly activates PAR1 independently of the receptor cleavage, thus mimicking the effects of thrombin.[57] In our experiment, both thrombin and TRAP-6 induced complete platelet aggregation within 100−150 s (black curve, Figure 12B,C). When supplemented to platelets, compound 21m showed partial (at 1 μM) or complete (at 10 μM) inhibition of thrombin-induced platelet aggregation (Figure 12B). Inactivated thrombin, now carrying the acyl fragment of 21m on its Ser195, is probably still able to bind to PAR-1, though without the ability to activate the receptor due to the catalytic activity loss. This finding correlates nicely with the compound 21m's ability to prevent MDA-MB-231-induced platelet aggregation (Figure 12A) and suggests that antiaggregatory properties of 21m are likely

linked to thrombin inhibition. This assumption finds further confirmation in the experiments with TRAP-6, in which 21m irrespective of dose tested showed no influence on thrombin-independent TRAP-6-induced platelet aggregation (Figure 12C).

In the second series of tests, platelet activation was studied by measuring the release of adenosine triphosphate (ATP) from platelets' dense granules employing the bioluminescent firefly luciferase assay.[54] Platelets were treated with compound 21m and activated with MDA-MB-231 cancer cells, thrombin, or TRAP-6. The luminescent signal corresponding to ATP released from platelets activated by TRAP-6 was selected as a functional control and set as 100% (Figure 13).
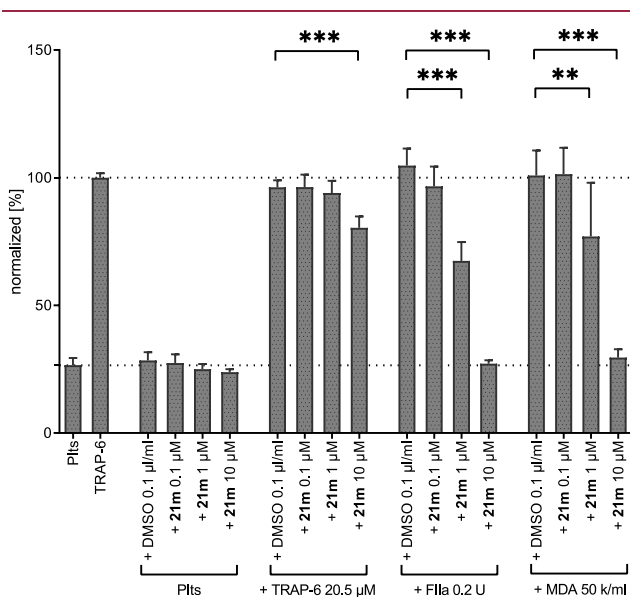
Figure 13. ATP release by activated platelets detected by luminescence measurements. MDA-MB-231 cancer cells, thrombin, and TRAP-6 strongly induce ATP release. TRAP-6-induced ATP release is set as 100%. Aminotriazole 21m dose-dependently reduces MDA-MB-231- and FIIa-induced ATP release. Tests were performed in triplicate, and the average with SD is given; ** $p < 0.0005$; *** $p < 0.0001$.

MDA-MB-231 cells, thrombin, and TRAP-6 strongly induced platelet activation as evidenced by maximal levels of ATP released upon platelet contact with listed activators (Figure 13). Compound 21m significantly suppressed both MDA-MB-231 cell- and thrombin-promoted platelet activation. This effect of 21m was dose-dependent, reaching its maximum at 10 μM (Figure 13). In contrast, compound 21m showed little (at 10 μM) to no (at 1 μM) influence on TRAP-6-induced platelet activation (Figure 13).

Altogether, two independent tests revealed the ability of aminotriazole 21m to suppress MDA-MB-231 cancer-cell-induced platelet activation. This effect was linked to the thrombin inhibitory activity of 21m. Two representative FXIIa inhibitors 21i and 21q showed practically no influence on the breast-cancer-cell-induced platelet aggregation.

Thrombin Generation Assay. For many anticoagulants, thrombin generation is an important measure of their efficacy. For this, thrombin generation assay (TGA) is employed, allowing to monitor the TF-induced thrombin generation by measuring the fluorogenic substrate cleavage. The assay outcome is expressed as a thrombogram (e.g., Figure 14),

which is characterized by several parameters shown in the footnote of Table 3.
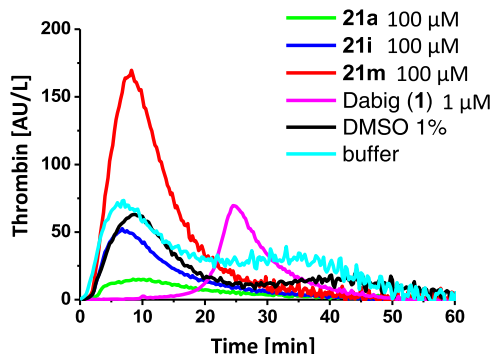
Figure 14. Representative thrombogram showing the TF-induced thrombin generation in the presence of **21a**, **21i**, **21m**, and dabigatran (**1**).

Selected compounds **21a**, **21i**, and **21m** exhibiting anticoagulant activity (Figure 7) and showing different preferences toward FXIIa and thrombin inhibition (Table 2) were assayed in TGA. As can be seen from the thrombogram (Figure 14), at 100 μM, α-naphthoylated aminotriazole **21i** showed a limited reduction of thrombin generation, which was expressed in the decreased amplitude of the thrombin peak (A_{max} reduction by 15% vs DMSO, Table 3) and reduced endogenous thrombin potential (ETP reduction by 38% vs DMSO, Table 3). The clotting time, however, was not extended; it was even slightly shortened ($T_{1/2}$ and T_{max}, Table 3). This limited effect of **21i** on thrombin generation was expected and is linked to the preference of **21i** to inhibit FXIIa over thrombin (Table 2). In contrast, being an unselective FXIIa and thrombin inhibitor, 3,4-dimethylbenzoic acid derivative **21a** (Table 2) showed a more pronounced reduction of thrombin generation at 100 μM (Figure 14), decreasing A_{max} and ETP by 73 and 69% compared to DMSO, respectively, and also extending $T_{1/2}$ by 27% (Table 3).

The β-naphthoylated aminotriazole **21m** exhibiting the lowest IC_{50} value (27 nM) toward thrombin was expected to show the strongest ability to reduce thrombin generation in TGA. Instead, **21m** demonstrated an unexpectedly paradoxical effect, amplifying thrombin generation (Figure 14). Thus, compared to DMSO, **21m** triggered higher amounts of thrombin generation (A_{max} and ETP increased 2.8- and 1.8-fold) and also shortened thrombin generation time (**21m** $T_{1/2}$ = 2.3 min vs DMSO $T_{1/2}$ = 3.0 min). This effect is unexpected, though not unusual, for thrombin inhibitors. A similar paradoxical effect was reported for known thrombin inhibitors dabigatran and melagatran, which being tested at low doses amplified thrombin generation in TGA.[58,59] This paradoxical effect is not completely understood but might be related to the inhibition of protein C activation by thrombin inhibitors.[60]

Cytotoxicity and Selectivity Profile of Synthesized Aminotriazoles. Before synthesized aminotriazoles could further proceed into animal studies, their safety profile should be evaluated in vitro. To get the initial impression about possible hepato- and neurotoxicity of prepared compounds, the most potent FXIIa and thrombin inhibitors **21i** and **21m**, respectively, along with the most selective FXIIa inhibitor **21q** were assayed in cytotoxicity tests employing HepG2 and CCF cells (Figure 15).

Performed cytotoxicity tests revealed a relatively low cytotoxicity profile of exemplary aminotriazoles (Figure 15). Thus, compounds **21i**, **21m**, and **21q** at the highest tested dose of 100 μM reduced the viability of HepG2 cells by only 8, 25, and 13%, respectively. CCF cells were found to be slightly more sensitive toward the addition of compounds **21m** and **21q**, which at the dose of 100 μM reduced the cell viability by 36 and 35%, respectively, which, however, was insufficient to obtain the IC_{50} values (extended cytotoxicity data are provided in the Supporting Information).

Even though synthesized compounds inhibited FXIIa and thrombin without affecting trypsin and FXa, considering their covalent reversible mechanism of action, other serine hydrolases might be affected by the compounds. Therefore, to verify that the synthesized aminotriazoles do not show aggressive acylating behavior toward other enzymes possessing catalytic Ser, selected compounds were assayed against the panel of physiologically relevant serine proteases (FXIa, urokinase, plasmin, and plasma kallikrein) and serine hydrolases MAGL (monoacylglycerol lipase)[61] and FAAH (fatty acid amide hydrolase).[62]

Performed experiments revealed that none of the assayed 1,2,4-triazol-5-amines was able to significantly inhibit serine proteases implicated in the blood coagulation cascade (except for targeted thrombin and FXIIa) as well as MAGL or FAAH (Table 4). This finding additionally underlines the selectivity of synthesized FXIIa and thrombin inhibitors, the inhibitory activity of which is not only driven by the presence of catalytic Ser in the enzymes' active site but is rather determined by the overall structural features of FXIIa and thrombin (Figure 11).

■ CONCLUSIONS

This study reports on selective small-molecule inhibitors of human blood coagulation factor XIIa and thrombin. The combination of conventional and microscale parallel synthetic

Table 3. Thrombin Generation Parameters under the Influence of 21a, 21i, 21m, and Dabigatran (1)[a]

	homogeneous thrombin generation (n = 3)			
	$T_{1/2}$ ± SD [min]	A_{max} ± SD [AU/L]	T_{max} ± SD [min]	ETP ± SD [AU*min/L]
21a	3.8 ± 0.5	16.9 ± 3.9	8.8 ± 0.4	370 ± 24
21i	2.7 ± 0.6	53.3 ± 1.1	7.0 ± 0.2	738 ± 250
21m	2.3 ± 0.6	175.5 ± 32.9	8.0 ± 0.7	2160 ± 278
Dabig (**1**)	15.2 ± 1.1	72.4 ± 3.5	25.5 ± 1.1	678 ± 110
DMSO	3.0 ± 0.5	63.0 ± 3.7	8.1 ± 0.6	1203 ± 44
Buffer	2.7 ± 0.5	73.0 ± 22.6	7.8 ± 1.3	1737 ± 344

[a]$T_{1/2}$, clotting time; A_{max}, the amplitude of the thrombin peak; T_{max}, time to peak; ETP, endogenous thrombin potential (the area under the thrombogram curve).
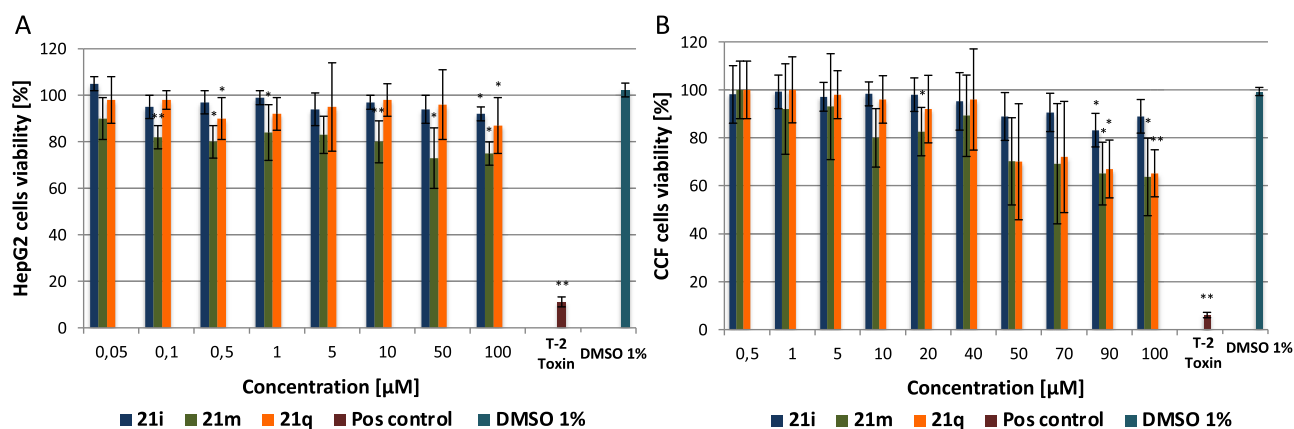
Figure 15. Cytotoxicity profile of synthesized FXIIa and thrombin inhibitors **21i**, **21m**, and **21q** tested on HepG2 and CCF-STTG-1 cell lines. T-2 toxin (10 μM) was used as a positive and DMSO (1%) as a negative control. Tests were performed in triplicate, and the average with SD is given; * $p < 0.05$; ** $p < 0.01$.

Table 4. Selectivity Profile of Acylated 1,2,4-Triazol-5-amines

protease IC$_{50}$, (nM)^a	10a	21a	21i	21m	21s
thrombin	235 ± 7	57 ± 6	375 ± 12	27 ± 2	1819 ± 155
FXa	>5000	>5000	>5000	48% @ 5 μM	>5000
FXIa	>5000	>5000	>5000	>5000	>5000
FXIIa	132 ± 10	91 ± 9	29 ± 5	138 ± 12	62 ± 22
uPA	7930 ± 2130	2942 ± 71	>5000	6762 ± 2408	41% @ 5 μM
plasmin	>5000	25820 ± 4880	>5000	>5000	>5000
PK	>5000	>5000	>5000	>5000	>5000
trypsin	>5000	>5000	>5000	>5000	
MAGL	>5000		>5000	>5000	
FAAH	>5000		>5000	>5000	

^{a}Screened @ 5 μM in at least two independent determinations; for active compounds, IC$_{50}$ measurements were performed in triplicate. Inhibition values of reference inhibitors: MAGL inhibitor CAY10499[63] IC$_{50}$ = 480 nM; FAAH inhibitor URB597[64] IC$_{50}$ = 43 nM.

approaches allowed us to access a library of diverse 1,2,4-triazol-5-amines, some of which potently inhibited FXIIa and/or thrombin but not other tested serine proteases of the blood coagulation cascade. Synthesized compounds preferentially affected the intrinsic blood coagulation, which is initiated by FXIIa and is implicated in thrombosis. Structure–activity relationship studies uncovered the inhibitors' structural features required for the FXIIa and thrombin successful inhibition and for the anticoagulant activity manifestation. The presence of a pyridyl moiety in the position 3 of the 1,2,4-triazol-5-amine scaffold was found to be crucial as its replacement with a phenyl or aminoaryl residue resulted in activity reduction. The 1,2,4-triazol-5-amines exhibiting a nonacylated annular secondary amino group or bearing a sulfonamide residue on the annular nitrogen atom demonstrated no ability to inhibit tested serine proteases as well as no influence on blood coagulation. Instead, N1-acylated compounds, especially bearing an aromatic acyl fragment, showed the highest ability to inhibit FXIIa and thrombin. Among them, derivative **21i** exhibiting the α-naphthoyl residue was found to be the most potent 29 nM inhibitor of FXIIa with improved selectivity over thrombin (**21i**: thrombin IC$_{50}$ = 375 nM), whereas its β-naphthoylated analogue **21m** was proved to be the most potent 27 nM inhibitor of thrombin with a reduced ability to affect FXIIa (IC$_{50}$ = 138 nM). More selective inhibitors of FXIIa were also found among synthesized aminotriazoles (*e.g.*, **21p**, **21s**, and **21q**), which demonstrated

almost no influence on the extrinsic blood coagulation while disrupting the intrinsic coagulation pathway.

Mass spectrometric analysis reinforced by the molecular modeling allowed us to discover previously unknown interactions between the synthesized inhibitors and the active site of FXIIa. It has been established that the carbonyl carbon atom of acylated 1,2,4-triazol-5-amines upon contact with FXIIa undergoes a nucleophilic attack, presumably, by the FXIIa catalytic Ser195, which results in the acyl moiety transfer, forming an FXIIa-Ser195-acyl covalent complex. A single transfer of the acyl moiety to FXIIa implies this process' specificity. Being an ester susceptible to slow hydrolytic cleavage, the resultant covalent complex (FXIIa-Ser195-acyl) was experimentally shown to degrade over time, recovering the native FXIIa. These experiments along with the observed time-dependent FXIIa and thrombin inhibition suggested acylated 1,2,4-triazol-5-amines as covalent reversible inhibitors. As suggested by the computational modeling, apart from the covalent interaction with Ser195, active inhibitors of FXIIa and thrombin form two hydrogen bonds with the backbone amides of the "oxyanion hole" (Gly193 and Ser195), thereby mimicking the interactions of the natural tetrahedral intermediate. Other interactions with S1–S3 and S1′ substrate-binding sites of FXIIa and thrombin are more specific for each enzyme and also depend on the compound's structure.

Apart from exhibiting direct anticoagulant properties, selected 1,2,4-triazol-5-amines reduced thrombin generation

in TGA and slowed down platelet activation and platelet aggregation. Thus, being tested at 100 μM, 3,4-dimethylbenzoic acid derivative **21a** practically diminished thrombin generation in TGA, whereas β-naphthoylated aminotriazole **21m** suppressed MDA-MB-231 cancer-cell-induced platelet activation. These effects were linked to the ability of **21a** and **21m** to inhibit thrombin.

Collectively, herein disclosed 1,2,4-triazol-5-amines with FXIIa and/or thrombin inhibitory activity, anticoagulant properties, elucidated mechanism of inhibition, selectivity profiles, and relatively low cytotoxicity represent a promising starting point for the development of novel antithrombotic drugs and also can find their application as chemical tools for studying the role of FXIIa and thrombin in physiological and pathological processes.

■ EXPERIMENTAL SECTION

Chemistry, General. Unless otherwise mentioned, THF was dried with sodium/benzophenone and was freshly distilled before use. Thin-layer chromatography (TLC): silica gel 60 F_{254} plates (Merck). Flash chromatography (FC): silica gel 60, 40−63 μm (Macherey-Nagel). Reversed-phase thin-layer chromatography (RP-TLC): silica gel 60 RP-18 F_{254}S plates (Merck). Automatic flash column chromatography: Isolera One (Biotage); brackets include eluent, cartridge-type. Melting point (m.p.): melting point apparatus SMP 3 (Stuart Scientific), uncorrected. ^{1}H NMR (400 MHz), ^{1}H NMR (600 MHz), and ^{13}C NMR (100 MHz): Agilent DD2 400 and 600 MHz spectrometers; chemical shifts (δ) are reported in ppm against the reference substance tetramethylsilane and calculated using the solvent residual peak of the undeuterated solvent. IR: IR Prestige-21 (Shimadzu). HRMS: MicrOTOF-QII (Bruker). The HPLC method to determine the purity of compounds: equipment 1: pump: L-7100, degasser: L-7614, autosampler: L-7200, UV detector: L-7400, interface: D-7000, data transfer: D-line, data acquisition: HSMS software (all from LaChrom, Merck Hitachi); equipment 2: pump: LPG-3400SD, degasser: DG-1210, autosampler: ACC-3000T, UV detector: VWD-3400RS, interface: Dionex UltiMate 3000, data acquisition: Chromeleon 7 (Thermo Fisher Scientific); column: LiChrospher 60 RP-select B (5 μm), LiChroCART 250−4 mm cartridge; flow rate: 1.0 mL/min; injection volume: 5.0 μL; detection at λ = 210 nm; solvents: A: demineralized water with 0.05% (v/v) trifluoroacetic acid, B: acetonitrile with 0.05% (v/v) trifluoroacetic acid; gradient elution (% A): 0−4 min: 90%; 4−29 min: gradient from 90 to 0%; 29−31 min: 0%; 31−31.5 min: gradient from 0 to 90%; 31.5−40 min: 90%. With the exception of compounds **7** (93.9%) and **21l** (94.0%), the purity of all test compounds was greater than 95%.

General Procedure A. To a stirred solution of 1*H*-1,2,4-triazol-5-amine **9a**−**c**, **15**, or **19a**−**c** (1 equiv) in dry THF/pyridine mixture (1:1), an acylating agent (acid chloride, sulfonyl chloride, or chloroformate, 1−2 equiv) in dry THF was added dropwise with a syringe pump over 30 min at 0 °C. The reaction mixture was stirred at 0 °C for 1 h and then at room temperature (for the indicated period of time). Then, the reaction mixture was diluted with water (100 mL), and the formed precipitate was filtrated off, washed with water and diethyl ether, and dried *in vacuo*. The crude product was purified, if required, by column chromatography.

General Procedure B (Synthesis of Acid Chlorides). The respective carboxylic acid (1 equiv) was dissolved in THF (3 mL, dry). At 0 °C, oxalyl chloride (2.3 equiv) was added dropwise to the reaction mixture over 3 min. One drop of DMF was added, and the reaction mixture was allowed to warm up to room temperature. After the mixture was stirred for 2 h, the solvent was evaporated under reduced pressure and the residue was dissolved in low amounts of dry THF (0.5 mL) to be used directly as an acylation agent in general procedure A.

General Procedure C. If not described otherwise, 1,2,4-triazol-5-amine **9a** (1 equiv), the respective carboxylic acid (1 equiv), EDCI

(1.3−2 equiv), and DMAP (1.3−2 equiv) were dissolved in DMF (3−4 mL, dry) at 0 °C. Under stirring, the reaction mixture was allowed to warm up to room temperature. After 3−18 h of stirring at room temperature, the mixture was cooled down to 0 °C and diluted with water (100 mL), and the formed precipitate was filtrated off and washed with water (10 mL) and diethyl ether (10 mL). The residue was dried under reduced pressure.

*(5-Amino-3-(pyridin-3-yl)-1H-1,2,4-triazol-1-yl)(phenyl)-methanone (**7**).* It was synthesized according to general procedure A from **9b** (195 mg, 1.2 mmol, 1 equiv) and benzoyl chloride (329 mg, 2.3 mmol, 1.9 equiv). Stirring at room temperature was continued for 4.5 h. The crude product was purified by flash column chromatography (DCM/MeOH = 1/0 → 9/1) to give **7** as a colorless solid (247 mg, 0.93 mmol, 77%); mp = 172−174 °C. TLC: 0.84 (EtOAc/MeOH, 9:1). ^{1}H NMR (600 MHz, DMSO-d_6) δ 7.51 (ddd, J = 8.0, 4.9, 0.9 Hz, 1H, 5′-H$_{pyridyl}$), 7.57−7.62 (m, 2H, 3″-H$_{phenyl}$, 5″-H$_{phenyl}$), 7.67−7.72 (m, 1H, 4″-H$_{phenyl}$), 7.94 (br s, 2H, NH$_2$), 8.19−8.13 (m, 2H, 2″-H$_{phenyl}$, 6″-H$_{phenyl}$), 8.25 (dt, J = 7.9, 1.9 Hz, 1H, 4′-H$_{pyridyl}$), 8.67 (dd, J = 4.9, 1.7 Hz, 1H, 6′-H$_{pyridyl}$), 9.11 (d, J = 2.1 Hz, 1H, 2′-H$_{pyridyl}$). ^{13}C NMR (151 MHz, DMSO-d_6) δ 123.9 (1C, C-5′$_{pyridyl}$), 126.0 (1C, C-3′$_{pyridyl}$), 128.1 (2C, C-3″$_{phenyl}$, C-5″$_{phenyl}$), 130.9 (2C, C-2″$_{phenyl}$, C-6″$_{phenyl}$), 132.0 (1C, C-1″$_{phenyl}$), 133.1 (1C, C-4″$_{phenyl}$), 133.8 (1C, C-4′$_{pyridyl}$), 147.5 (1C, C-2′$_{pyridyl}$), 150.9 (1C, C-6′$_{pyridyl}$), 157.7 (1C, C-3$_{triazole}$), 159.1 (1C, C-5$_{triazole}$), 167.6 (C=O). IR (neat): $\tilde{\nu}$ [cm^{-1}] = 3426, 3059, 1690, 1659, 1582, 1524, 1489, 1412, 1373, 1339, 1180, 1146, 1072, 1026, 964, 799, 748, 687, 625. HRMS (m/z): [M + H]$^+$ calcd for C$_{14}$H$_{11}$N$_5$O$^+$ 266.1036, found 266.1017. HPLC: t_R = 13.95 min, purity 93.9%.

*(5-Amino-3-(pyridin-2-yl)-1H-1,2,4-triazol-1-yl)(phenyl)-methanone (**10a**).* It was synthesized according to general procedure A from **9a** (305 mg, 1.89 mmol, 1 equiv) and benzoyl chloride (346 mg, 2.46 mmol, 1.3 equiv). Stirring at room temperature was continued for 4.5 h. The crude product was purified by flash column chromatography (DCM/MeOH = 1/0 → 9/1) to give **10a** as a colorless solid (210 mg, 0.79 mmol, 42%); mp = 174−175 °C. TLC: 0.72 (EtOAc/MeOH, 9:1). ^{1}H NMR (600 MHz, DMSO-d_6) δ 7.47 (ddd, J = 7.5, 4.7, 1.2 Hz, 1H, 5′-H$_{pyridyl}$), 7.56−7.62 (m, 2H, 3″-H$_{phenyl}$, 5″-H$_{phenyl}$), 7.70 (ddt, J = 8.7, 7.0, 1.3 Hz, 1H, 4″-H$_{phenyl}$), 7.85 (br s, 2H, NH$_2$), 7.92 (td, J = 7.7, 1.8 Hz, 1H, 4′-H$_{pyridyl}$), 8.00 (dt, J = 7.8, 1.1 Hz, 1H, 3′-H$_{pyridyl}$), 8.10−8.16 (m, 2H, 2″-H$_{phenyl}$, 6″-H$_{phenyl}$), 8.66 (ddd, J = 4.7, 1.8, 0.9 Hz, 1H, 6′-H$_{pyridyl}$). ^{13}C NMR (151 MHz, DMSO-d_6) δ 122.5 (1C, C-3′$_{pyridyl}$), 124.7 (1C, C-5′$_{pyridyl}$), 128.1 (2C, 3″-C$_{phenyl}$, 5″-C$_{phenyl}$), 130.7 (2C, 2″-C$_{phenyl}$, 6″-C$_{phenyl}$), 132.1 (1C, 1″-C$_{phenyl}$), 133.0 (1C, 4″-C$_{phenyl}$), 137.0 (1C, C-4′$_{pyridyl}$), 148.9 (1C, C-2′$_{pyridyl}$), 149.7 (1C, C-6′$_{pyridyl}$), 159.0 (1C, 3-C$_{triazole}$), 159.6 (1C, 5-C$_{triazole}$), 167.9 (C=O). IR (neat): $\tilde{\nu}$ [cm^{-1}] = 3460, 3063, 2928, 1686, 1632, 1535, 1447, 1385, 1358, 1327, 1153, 1076, 968, 918, 799, 745, 691. HRMS (m/z): [M + H]$^+$ calcd for C$_{14}$H$_{11}$N$_5$O$^+$ 266.1036, found 266.1015. HPLC: t_R = 14.83 min, purity 96.6%.

*(5-Amino-3-(pyridin-4-yl)-1H-1,2,4-triazol-1-yl)(phenyl)-methanone (**10c**).* It was synthesized according to general procedure A from **9c** (499 mg, 3.1 mmol, 1 equiv) and benzoyl chloride (479 mg, 3.41 mmol, 1.1 equiv). Stirring at room temperature was continued for 4.5 h. After the washing steps, pure product **10c** was obtained as a colorless solid (716 mg, 2.70 mmol, 87%); mp = 216−217 °C. TLC: 0.74 (EtOAc/MeOH, 9:1). ^{1}H NMR (600 MHz, DMSO-d_6) δ 7.56−7.62 (m, 2H, 3″-H$_{phenyl}$, 5″-H$_{phenyl}$), 7.68−7.74 (m, 1H, 4″-H$_{phenyl}$), 7.81−7.86 (m, 2H, 3′-H$_{pyridyl}$, 5′-H$_{pyridyl}$), 7.94 (br s, 2H, NH$_2$), 8.11−8.18 (m, 2H, 2″-H$_{phenyl}$, 6″-H$_{phenyl}$), 8.64−8.70 (m, 2H, 2′-H$_{pyridyl}$, 6′-H$_{pyridyl}$). ^{13}C NMR (151 MHz, DMSO-d_6) δ 120.5 (2C, C-3′$_{pyridyl}$, C-5′$_{pyridyl}$), 128.1 (2C, C-3″$_{phenyl}$, C-5″$_{phenyl}$), 130.8 (2C, C-2″$_{phenyl}$, C-6″$_{phenyl}$), 131.9 (1C, C-1″$_{phenyl}$), 133.1 (1C, C-4″$_{phenyl}$), 137.3 (1C, C-4′$_{pyridyl}$), 150.4 (2C, C-2′$_{pyridyl}$, C-6′$_{pyridyl}$), 157.8 (1C, C-3$_{triazole}$), 159.2 (1C, C-5$_{triazole}$), 167.6 (C=O). IR (neat): $\tilde{\nu}$ [cm^{-1}] = 3302, 3125, 1701, 1651, 1605, 1524, 1489, 1366, 1307, 922, 752, 675, 675. HRMS (m/z): [M + H]$^+$ calcd for C$_{14}$H$_{11}$N$_5$O$^+$ 266.1036, found 266.1051. HPLC: t_R = 13.59 min, purity 99.1%.

*(5-Amino-3-(pyridin-4-yl)-1H-1,2,4-triazol-1-yl)(cyclohexyl)-methanone (**11c**).* It was synthesized according to general procedure

A from **9c** (300 mg, 1.86 mmol, 1 equiv) and cyclohexanecarbonyl chloride (355 mg, 2.42 mmol, 1.3 equiv). Stirring at room temperature was continued for 4.5 h. After the washing steps, pure product **11c** was obtained as a colorless solid (287 mg, 1.06 mmol, 57%); mp = 193−195 °C. TLC: 0.83 (EtOAc/MeOH, 9:1).^{1}H NMR (600 MHz, DMSO-d_6) δ 1.18−1.29 (m, 1H, CH(CH$_2$CH$_2$)$_2$CH_2), 1.31−1.49 (m, 4H, CH(CH_2CH$_2$)$_2$CH$_2$), 1.65−1.72 (m, 1H, CH(CH$_2$CH$_2$)$_2$CH_2), 1.78 (dt, J = 12.8, 3.2 Hz, 2H, CH-(CH$_2$CH_2)$_2$CH$_2$), 1.98 (dd, J = 11.5, 4.3 Hz, 2H, CH-(CH_2CH$_2$)$_2$CH$_2$), 3.42 (tt, J = 11.2, 3.4 Hz, 1H, CH(CH$_2$CH$_2$)$_2$CH$_2$), 7.74 (br s, 2H, NH$_2$), 7.84−7.89 (m, 2H, 3′-H$_{pyridyl}$, 5′-H$_{pyridyl}$), 8.68−8.73 (m, 2H, 2′-H$_{pyridyl}$, 6′-H$_{pyridyl}$). ^{13}C NMR (151 MHz, DMSO-d_6) δ 24.9 (2C, CH(CH$_2$CH$_2$)$_2$CH$_2$), 25.4 (1C, CH(CH$_2$CH$_2$)$_2$CH$_2$), 28.1 (2C, CH(CH$_2$CH$_2$)$_2$CH$_2$), 42.2 (1C, CH(CH$_2$CH$_2$)$_2$CH$_2$), 120.4 (2C, C-3′$_{pyridyl}$, C-5′$_{pyridyl}$), 137.4 (1C, C-4′$_{pyridyl}$), 150.4 (2C, C-2′$_{pyridyl}$, C-6′$_{pyridyl}$), 157.5 (1C, C-3$_{triazole}$), 158.0 (1C, C-5$_{triazole}$), 176.5 (C═O). IR (neat): $\tilde{\nu}$ [cm^{-1}] = 3421, 3105, 2935, 2854, 1717, 1647, 1605, 1524, 1489, 1416, 1362, 1331, 1277, 1234, 1138, 976, 833, 752, 675. HRMS (m/z): [M + H]$^+$ calcd for C$_{14}$H$_{17}$N$_5$O$^+$ 272.1506, found 272.1178. HPLC: t_R = 15.86 min, purity 95.1%.

Phenyl 5-Amino-3-(pyridin-2-yl)-1H-1,2,4-triazole-1-carboxylate (12a). It was synthesized according to general procedure A from **9a** (100 mg, 0.62 mmol, 1 equiv) and phenyl chloroformate (107 mg, 0.68 mmol, 1.1 equiv). Stirring at room temperature was continued for 2 h. The crude product was purified by flash column chromatography (DCM/ACN = 7/3 → 0/1) to give **12a** as a colorless solid (25.9 mg, 0.092 mmol, 15%); mp = >300 °C. TLC: 0.39 (DCM/MeOH, 9:1). ^{1}H NMR (600 MHz, DMSO-d_6) δ 7.38 (t, J = 7.4 Hz, 1H, 4″-H$_{phenyl}$), 7.42 (d, J = 7.9 Hz, 2H, 2″-H$_{phenyl}$, 6″-H$_{phenyl}$), 7.49 (dd, J = 6.7, 4.9 Hz, 1H, 5′-H$_{pyridyl}$), 7.52 (t, J = 7.9 Hz, 2H, 3″-H$_{phenyl}$, 5″-H$_{phenyl}$), 7.61 (br s, 2H, NH$_2$), 7.93 (td, J = 7.7, 1.8 Hz, 1H, 4′-H$_{pyridyl}$), 8.03 (d, J = 7.8, 1H, 3′-H$_{pyridyl}$), 8.68 (d, J = 4.3 Hz, 1H, 6′-H$_{pyridyl}$). ^{13}C NMR (151 MHz, DMSO-d_6) δ 121.7 (2C, C-2″$_{phenyl}$, C-6″$_{phenyl}$), 122.4 (1C, C-3′$_{pyridyl}$), 124.8 (1C, C-5′$_{pyridyl}$), 126.8 (1C, C-4″$_{phenyl}$), 129.8 (2C, C-3″$_{phenyl}$, C-5″$_{phenyl}$), 137.1 (1C, C-4′$_{pyridyl}$), 148.7 (C═O), 148.9 (1C, C-2′$_{pyridyl}$), 149.7 (1C, C-6′$_{pyridyl}$), 149.8 (1C, C-1″$_{phenyl}$), 158.6 (1C, C-5$_{triazole}$), 159.8 (1C, C-3$_{triazole}$). IR (neat): $\tilde{\nu}$ [cm^{-1}] =1325, 1589, 1748, 3310, 3435. HRMS (m/z): [M + H]$^+$ calcd for C$_{14}$H$_{12}$N$_5$O$_2^+$ 282.0986, found 282.0977. HPLC: t_R = 14.40 min, purity 99.8%.

3-(Pyridin-4-yl)-1-tosyl-1H-1,2,4-triazol-5-amine (13c). It was synthesized according to general procedure A from **9c** (250 mg, 1.55 mmol, 1 equiv) and 4-toluenesulfonyl chloride (444 mg, 2.33 mmol, 1.5 equiv). Stirring at room temperature was continued for 4.5 h. After the washing steps, pure product **13c** was obtained as a colorless solid (342 mg, 1.08 mmol, 70%); mp = 222 °C (decomp.). TLC: 0.80 (EtOAc/MeOH, 9:1). ^{1}H NMR (600 MHz, DMSO-d_6) δ 2.39 (s, 3H, CH_3), 7.48−7.54 (m, 2H, 3″-H$_{tosyl}$, 5″-H$_{tosyl}$), 7.59 (br s, 2H, NH$_2$), 7.70−7.79 (m, 2H, 3′-H$_{pyridyl}$, 5′-H$_{pyridyl}$), 7.92−7.99 (m, 2H, 2″-H$_{tosyl}$, 6″-H$_{tosyl}$), 8.62−8.69 (m, 2H, 2′-H$_{pyridyl}$, 6′-H$_{pyridyl}$). ^{13}C NMR (151 MHz, DMSO-d_6) δ 21.2 (1C, CH$_3$), 120.3 (2C, C-3′$_{pyridyl}$ and C-5′$_{pyridyl}$), 127.6 (2C, C-2″$_{tosyl}$, C-6″$_{tosyl}$), 130.5 (2C, C-3″$_{tosyl}$, C-5″$_{tosyl}$), 133.2 (1C, C-1″$_{tosyl}$), 136.7 (1C, C-4′$_{pyridyl}$), 146.6 (1C, C-4″$_{tosyl}$), 150.4 (2C, C-2′$_{pyridyl}$, C-6′$_{pyridyl}$), 157.7 (1C, C-5$_{triazole}$), 159.0 (1C, C-3$_{triazole}$). IR (neat): $\tilde{\nu}$ [cm^{-1}] = 3429, 3144, 3117, 1717, 1647, 1562, 1520, 1485, 1415, 1377, 1169, 1076, 968, 810, 664, 602. HRMS (m/z): [M + H]$^+$ calcd for C$_{14}$H$_{13}$N$_5$O$_2$S$^+$ 316.0863, found 316.0824. HPLC: t_R = 15.63 min, purity 99.4%.

(5-Amino-3-phenyl-1H-1,2,4-triazol-1-yl)(phenyl)methanone (16). It was synthesized according to modified general procedure A from **15** (100 mg, 0.62 mmol, 1 equiv) and benzoyl chloride (88 mg, 0.62 mmol, 1 equiv). Benzoyl chloride in 2 mL of dry THF was added to the reaction mixture with a syringe pump over a period of 2 h at 0 °C, and stirring was continued at room temperature for another 2 h. Then, H$_2$O (15 mL) was added and the aqueous layer was extracted with EtOAc (3×). The combined organic layers were dried (Na$_2$SO$_4$) and concentrated under reduced pressure. The residue was purified by flash chromatography (cyclohexane/EtOAc = 1/0 → 0/1), yielding **16** as a colorless solid (152 mg, 0.58 mmol, 92%); mp = 159 °C.

TLC: 0.27 (EtOAc/cyclohexane, 2:8).^{1}H NMR (600 MHz, DMSO-d_6) δ 7.45−7.50 (m, 3H, 3′-H$_{phenyl}$, 4′-H$_{phenyl}$, 5′-H$_{phenyl}$), 7.56−7.62 (m, 2H, 3″-H$_{benzoyl}$, 5″-H$_{benzoyl}$), 7.67−7.72 (m, 1H, 4″-H$_{benzoyl}$), 7.85 (br s, 2H, NH$_2$), 7.92−7.99 (m, 2H, 2′-H$_{phenyl}$, 6′-H$_{phenyl}$), 8.13−8.18 (m, 2H, 2″-H$_{benzoyl}$, 6″-H$_{benzoyl}$). ^{13}C NMR (151 MHz, DMSO-d_6) δ 126.4 (2C, C-2′$_{phenyl}$, C-6′$_{phenyl}$), 128.1 (2C, C-3″$_{benzoyl}$ and C-5″$_{benzoyl}$), 128.7 (2C, C-3′$_{phenyl}$, C-5′$_{phenyl}$), 130.10 (1C, C-1′$_{phenyl}$), 130.11 (1C, C-4′$_{phenyl}$), 130.8 (2C, C-2″$_{benzoyl}$, C-6″$_{benzoyl}$), 132.1 (1C, C-1″$_{benzoyl}$), 133.0 (1C, C-2″$_{benzoyl}$), 159.0 (1C, C-5$_{triazole}$), 159.7 (1C, C-3$_{triazole}$), 167.6 (C═O). IR (neat): $\tilde{\nu}$ [cm^{-1}] = 3421, 3287, 3190, 1690, 1535, 1362, 1296, 737. HRMS (m/z): [M + H]$^+$ calcd for C$_{15}$H$_{12}$N$_4$O$^+$ 265.1084, found 265.1108. HPLC: t_R = 20.1 min, purity 98.5%.

(5-Amino-3-(pyridin-3-ylamino)-1H-1,2,4-triazol-1-yl)(phenyl)-methanone (20a). It was synthesized according to general procedure A from **19a** (89 mg, 0.51 mmol) and benzoyl chloride (71 mg, 0.51 mmol). Stirring at room temperature was continued for 30 min. The crude product was purified by flash column chromatography (DCM/MeOH = 1/0 → 88/12) to give **20a** as a colorless solid (24.1 mg, 0.09 mmol, 17%); mp > 300 °C. TLC: 0.53 (DCM/MeOH, 92:8). ^{1}H NMR (400 MHz, DMSO-d_6) δ 7.23 (m, 1H, 5′-H$_{pyridyl}$), 7.54−7.60 (m, 2H, 3′-H$_{phenyl}$, 5′-H$_{phenyl}$), 7.64−7.69 (m, 1H, 4′-H$_{phenyl}$), 7.86 (s, 2H, NH$_2$), 7.87−7.91 (m, 1H, 4′-H$_{pyridyl}$), 8.05 (s, 1H, 6′-H$_{pyridyl}$), 8.10−8.16 (m, 2H, 2′-H$_{phenyl}$, 6′-H$_{phenyl}$), 8.71 (s, 1H, 2′-H$_{pyridyl}$), 9.53 (s, 1H, NH). ^{13}C NMR (100 MHz, DMSO-d_6) δ 122.8 (1C, C-4′$_{pyridyl}$), 123.4 (1C, C-5′$_{pyridyl}$), 127.9 (2C, C-3′$_{phenyl}$, C-5′$_{phenyl}$), 130.2 (2C, C-2′$_{phenyl}$, C-6′$_{phenyl}$), 132.5 (1C, C-4′$_{phenyl}$), 132.7 (1C, C-1′$_{phenyl}$), 137.6 (1C, C-3′$_{pyridyl}$), 138.8 (1C, C-2′$_{pyridyl}$), 141.0 (1C, C-6′$_{pyridyl}$), 157.5 (1C, C-3′$_{triazole}$, C-5′$_{triazole}$), 158.0 (1C, C-3′$_{triazole}$, C-5′$_{triazole}$), 166.7 (1C, C═O). IR (neat): $\tilde{\nu}$ [cm^{-1}] = 3410, 3121, 2963, 1678, 1612, 1574, 1555, 1431, 1346, 1308, 1177, 1096, 926, 799, 752, 683. HRMS (m/z): [M + H]$^+$ calcd for C$_{14}$H$_{13}$N$_6$O$^+$ 281.1145, found 281.1148. HPLC: t_R = 13.3 min, purity 99.2%.

(5-Amino-3-(phenylamino)-1H-1,2,4-triazol-1-yl)(phenyl)-methanone (20b). It was synthesized according to general procedure A from **19b** (61.5 mg, 0.35 mmol) and benzoyl chloride (49 mg, 0.35 mmol). Stirring at 0 °C was continued for 2 h without further stirring at room temperature. The crude product was purified by flash column chromatography (cyclohexane/EtOAc = 3/1 → 1/1) to give **20b** as a colorless solid (49.6 mg, 0.18 mmol, 51%); mp = 168−169 °C. TLC: 0.37 (DCM/MeOH, 95:5).^{1}H NMR (400 MHz, DMSO-d_6) δ 6.81−6.85 (m, 1H, 4′-H$_{phenyl}$), 7.17−7.24 (m, 2H, 3′-H$_{phenyl}$, 5′-H$_{phenyl}$), 7.48−7.53 (m, 2H, 2′-H$_{phenyl}$, 6′-H$_{phenyl}$), 7.54−7.60 (m, 2H, 3′-H$_{benzoyl}$, 5′-H$_{benzoyl}$), 7.62−7.71 (m, 1H, 4′-H$_{benzoyl}$), 7.80 (s, 2H, NH$_2$), 8.10−8.19 (m, 2H, 2′-H$_{benzoyl}$, 6′-H$_{benzoyl}$), 9.27 (s, 1H, NH). ^{13}C NMR (100 MHz, DMSO-d_6) δ 116.6 (2C, C-2′$_{phenyl}$, C-6′$_{phenyl}$), 120.0 (1C, C-4′$_{phenyl}$), 127.9 (2C, C-3′$_{benzoyl}$, C-5′$_{benzoyl}$), 128.6 (2C, C-3′$_{phenyl}$, C-5′$_{phenyl}$), 130.3 (2C, C-2′$_{benzoyl}$, C-6′$_{benzoyl}$), 132.5 (1C, C-4′$_{benzoyl}$), 132.8 (1C, C-1′$_{benzoyl}$), 141.0 (1C, C-1′$_{phenyl}$), 157.3 (C-3′$_{triazole}$, C-5′$_{triazole}$), 158.2 (C-3′$_{triazole}$, C-5′$_{triazole}$), 166.6 (1C, C═O). IR (neat): $\tilde{\nu}$ [cm^{-1}] = 3379, 1670, 1582, 1555, 1450, 1358, 1200, 1084, 860, 745, 687. HRMS (m/z): [M + H]$^+$ calcd for C$_{15}$H$_{14}$N$_5$O$^+$ 280.1193, found 280.1202. HPLC: t_R = 19.9 min, purity 99.3%.

(5-Amino-3-((4-ethoxyphenyl)amino)-1H-1,2,4-triazol-1-yl)-(phenyl)-methanone (20c). It was synthesized according to general procedure A from **19c** (200 mg, 0.91 mmol) and benzoyl chloride (141 mg, 1.0 mmol). Stirring at room temperature was continued for 18 h. The crude product was purified by flash column chromatography (DCM/EtOAc = 1/0 → 45/55) to give **20c** as a yellowish solid (157 mg, 0.49 mmol, 53%); mp = 163 °C. TLC: 0.30 (DCM/MeOH, 95:5). ^{1}H NMR (400 MHz, DMSO-d_6) δ 1.28 (t, J = 7.0 Hz, 3H, CH$_3$), 3.94 (q, J = 7.0 Hz, 2H, CH$_2$), 6.75−6.83 (m, 2H, 3′-H$_{4-ethoxyphenyl}$, 5′-H$_{4-ethoxyphenyl}$), 7.39−7.44 (m, 2H, 2′-H$_{4-ethoxyphenyl}$, 6′-H$_{4-ethoxyphenyl}$), 7.53−7.60 (m, 2H, 3′-H$_{benzoyl}$, 5′-H$_{benzoyl}$), 7.62−7.69 (m, 1H, 4′-H$_{benzoyl}$), 7.77 (s, 2H, NH$_2$), 8.14−8.19 (m, 2H, 2′-H$_{benzoyl}$, 6′-H$_{benzoyl}$), 9.04 (s, 1H, NH). ^{13}C NMR (100 MHz, DMSO-d_6) δ 14.8 (1C, CH$_3$), 63.1 (1C, CH$_2$), 114.6 (2C, C-3′$_{4-ethoxyphenyl}$, C-5′$_{4-ethoxyphenyl}$), 117.9 (2C, C-2′$_{4-ethoxyphenyl}$, C-6′$_{4-ethoxyphenyl}$), 127.9 (2C, C-3′$_{benzoyl}$, C-5′$_{benzoyl}$), 130.3 (2C, C-2′$_{benzoyl}$, C-6′$_{benzoyl}$), 132.5 (1C, C-4′$_{benzoyl}$), 132.8 (1C, C-1′$_{benzoyl}$), 134.3 (1C, C-1′$_{4-ethoxyphenyl}$), 152.4

(1C, C-4′$_{4\text{-ethoxyphenyl}}$), 157.3 (1C, C-3′$_{triazole}$, C-5′$_{triazole}$), 158.4 (1C, C-3′$_{triazole}$, C-5′$_{triazole}$), 166.4 (1C, C=O). IR (neat): $\tilde{\nu}$ [cm^{-1}] = 3483, 3356, 3256, 2970, 1663, 1562, 1508, 1362, 1231, 1053, 922, 833, 748, 691. HRMS (m/z): [M + H]$^+$ calcd for C$_{17}$H$_{17}$N$_5$O$_2^+$ 324.1455, found 324.1479. HPLC: t_R = 20.5 min, purity 98.9%.

(5-Amino-3-(pyridin-2-yl)-1H-1,2,4-triazol-1-yl)(3,4-dimethyl-phenyl)-methanone (21a). It was synthesized according to general procedure A from **9a** (100 mg, 620 μmol, 1 equiv) and 3,4-dimethylbenzoyl chloride, which was obtained from 3,4-dimethylbenzoic acid (121 mg, 807 μmol, 1.3 equiv) and oxalyl chloride (236 mg, 1.86 mmol, 3 equiv), according to general procedure B. The reaction mixture was gradually heated to room temperature over 18 h. After the washing steps, pure product **21a** was obtained as a colorless solid (109 mg, 372 μmol, 60%); mp = 194−195 °C. TLC: 0.54 (DCM/MeOH = 92:8). ^{1}H NMR (600 MHz, DMSO-d_6) δ 2.32 (s, 3H, 3′-CH$_3$), 2.33 (s, 3H, 4′-CH$_3$), 7.35 (d, J = 8.0 Hz, 1H, 5′-H$_{phenyl}$), 7.46 (ddd, J = 7.5, 4.7, 1.3 Hz, 1H, 5′-H$_{pyridinyl}$), 7.80 (s, 2H, NH$_2$), 7.89 (s, 1H, 2′-H$_{phenyl}$), 7.90−7.93 (m, 1H, 4′-H$_{pyridinyl}$), 7.93−7.95 (m, 1H, 6′-H$_{benzoyl}$), 8.00 (d, J = 8.0 Hz, 1H, 3′-H$_{pyridinyl}$), 8.66 (d, J = 4.7 Hz, 1H, 6′-H$_{pyridinyl}$). ^{13}C NMR (151 MHz, DMSO-d_6) δ 19.4 (1C, 3′-CH$_3$), 19.6 (1C, 4′-CH$_3$), 122.5 (1C, C-3′$_{pyridyl}$), 124.7 (1C, C-5′$_{pyridyl}$), 128.7 (1C, C-6′$_{phenyl}$), 129.1 (1C, C-5′$_{phenyl}$), 129.5 (1C, C-1′$_{phenyl}$), 131.5 (1C, C-2′$_{phenyl}$), 136.2 (1C, C-3′$_{phenyl}$), 137.0 (1C, C-4′$_{pyridyl}$), 142.4 (1C, C-4′$_{phenyl}$), 149.0 (1C, C-2′$_{pyridyl}$), 149.7 (1C, C-6′$_{pyridyl}$), 159.0 (1C, C-5′$_{triazole}$), 159.4 (1C, C-3′$_{triazole}$), 167.9 (1C, C=O). IR (neat): $\tilde{\nu}$ [cm^{-1}] = 3406, 3275, 3194, 3132, 1674, 1636, 1531, 1404, 1362, 1327, 1285, 1173, 1157, 1115, 976, 783, 748, 687. HRMS (m/z): [M + H]$^+$ calcd for C$_{16}$H$_{16}$N$_5$O$^+$ 294.1349, found 294.1368. HPLC: t_R = 17.6 min, purity 98.0%.

(5-Amino-3-(pyridin-2-yl)-1H-1,2,4-triazol-1-yl)(4-methoxyphenyl)-methanone (21b). It was synthesized according to general procedure A from **9a** (100 mg, 620 μmol, 1 equiv) and 4-methoxylbenzoyl chloride (138 mg, 807 μmol, 1.30 equiv). The reaction mixture was gradually heated to room temperature over 18 h. After the washing steps, pure product **21b** was obtained as a colorless solid (131 mg, 445 μmol, 72%); mp = 189−190 °C. TLC: 0.50 (DCM/MeOH = 92:8). ^{1}H NMR (600 MHz, DMSO-d_6) δ 3.89 (s, 3H, CH$_3$), 7.13 (d, J = 8.7 Hz, 2H, 3′-H$_{phenyl}$, 5′-H$_{phenyl}$), 7.47 (ddd, J = 7.6, 4.8, 1.2 Hz, 1H, 5′-H$_{pyridyl}$), 7.79 (s, 2H, NH$_2$), 7.92 (td, J = 7.7, 1.9 Hz, 1H, 4-H$_{pyridyl}$), 8.02 (d, J = 7.8 Hz, 1H, 3′-H$_{pyridyl}$), 8.26 (d, J = 8.9 Hz, 2H, 2′-H$_{phenyl}$, 6′-H$_{phenyl}$), 8.68 (d, J = 4.1 Hz, 1H, 6′-H$_{pyridyl}$). ^{13}C NMR (151 MHz, DMSO-d_6) δ 55.6 (1C, CH$_3$), 113.6 (2C, C-3′$_{phenyl}$, C-5′$_{phenyl}$), 122.5 (1C, C-3′pyridyl), 123.7 (1C, C-1′$_{phenyl}$), 124.7 (1C, C-5′pyridyl), 133.7 (2C, C-2′$_{phenyl}$, C-6′$_{phenyl}$), 137.0 (1C, C-4′pyridyl), 149.0 (1C, C-2′pyridyl), 149.7 (1C, C-6′pyridyl), 159.1 (1C, C-5′triazole), 159.3 (1C, C-3′triazole), 163.2 (1C, C-4′$_{phenyl}$), 166.8 (1C, C=O). IR (neat): $\tilde{\nu}$ [cm^{-1}] = 3433, 3063, 1674, 1636, 1601, 1508, 1358, 1312, 1254, 1177, 1150, 1022, 968, 922, 845, 802, 756, 687, 648. HRMS (m/z): [M + H]$^+$ calcd for C$_{15}$H$_{14}$N$_5$O$_2^+$ 296.1142, found 296.1164. HPLC: t_R = 15.7 min, purity 97.9%.

(5-Amino-3-(pyridin-2-yl)-1H-1,2,4-triazol-1-yl)(4-ethylphenyl)-methanone (21c). It was synthesized according to general procedure A from **9a** (100 mg, 620 μmol, 1 equiv) and 4-ethylbenzoyl chloride, which was obtained from 4-ethylbenzoic acid (121 mg, 807 μmol, 1.3 equiv) and oxalyl chloride (236 mg, 1.86 mmol, 3 equiv), according to general procedure B. Stirring at room temperature was continued for 1 h. After the washing steps, pure product **21c** was obtained as a colorless solid (135 mg, 459 μmol, 74%); mp = 173−174 °C. TLC: 0.35 (DCM/MeOH = 9:1). ^{1}H NMR (600 MHz, DMSO-d_6) δ 1.24 (t, J = 7.6 Hz, 3H, CH$_3$), 2.72 (q, J = 7.6 Hz, 2H, CH$_2$), 7.43 (d, J = 8.1 Hz, 2H, 3′-H$_{phenyl}$, 5′-H$_{phenyl}$), 7.47 (ddd, J = 7.6, 4.7, 1.3 Hz, 1H, 5′-H$_{pyridyl}$), 7.82 (s, 2H, NH$_2$), 7.92 (td, J = 7.7, 1.8 Hz, 1H, 4′-H$_{pyridyl}$), 8.01 (d, J = 7.8 Hz, 1H, 3′-H$_{pyridyl}$), 8.09 (d, J = 8.2 Hz, 2H, 2′-H$_{phenyl}$, 6′-H$_{phenyl}$), 8.66 (d, J = 4.3 Hz, 1H, 6′-H$_{pyridyl}$). ^{13}C NMR (151 MHz, DMSO-d_6) δ 15.2 (1C, CH$_3$), 28.3 (1C, CH$_2$), 122.5 (1C, C-3′$_{pyridyl}$), 124.7 (1C, C-5′$_{pyridyl}$), 127.6 (2C, C-3′$_{phenyl}$, C-5′$_{phenyl}$), 129.4 (1C, C-1′$_{phenyl}$), 131.1 (2C, C-2′$_{phenyl}$, C-6′$_{phenyl}$), 137.0 (1C, C-4′$_{pyridyl}$), 149.0 (1C, C-2′$_{pyridyl}$), 149.6 (1C, C-4′$_{phenyl}$), 149.7 (1C, C-6′$_{pyridyl}$), 159.0 (1C, C-5′$_{triazole}$), 159.5 (1C, C-3′$_{triazole}$), 167.7 (1C, C=O). IR (neat): $\tilde{\nu}$ [cm^{-1}] = 3449, 3075, 2970, 1678, 1632, 1535,

1362, 1323, 1188, 1153, 926, 849, 745, 691. HRMS (m/z): [M + H]$^+$ calcd for C$_{16}$H$_{16}$N$_5$O$^+$ 294.1349, found 294.1369. HPLC: t_R = 17.9 min, purity 96.7%.

(5-Amino-3-(pyridin-2-yl)-1H-1,2,4-triazol-1-yl)(4-(trifluoromethyl)-phenyl)-methanone (21d). It was synthesized according to general procedure A from **9a** (100 mg, 620 μmol, 1 equiv) and 4-trifluoromethylbenzoyl chloride (233 mg, 1.12 mmol, 1.2 equiv). The reaction mixture was gradually heated to room temperature over 18 h. The crude product was purified by flash column chromatography (DCM/MeOH = 1/0 → 88/12) to give **21d** as a yellow solid (78.1 mg, 234 μmol, 25%); mp = 272−273 °C. TLC: 0.54 (DCM/MeOH = 92:8). ^{1}H NMR (400 MHz, DMSO-d_6) δ 7.47 (ddd, J = 7.5, 4.7, 1.3 Hz, 1H, 5′-H$_{pyridyl}$), 7.86−7.95 (m, 3H, NH$_2$, 4′-H$_{pyridyl}$), 7.97 (d, J = 8.2 Hz, 2H, 3′-H$_{phenyl}$, 5′-H$_{phenyl}$), 7.99−8.02 (m, 1H, 3′-H$_{pyridyl}$), 8.27 (d, J = 8.2 Hz, 2H, 2′-H$_{phenyl}$, /6′-H$_{phenyl}$), 8.65 (ddd, J = 4.8, 1.8, 0.9 Hz, 1H, 6′-H$_{pyridyl}$). ^{13}C NMR (151 MHz, DMSO-d_6) δ 122.6 (1C, C-3′$_{pyridyl}$), 123.8 (q, $J_{C,F}$ = 272.7 Hz, 1C, CF$_3$), 124.8 (1C, C-5′$_{pyridyl}$), 125.0 (q, $J_{C,F}$ = 3.8 Hz 2C, C-3$_{phenyl}$′, C-5′$_{phenyl}$), 131.3 (2C, C-2′$_{phenyl}$, C-6′$_{phenyl}$), 132.1 (q, $J_{C,F}$ = 32.0 Hz 1C, C-4$_{phenyl}$′), 136.2 (1C, C-1$_{phenyl}$′), 137.0 (1C, C-4′$_{pyridyl}$), 148.8 (1C, C-2′$_{pyridyl}$), 149.7 (1C, C-6′$_{pyridyl}$), 158.9 (1C, C-5$_{triazole}$), 159.9 (1C, C-3$_{triazole}$), 167.0 (1C, C=O). IR (neat): $\tilde{\nu}$ [cm^{-1}] = 3468, 3075, 1690, 1636, 1535, 1389, 1354, 1319, 1161, 1115, 1065, 961, 922, 849, 764, 741, 687. HRMS (m/z): [M + H]$^+$ calcd for C$_{15}$H$_{11}$F$_3$N$_5$O$^+$ 334.0941, found 334.0934. HPLC: t_R = 18.1 min, purity 98.3%.

(5-Amino-3-(pyridin-2-yl)-1H-1,2,4-triazol-1-yl)(2-nitrophenyl)-methanone (21e). It was synthesized according to general procedure A from **9a** (100 mg, 620 μmol, 1 equiv) and 2-nitrobenzoyl chloride (150 mg, 807 μmol, 1.3 equiv). Stirring at room temperature was continued for 2.5 h. The crude product was purified by recrystallization from an EtOAc/DMSO mixture to obtain **21e** as a yellow solid (83.4 mg, 269 μmol, 43%); mp = 229−230 °C. TLC: 0.55 (H$_2$O/ACN = 4:6, RP). ^{1}H NMR (600 MHz, DMSO-d_6) δ 7.43 (t, J = 6.1 Hz, 1H, 5′-H$_{pyridyl}$), 7.82−7.85 (m, 1H, 3′-H$_{pyridyl}$), 7.86−7.89 (m, 1H, 4′-H$_{pyridyl}$), 7.89−7.92 (m, 1H, 4′-H$_{phenyl}$), 7.92−7.98 (m, 3H, NH$_2$, 6′-H$_{phenyl}$), 7.99−8.03 (m, 1H, 3′-H$_{phenyl}$), 8.32 (d, J = 8.3 Hz, 1H, 5′-H$_{phenyl}$), 8.57 (d, J = 4.8 Hz, 1H, 6′-H$_{pyridyl}$). ^{13}C NMR (151 MHz, DMSO-d_6) δ 122.5 (1C, C-2′$_{phenyl}$), 124.2 (1C, C-5′$_{phenyl}$), 124.9 (1C, C-5′$_{pyridyl}$), 129.4 (1C, C-1′$_{phenyl}$), 129.8 (1C, C-6′$_{phenyl}$), 132.3 (1C, C-4′$_{phenyl}$), 135.1 (1C, C-3′$_{phenyl}$), 137.0 (1C, C-4′$_{pyridyl}$), 146.0 (1C, C-2′$_{phenyl}$), 148.4 (1C, C-2′$_{pyridyl}$), 149.7 (1C, C-6′$_{pyridyl}$), 157.9 (1C, C-5′$_{triazole}$), 160.3 (1C, C-3′$_{triazole}$), 166.2 (1C, C=O). IR (neat): $\tilde{\nu}$ [cm^{-1}] = 3456, 3001, 1697, 1647, 1524, 1350, 1165, 968, 930, 791, 941, 691, 656. HRMS (m/z): [M + H]$^+$ calcd for C$_{14}$H$_{11}$N$_6$O$_3^+$ 311.0877, found 311.0887. HPLC: t_R = 15.0 min, purity 99.2%.

(5-Amino-3-(pyridin-2-yl)-1H-1,2,4-triazol-1-yl)(4-nitrophenyl)-methanone (21f). It was synthesized according to general procedure A from **9a** (100 mg, 620 μmol, 1 equiv) and 4-nitrobenzoyl chloride (230 mg, 1.24 mmol, 2 equiv). The reaction mixture was gradually heated to room temperature over 18 h. The crude product was purified by recrystallization from an EtOAc/DMSO mixture to obtain **21f** as a yellow solid (87.8 mg, 283 μmol, 46%); mp = 299−300 °C. TLC: 0.43 (H$_2$O/ACN = 4:6). ^{1}H NMR (600 MHz, DMSO-d_6) δ 7.47 (ddd, J = 7.6, 4.7, 1.3 Hz, 1H, 5′-H$_{pyridyl}$), 7.89−7.97 (m, 3H, NH$_2$, 4′-H$_{pyridyl}$), 8.00 (d, J = 7.8 Hz, 1H, 3′-H$_{pyridyl}$), 8.29 (d, J = 8.9 Hz, 2H, 2′-H$_{phenyl}$, 6′-H$_{phenyl}$), 8.40 (d, J = 8.9 Hz, 2H, 3′-H$_{phenyl}$, 5′-H$_{phenyl}$), 8.65 (d, J = 4.3 Hz, 1H, 6′-H$_{pyridyl}$). ^{13}C NMR (151 MHz, DMSO-d_6) δ 122.6 (1C, C-3′$_{pyridyl}$), 123.1 (2C, C-3′$_{phenyl}$, C-5′$_{phenyl}$), 124.9 (1C, C-5′$_{pyridyl}$), 131.8 (2C, C-2′$_{phenyl}$, C-6′$_{phenyl}$), 137.0 (1C, C-4′$_{pyridyl}$), 138.0 (1C, C-1′$_{phenyl}$), 148.7 (1C, C-2′$_{pyridyl}$), 149.5 (1C, C-4′$_{phenyl}$), 149.7 (1C, C-6′$_{pyridyl}$), 158.8 (1C, C-5′$_{triazole}$), 160.0 (1C, C-3′$_{triazole}$), 166.6 (1C, C=O). IR (neat): $\tilde{\nu}$ [cm^{-1}] = 3441, 3055, 1694, 1639, 1520, 1400, 1373, 1339, 1288, 1246, 1157, 968, 853, 741, 710, 691. HRMS (m/z): [M + H]$^+$ calcd for C$_{14}$H$_{11}$N$_6$O$_3^+$ 311.0877, found 311.0891. HPLC: t_R = 15.7 min, purity 96.3%.

(5-Amino-3-(pyridin-2-yl)-1H-1,2,4-triazol-1-yl)(4-fluorophenyl)-methanone (21g). It was synthesized according to general procedure A from **9a** (300 mg, 1.86 mmol, 1 equiv) and 4-fluorobenzoyl chloride (384 mg, 2.42 mmol, 1.3 equiv). Stirring at room temperature was

continued for 3 h. After the washing steps, pure product **21g** was obtained as a colorless solid (366 mg, 1.29 mmol, 69%); mp = 202–204 °C. TLC: 0.78 (EtOAc/MeOH = 9:1). ^{1}H NMR (600 MHz, DMSO-d_6) δ 7.41–7.46 (m, 2H, 3′-H$_{phenyl}$, 5′-H$_{phenyl}$), 7.47 (ddd, J = 7.6, 4.8, 1.2 Hz, 1H, 5′-H$_{pyridyl}$), 7.86 (s, 2H, NH$_2$), 7.92 (td, J = 7.7, 1.8 Hz, 1H, 4-H$_{pyridyl}$), 8.02 (dt, J = 7.9, 1.1 Hz, 1H, 3′-H$_{pyridyl}$), 8.24–8.30 (m, 2H, 2′-H$_{phenyl}$, 6′-H$_{phenyl}$), 8.67 (ddd, J = 4.6, 1.9, 0.9 Hz, 1H, 6′-H$_{pyridyl}$). ^{13}C NMR (151 MHz, DMSO-d_6) δ 115.3 (d, $J_{C,F}$ = 22.0 Hz, 2C, C-3′$_{phenyl}$, C-5′$_{phenyl}$), 122.5 (1C, C-3′$_{pyridyl}$), 124.8 (1C, C-5′$_{pyridyl}$), 128.5 (d, $J_{C,F}$ = 2.9 Hz, 1C, C-1′$_{phenyl}$), 134.0 (d, $J_{C,F}$ = 9.3 Hz, 2C, C-2′$_{phenyl}$, C-6′$_{phenyl}$), 137.0 (1C, C-4′$_{pyridyl}$), 148.9 (1C, C-2′$_{pyridyl}$), 149.7 (1C, C-6′$_{pyridyl}$), 159.0 (1C, C-5′$_{triazole}$), 159.6 (1C, C-3′$_{triazole}$), 164.8 (d, $J_{C,F}$ = 252.4 Hz, 1C, C-4′$_{phenyl}$), 166.6 (1C, C=O). IR (neat): $\tilde{\nu}$ [cm^{-1}] = 3460, 3075, 2978, 1690, 1624, 1597, 1535, 1501, 1358, 1335, 1231, 1196, 1158, 1088, 972, 930, 845, 787, 741, 679, 610. HRMS (m/z): [M + H]$^+$ calcd for C$_{14}$H$_{10}$FN$_5$O$^+$ 284.0942, found 284.0919. HPLC: t_R = 19.3 min, purity 99.0%.

(5-Amino-3-(pyridin-2-yl)-1H-1,2,4-triazol-1-yl)(4-bromophenyl)-methanone (21h). It was synthesized according to general procedure A from **9a** (100 mg, 620 μmol, 1 equiv) and 4-bromobenzoyl chloride (136 mg, 620 μmol, 1.00 equiv). Stirring at room temperature was continued for 1 h. After the washing steps, pure product **21h** was obtained as a colorless solid (138 mg, 400 μmol, 64%); mp = 205 °C. TLC: 0.52 (DCM/MeOH = 92:8). ^{1}H NMR (600 MHz, DMSO-d_6) δ 7.47 (ddd, J = 7.6, 4.7, 1.3 Hz, 1H, 5′-H$_{pyridyl}$), 7.82 (d, J = 8.5 Hz, 2H, 3′-H$_{phenyl}$, 5′-H$_{phenyl}$), 7.87 (s, 2H, NH$_2$), 7.92 (td, J = 7.7, 1.8 Hz, 1H, 4′-H$_{pyridyl}$), 8.00 (d, J = 7.8 Hz, 1H, 3′-H$_{pyridyl}$), 8.07 (d, J = 8.5 Hz, 2H, 2′-H$_{phenyl}$, 6′-H$_{phenyl}$), 8.66 (d, J = 4.3 Hz, 1H, 6′-H$_{pyridyl}$). ^{13}C NMR (151 MHz, DMSO-d_6) δ 122.6 (1C, C-3′$_{pyridyl}$), 124.8 (1C, C-5′$_{pyridyl}$), 127.0 (1C, C-4′$_{phenyl}$), 131.2 (2C, C-3′$_{phenyl}$, C-5′$_{phenyl}$), 131.2 (1C, C-1′$_{phenyl}$), 132.8 (2C, C-2′$_{phenyl}$, C-6′$_{phenyl}$), 137.0 (1C, C-4′$_{pyridyl}$), 148.8 (1C, C-2′$_{pyridyl}$), 149.7 (1C, C-6′$_{pyridyl}$), 158.9 (1C, C-5′$_{triazole}$), 159.7 (1C, C-3′$_{triazole}$), 167.0 (1C, C=O). IR (neat): $\tilde{\nu}$ [cm^{-1}] = 3453, 3098, 1682, 1636, 1582, 1535, 1396, 1366, 1339, 1288, 1157, 1072, 976, 918, 841, 791, 745, 691, 671. HRMS (m/z): [M + H]$^+$ calcd for C$_{14}$H$_{11}$Br^{79}N$_5$O$^+$ 344.0141, found 344.0165, calcd for C$_{14}$H$_{11}$Br^{81}N$_5$O$^+$ 346.0121, found 346.0149. HPLC: t_R = 17.3 min, purity 95.5%.

(5-Amino-3-(pyridin-2-yl)-1H-1,2,4-triazol-1-yl)(naphthalen-1-yl)-methanone (21i). It was synthesized according to general procedure A from **9a** (100 mg, 620 μmol, 1 equiv) and 1-napthoyl chloride (244 mg, 1.24 mmol, 2 equiv). The reaction mixture was gradually heated to room temperature over 18 h. After the washing steps, pure product **21i** was obtained as a colorless solid (151 mg, 479 μmol, 77%); mp = 227–228 °C. TLC: 0.59 (DCM/MeOH = 92:8). ^{1}H NMR (600 MHz, DMSO-d_6) δ 7.40 (ddd, J = 7.3, 4.7, 1.4 Hz, 1H, 5′-H$_{pyridyl}$), 7.58–7.64 (m, 2H, 7′-H$_{naphthoyl}$, 8′-H$_{naphthoyl}$), 7.67 (dd, J = 8.3, 7.1 Hz, 1H, 3′-H$_{naphthoyl}$), 7.85 (td, J = 7.6, 1.8 Hz, 1H, 4′-H$_{pyridyl}$), 7.87–7.89 (m, 1H, 3′-H$_{pyridyl}$), 7.89–7.90 (m, 1H, 9′-H$_{naphthoyl}$), 7.90–7.92 (m, 1H, 2′-H$_{naphthoyl}$), 7.98 (s, 2H, NH$_2$), 8.06–8.10 (m, 1H, 6′-H$_{naphthoyl}$), 8.19 (dt, J = 8.2, 1.1 Hz, 1H, 4′-H$_{naphthoyl}$), 8.52 (ddd, J = 4.7, 1.7, 1.0 Hz, 1H, 6′-H$_{pyridyl}$). ^{13}C NMR (151 MHz, DMSO-d_6) δ 122.5 (1C, C-3′$_{pyridyl}$), 124.6 (1C, C-9′$_{naphthoyl}$), 124.7 (1C, C-5′$_{pyridyl}$), 124.8 (1C, C-3′$_{naphthoyl}$), 126.6 (1C, C-7′$_{naphthoyl}$), 127.5 (1C, C-8′$_{naphthoyl}$), 127.6 (1C, C-2′$_{naphthoyl}$), 128.5 (1C, C-6′$_{naphthoyl}$), 129.4 (1C, C-10′$_{naphthoyl}$), 130.8 (1C, C-1′$_{naphthoyl}$), 131.3 (1C, C-4′$_{naphthoyl}$), 132.9 (1C, C-5′$_{naphthoyl}$), 137.0 (1C, C-4′$_{pyridyl}$), 148.8 (1C, H-2′$_{pyridyl}$), 149.6 (1C, C-6′$_{pyridyl}$), 158.6 (1C, C-5′$_{triazole}$), 159.7 (1C, C-3′$_{triazole}$), 169.2 (1C, C=O). IR (neat): $\tilde{\nu}$ [cm^{-1}] = 3460, 2978, 1694, 1632, 1354, 1308, 1153, 1053, 910, 779, 748, 694. HRMS (m/z): [M + H]$^+$ calcd for C$_{18}$H$_{14}$N$_5$O$^+$ 316.1193, found 316.1187. HPLC: t_R = 16.9 min, purity 98.4%.

(5-Amino-3-(pyridin-2-yl)-1H-1,2,4-triazol-1-yl)(cyclohexyl)-methanone (21j). It was synthesized according to general procedure A from **9c** (301 mg, 1.87 mmol, 1 equiv) and cyclohexanecarbonyl chloride (356 mg, 2.43 mmol, 1.3 equiv). Stirring at room temperature was continued for 4.5 h. After the washing steps, pure product **11c** was obtained as a colorless solid (418 mg, 1.54 mmol, 83%); mp = 204–206 °C. TLC: 0.76 (EtOAc/MeOH, 9:1). ^{1}H NMR (600 MHz, DMSO-d_6) δ 1.23 (qt, J = 12.4, 3.6 Hz, 1H,

CH(CH$_2$CH$_2$)$_2$CH$_2$), 1.31–1.50 (m, 4H, CH(CH$_2$CH$_2$)$_2$CH$_2$), 1.69 (dtd, J = 12.7, 3.4, 1.6 Hz, 1H, CH(CH$_2$CH$_2$)$_2$CH$_2$), 1.78 (dt, J = 13.1, 3.4 Hz, 2H, CH(CH$_2$CH$_2$)$_2$CH$_2$), 1.94–2.02 (m, 2H, CH(CH$_2$CH$_2$)$_2$CH$_2$), 3.42 (tt, J = 11.3, 3.4 Hz, 1H, CH(CH$_2$CH$_2$)$_2$CH$_2$), 7.48 (ddd, J = 7.5, 4.7, 1.2 Hz, 1H, 5′-H$_{pyridyl}$), 7.66 (br s, 2H, NH$_2$), 7.85 (td, J = 7.7, 1.8 Hz, 1H, 4′-H$_{pyridyl}$), 8.00 (dt, J = 7.9, 1.1 Hz, 1H, 3′-H$_{pyridyl}$), 8.68 (ddd, J = 4.7, 1.8, 0.9 Hz, 1H, 6′-H$_{pyridyl}$). ^{13}C NMR (151 MHz, DMSO-d_6) δ 24.9 (2C, CH(CH$_2$CH$_2$)$_2$CH$_2$), 25.4 (1C, CH(CH$_2$CH$_2$)$_2$CH$_2$), 28.2 (2C, CH(CH$_2$CH$_2$)$_2$CH$_2$), 42.0 (1C, CH(CH$_2$CH$_2$)$_2$CH$_2$), 122.5 (1C, C-3′$_{pyridyl}$), 124.7 (1C, C-5′$_{pyridyl}$), 137.0 (1C, C-4′$_{pyridyl}$), 149.0 (1C, C-2′$_{pyridyl}$), 149.7 (1C, C-6′$_{pyridyl}$), 157.7 (1C, C-5$_{triazole}$), 159.2 (1C, C-3$_{triazole}$), 176.7 (C=O). IR (neat): $\tilde{\nu}$ [cm^{-1}] = 3441, 3256, 3198, 3125, 2936, 2855, 1717, 1620, 1528, 1485, 1404, 1381, 1358, 1273, 1173, 1150, 1080, 976, 806, 745, 683. HRMS (m/z): [M + H]$^+$ calcd for C$_{14}$H$_{17}$N$_5$O$^+$ 272.1506, found 272.1467. HPLC: t_R = 15.80 min, purity 99.5%.

(5-Amino-3-(pyridin-2-yl)-1H-1,2,4-triazol-1-yl)(m-tolyl)-methanone (21k). It was synthesized according to general procedure C from **9a** (100 mg, 621 μmol, 1 equiv) and 3-methylbenzoic acid (84.5 mg, 621 μmol, 1 equiv), with EDCI (238 mg, 1.24 mmol, 2 equiv) and DMAP (152 mg, 1.24 mmol, 2 equiv) in DMF (4 mL). Stirring at 0 °C was continued for 2 h, followed by 2 h at room temperature. After the washing steps, pure product **21k** was obtained as a colorless solid (112 mg, 402 μmol, 65%); mp = 172 °C. TLC: 0.43 (DCM/MeOH = 9:1). ^{1}H NMR (600 MHz, DMSO-d_6) δ 2.41 (s, 3H, CH$_3$), 7.45–7.49 (m, 2H, 5′-H$_{phenyl}$, 5′-H$_{pyridyl}$), 7.51 (d, J = 7.6 Hz, 1H, 4′-H$_{phenyl}$), 7.83 (s, 2H, NH$_2$), 7.87 (s, 1H, 2′-H$_{phenyl}$), 7.91 (td, J = 7.7, 1.8 Hz, 1H, 4′-H$_{pyridyl}$), 7.94 (d, J = 7.5 Hz, 1H, 6′-H$_{phenyl}$), 7.99 (d, J = 7.7 Hz, 1H, 3′-H$_{pyridyl}$), 8.66 (d, J = 4.5 Hz, 1H, 6′-H$_{pyridyl}$). ^{13}C NMR (151 MHz, DMSO-d_6) δ 20.9 (1C, CH$_3$), 122.5 (1C, C-3′$_{pyridyl}$), 124.7 (1C, C-5′$_{pyridyl}$), 128.0 (2C, C-5′$_{phenyl}$, C-6′$_{phenyl}$), 130.8 (1C, C-2′$_{phenyl}$), 132.1 (1C, C-1′$_{phenyl}$), 133.6 (1C, C-4′$_{phenyl}$), 137.0 (1C, C-4′$_{pyridyl}$), 137.5 (1C, C-3′$_{phenyl}$), 149.0 (1C, C-2′$_{pyridyl}$), 149.7 (1C, C-6′$_{pyridyl}$), 158.9 (1C, C-5′$_{triazole}$), 159.5 (1C, C-3′$_{triazole}$), 168.1 (1C, C=O). IR (neat): $\tilde{\nu}$ [cm^{-1}] = 3460, 3063, 1856, 1636, 1537, 1464, 1389, 1362, 1325, 1288, 1179, 972. HRMS (m/z): [M + H]$^+$ calcd for C$_{15}$H$_{14}$N$_5$O$^+$ 280.1193, found 280.1206. HPLC: t_R = 16.3 min, purity 98.9%.

(5-Amino-3-(pyridin-2-yl)-1H-1,2,4-triazol-1-yl)(pyridin-3-yl)-methanone (21l). It was synthesized according to general procedure C from **9a** (100 mg, 621 μmol, 1 equiv) and nicotinic acid (76.4 mg, 621 μmol, 1 equiv), with EDCI (238 mg, 1.24 mmol, 2 equiv) and DMAP (152 mg, 1.24 mmol, 2 equiv) in DMF (4 mL). Stirring at 0 °C was continued for 2 h, followed by 4 h at room temperature. After the washing steps, pure product **21l** was obtained as a colorless solid (42.3 mg, 159 μmol, 26%); mp = 193 °C. TLC: 0.64 (DCM/MeOH = 85:15). ^{1}H NMR (600 MHz, DMSO-d_6) δ 7.48 (dd, J = 7.4, 4.7 Hz, 1H, 5′-H$_{pyridyl}$), 7.64 (dd, J = 7.9, 4.8 Hz, 1H, 5′-H$_{nicotinoyl}$), 7.87–7.96 (m, 3H, NH$_2$, 4′-H$_{pyridyl}$), 8.01 (d, J = 7.8 Hz, 1H, 3′-H$_{pyridyl}$), 8.48 (dt, J = 8.1, 2.0 Hz, 1H, 4′-H$_{nicotinoyl}$), 8.67 (d, J = 4.0 Hz, 1H, 6′-H$_{pyridyl}$), 8.83 (dd, J = 4.9, 1.7 Hz, 1H, 6′-H$_{nicotinoyl}$), 9.25 (d, J = 2.2 Hz, 1H, 2′-H$_{nicotinoyl}$). ^{13}C NMR (151 MHz, DMSO-d_6) δ 122.6 (1C, C-3′$_{pyridyl}$), 123.2 (1C, C-5′$_{nicotinoyl}$), 124.8 (1C, C-5′$_{pyridyl}$), 128.5 (1C, C-3′$_{nicotinoyl}$), 137.1 (1C, C-4′$_{pyridyl}$), 138.4 (1C, C-4′$_{nicotinoyl}$), 148.8 (1C, C-2′$_{pyridyl}$), 149.8 (1C, C-6′$_{pyridyl}$), 151.0 (1C, C-2′$_{nicotinoyl}$), 152.9 (1C, C-6′$_{nicotinoyl}$), 158.8 (1C, C-5′$_{triazole}$), 159.9 (1C, C-3′$_{triazole}$), 166.5 (1C, C=O). IR (neat): $\tilde{\nu}$ [cm^{-1}] = 3443, 3107, 1688, 1632, 1589, 1530, 1464, 1366, 1329, 1290, 1248, 1155, 1094, 970, 942, 912. HRMS (m/z): [M + H]$^+$ calcd for C$_{13}$H$_{11}$N$_6$O$^+$ 267.0989, found 267.0994. Unstable under HPLC conditions, qNMR: purity 94%.

(5-Amino-3-(pyridin-2-yl)-1H-1,2,4-triazol-1-yl)(naphthalen-2-yl)-methanone (21m). It was synthesized according to general procedure C from **9a** (80 mg, 496 μmol, 1 equiv) and 2-naphthoic acid (85.5 mg, 496 μmol, 1 equiv), with EDCI (190 mg, 993 μmol, 2 equiv) and DMAP (121 mg, 993 μmol, 2 equiv) in DMF (3 mL). Stirring at 0 °C was continued for 1 h, followed by 2 h at room temperature. The crude product was purified by flash column chromatography (DCM/ACN = 1/0 → 0/1) to give **21m** as a colorless solid (58.3 mg, 271 μmol, 55%); mp = 200–201 °C. TLC:

0.41 (DCM/MeOH = 9:1). ^{1}H NMR (600 MHz, DMSO-d_6) δ 7.47 (ddd, J = 7.5, 4.7, 1.2 Hz, 1H, 5′-H$_{pyridyl}$), 7.65 (ddd, J = 8.1, 6.8, 1.3 Hz, 1H, 7′-H$_{naphthoyl}$), 7.72 (ddd, J = 8.2, 6.8, 1.3 Hz, 1H, 6′-H$_{naphthoyl}$), 7.89 (br s, 2H, NH$_2$), 7.92 (td, J = 7.7, 1.8 Hz, 1H, 4′-H$_{pyridyl}$), 8.02 (d, J = 7.9 Hz, 1H, 3′-H$_{pyridyl}$), 8.05 (d, J = 8.3 Hz, 1H, 5′-H$_{naphthoyl}$), 8.09 (d, J = 8.7 Hz, 1H, 4′-H$_{naphthoyl}$), 8.12−8.15 (m, 2H, 3′-H$_{naphthoyl}$, 8′-H$_{naphthoyl}$), 8.64−8.66 (m, 1H, 6′-H$_{pyridyl}$), 8.79 (s, 1H, 1′-H$_{naphthoyl}$). ^{13}C NMR (151 MHz, DMSO-d_6) δ 122.5 (1C, C-3′$_{pyridyl}$), 124.7 (1C, C-5$_{pyridyl}$), 126.3 (1C, C-3′$_{naphthoyl}$), 127.0 (1C, C-7′$_{naphthoyl}$), 127.5 (1C, C-4′$_{naphthoyl}$), 127.7 (1C, C-5′$_{naphthoyl}$), 128.8 (1C, C-6′$_{naphthoyl}$), 129.5 (2C, C-2′$_{naphthoyl}$, C-8$_{naphthoyl}$), 131.6 (1C, C-8a′$_{naphthoyl}$), 132.2 (1C, C-1′$_{naphthoyl}$), 134.7 (1C, C-4a′$_{naphthoyl}$), 137.0 (1C, C-4′$_{pyridyl}$), 149.0 (1C, C-2′$_{pyridyl}$), 149.7 (1C, C-6′$_{pyridyl}$), 159.0 (1C, C-5′$_{triazole}$), 159.7 (1C, C-3′$_{triazole}$), 168.0 (1C, C=O). IR (neat): $\tilde{\nu}$ [cm^{-1}] = 3451, 3051, 1678, 1634, 1531, 1462, 1387, 1356, 1317, 1271, 1248, 1209, 1179, 1150, 1115, 1092, 1082, 1047, 986, 932, 899, 864, 818. HRMS (m/z): [M + H]$^+$ calcd for C$_{18}$H$_{14}$N$_5$O$^+$ 316.1193, found 316.1188. HPLC: t_R = 18.1 min, purity 99.5%.

(5-Amino-3-(pyridin-2-yl)-1H-1,2,4-triazol-1-yl)(furan-2-yl)-methanone (21n). It was synthesized according to general procedure C from **9a** (80 mg, 496 μmol, 1 equiv) and 2-furoic acid (55.0 mg, 496 μmol, 1 equiv), with EDCI (190 mg, 993 μmol, 2 equiv) and DMAP (121 mg, 993 μmol, 2 equiv) in DMF (3 mL). Stirring at 0 °C was continued for 1 h, followed by 2 h at room temperature. After the washing steps, pure product **21n** was obtained as a colorless solid (98.8 mg, 387 μmol, 78%); mp = 213 °C. TLC: 0.44 (DCM/MeOH = 92:8). ^{1}H NMR (600 MHz, DMSO-d_6) δ 6.88 (dd, J = 3.6, 1.7 Hz, 1H, 4′-H$_{furanoyl}$), 7.50 (ddd, J = 7.6, 4.7, 1.3 Hz, 1H, 5′-H$_{pyridyl}$), 7.84 (br s, 2H, NH$_2$), 7.95 (td, J = 7.7, 1.8 Hz, 1H, 4′-H$_{pyridyl}$), 8.10 (dt, J = 7.9, 1.1 Hz, 1H, 3′-H$_{pyridyl}$), 8.21−8.22 (m, 2H, 3′-H$_{furanoyl}$, 5′-H$_{furanoyl}$), 8.72 (ddd, J = 4.6, 1.7, 0.9 Hz, 1H, 6′-H$_{pyridyl}$). ^{13}C NMR (151 MHz, DMSO-d_6) δ 113.1 (1C, C-4′$_{furanoyl}$), 122.6 (1C, C-3′$_{pyridyl}$), 124.9 (1C, C-5′$_{pyridyl}$), 125.0 (1C, C-5′$_{furanoyl}$), 137.1 (1C, C-4′$_{pyridyl}$), 143.9 (1C, C-2′$_{furanoyl}$), 148.8 (1C, C-2′$_{pyridyl}$), 149.7 (1C, C-3′$_{furanoyl}$), 149.8 (1C, C-6′$_{pyridyl}$), 155.9 (1C, C=O), 158.9 (1C, C-5′$_{triazole}$), 160.1 (1C, C-3′$_{triazole}$). IR (neat): $\tilde{\nu}$ [cm^{-1}] = 3441, 3279, 3186, 3117, 3088, 1670, 1638, 1562, 1533, 1466, 1404, 1391, 1373, 1339, 1288, 1175, 1153, 1078, 1026, 970, 959, 878. HRMS (m/z): [M + H]$^+$ calcd for C$_{12}$H$_{10}$N$_5$O$_2$$^+$ 256.0829, found 256.0840. t_R = 13.0 min, purity 97.9%.

(5-Amino-3-(pyridin-2-yl)-1H-1,2,4-triazol-1-yl)-(tetrahydropyran-4-yl)methanone (21o). It was synthesized according to general procedure C from **9a** (100 mg, 621 μmol, 1 equiv) and tetrahydro-2H-pyran-4-carboxylic acid (80.8 mg, 621 μmol, 1 equiv), with EDCI (238 mg, 1.24 mmol, 2 equiv) and DMAP (152 mg, 1.24 mmol, 2 equiv) in DMF (4 mL). The reaction mixture was gradually heated from 0 °C to room temperature over 18 h. After the washing steps, pure product **21o** was obtained as a colorless solid (131 mg, 480 μmol, 77%); mp = 215 °C. TLC: 0.53 (DCM/MeOH = 92:8). ^{1}H NMR (600 MHz, DMSO-d_6) δ 1.70 (dtd, J = 13.3, 11.7, 4.4 Hz, 2H, 3′-H$_{tetrahydropyranyl}$, 5′-H$_{tetrahydropyranyl}$), 1.90 (ddd, J = 12.8, 4.1, 2.0 Hz, 2H, 3′-H$_{tetrahydropyranyl}$, 5′-H$_{tetrahydropyranyl}$), 3.47 (td, J = 11.7, 2.2 Hz, 2H, 2′-H$_{tetrahydropyranyl}$, 6′-H$_{tetrahydropyranyl}$), 3.69 (tt, J = 11.5, 3.9 Hz, 1H, 4′-H$_{tetrahydropyranyl}$), 3.92 (ddd, J = 11.5, 4.4, 2.1 Hz, 2H, 2′-H$_{tetrahydropyranyl}$, 6′-H$_{tetrahydropyranyl}$), 7.48 (ddd, J = 7.5, 4.7, 1.2 Hz, 1H, 5′-H$_{pyridyl}$), 7.69 (br s, 2H, NH$_2$), 7.92 (td, J = 7.7, 1.8 Hz, 1H, 4′-H$_{pyridyl}$), 8.01 (dt, J = 7.9, 1.1 Hz, 1H, 3′-H$_{pyridyl}$), 8.68 (ddd, J = 4.7, 1.8, 0.9 Hz, 1H, 6′-H$_{pyridyl}$). ^{13}C NMR (151 MHz, DMSO-d_6) δ 27.9 (2C, C-3′$_{tetrahydropyranyl}$, C-5′$_{tetrahydropyranyl}$), 39.5 (1C, C-4′$_{tetrahydropyranyl}$), 66.0 (2C, C-2′$_{tetrahydropyranyl}$, 6′-C$_{tetrahydropyranyl}$), 122.5 (1C, C-3′$_{pyridyl}$), 124.7 (1C, C-5′$_{pyridyl}$), 137.0 (1C, C-4′$_{pyridyl}$), 148.9 (1C, C-2′$_{pyridyl}$), 149.7 (1C, C-6′$_{pyridyl}$), 157.7 (1C, C-5′$_{triazole}$), 159.4 (1C, C-3′$_{triazole}$), 175.3 (1C, C=O). IR (neat): $\tilde{\nu}$ [cm^{-1}] = 3456, 3096, 2965, 2941, 2855, 1717, 1622, 1530, 1483, 1429, 1981, 1356, 1335, 1323, 1304, 1281, 1238, 1169, 1152, 1132, 1115, 1082, 1049, 1011, 982, 970, 912, 872, 829, 820, 806. HRMS (m/z): [M + H]$^+$ calcd for C$_{13}$H$_{16}$N$_5$O$^+$ 274.1299, found 274.1306. HPLC: t_R = 12.0 min, purity 99.1%.

N-(4-(5-Amino-3-(pyridin-2-yl)-1H-1,2,4-triazole-1-carbonyl)-phenyl)-2,2,2-trifluoroacetamide (21p). It was synthesized according to general procedure C from **9a** (100 mg, 621 μmol, 1 equiv) and 4-(2,2,2-trifluoroacetamido)benzoic acid (145 mg, 621 μmol, 1 equiv), with EDCI (238 mg, 1.24 mmol, 2 equiv) and DMAP (152 mg, 1.24 mmol, 2 equiv) in DMF (4 mL). Stirring at 0 °C was continued for 2 h, followed by 3 h at room temperature. After the washing steps, pure product **21p** was obtained as a yellow solid (164 mg, 436 μmol, 70%); mp = 230 °C. TLC: 0.65 (DCM/MeOH = 85:15). ^{1}H NMR (600 MHz, DMSO-d_6) δ 7.48 (ddd, J = 7.5, 4.8, 1.3 Hz, 1H, 5′-H$_{pyridyl}$), 7.84 (s, 2H, NH$_2$), 7.89 (dt, J = 8.8, 1.9 Hz, 2H, 3′-H$_{phenyl}$, 5′-H$_{phenyl}$), 7.92 (td, J = 7.7, 1.8 Hz, 1H, 4′-H$_{pyridyl}$), 8.02 (dt, J = 7.9, 1.2 Hz, 1H, 3′-H$_{pyridyl}$), 8.24 (dt, J = 8.9; 1.8 Hz, 2H, 2′-H$_{phenyl}$, 6′-H$_{phenyl}$), 8.67 (ddd, J = 4.7, 1.7, 0.9 Hz, 1H, 6′-H$_{pyridyl}$), 11.62 (s, 1H, NH). ^{13}C NMR (151 MHz, DMSO-d_6) δ 115.6 (q, J = 289 Hz, 1C, CF$_3$), 120.0 (2C, C-3′$_{phenyl}$, C-5′$_{phenyl}$), 122.6 (1C, C-3′$_{pyridyl}$), 124.8 (1C, C-5′$_{pyridyl}$), 128.5 (1C, C-1′$_{phenyl}$), 132.2 (2C, C-2′$_{phenyl}$, C-6′$_{phenyl}$), 137.0 (1C, C-4′$_{pyridyl}$), 140.6 (1C, C-4′$_{phenyl}$), 148.9 (1C, C-2′$_{pyridyl}$), 149.7 (1C, C-6′$_{pyridyl}$), 154.9 (q, J = 37.2 Hz, 1C, CF$_3$C=O), 159.0 (1C, C-5′$_{triazole}$); 159.6 (1C, C-3′$_{triazole}$), 166.9 (1C, PhC=O). IR (neat): $\tilde{\nu}$ [cm^{-1}] = 3464, 3308, 3098, 1711, 1686, 1605, 1539, 1452, 1416, 1395, 1360, 1337, 1287, 1250, 1204, 1186, 1153, 1123, 995, 972, 922, 901, 851. HRMS (m/z): [M + H]$^+$ calcd for C$_{16}$H$_{12}$F$_3$N$_6$O$_2$$^+$ 377.0968, found 377.0965. HPLC: t_R = 16.7 min, purity 99.4%.

N-(4-(5-Amino-3-(pyridin-2-yl)-1H-1,2,4-triazole-1-carbonyl)-phenyl)benz-amide (21q). It was synthesized according to general procedure C from **9a** (80 mg, 496 μmol, 1 equiv) and 4-benzamidobenzoic acid (112 mg, 496 μmol, 1 equiv), with EDCI (190 mg, 993 μmol, 2 equiv) and DMAP (121 mg, 993 μmol, 2 equiv) in DMF (3 mL). Stirring at 0 °C was continued for 1 h, followed by 2 h at room temperature. After the washing steps, pure product **21q** was obtained as a yellow solid (169 mg, 440 μmol, 89%); mp = 214 °C. TLC: 0.64 (DCM/MeOH = 85:15). ^{1}H NMR (600 MHz, DMSO-d_6) δ 7.48 (dd, J = 7.0, 5.2 Hz, 1H, 5′-H$_{pyridyl}$), 7.57 (t, J = 7.6 Hz, 2H, 3′-H$_{benzamidyl}$, 5′-H$_{benzamidyl}$), 7.63 (t, J = 7.3 Hz, 1H, 4′-H$_{benzamidyl}$), 7.82 (br s, 2H, NH$_2$), 7.93 (td, J = 7.7, 1.8 Hz, 1H, 4′-H$_{pyridyl}$), 7.98−8.02 (m, 4H, 2′-H$_{benzamidyl}$, 6′-H$_{benzamidyl}$, 3′-H$_{4-amidobenzoyl}$, 5′-H$_{4-amidobenzoyl}$), 8.04 (d, J = 7.9 Hz, 1H, 3′-H$_{pyridyl}$), 8.25 (0, J = 8.7 Hz, 2H, 2′-H$_{4-amidobenzoyl}$, 6′-H$_{4-amidobenzoyl}$), 8.68 (dd, J = 4.8, 1.7 Hz, 1H, 6′-H$_{pyridyl}$), 10.65 (s, 1H, NH). ^{13}C NMR (151 MHz, DMSO-d_6) δ 119.0 (2C, C-3′$_{4-amidobenzoyl}$, C-5′$_{4-amidobenzoyl}$), 122.5 (1C, C-3′$_{pyridyl}$), 124.7 (1C, C-5′$_{pyridyl}$), 126.3 (1C, C-1′$_{4-amidobenzoyl}$), 127.9 (2C, C-2′$_{benzamidyl}$, C-6′$_{benzamidyl}$), 128.5 (2C, C-3′$_{benzamidyl}$, C-5′$_{benzamidyl}$), 132.0 (1C, C-4′$_{benzamidyl}$), 132.3 (2C, C-2′$_{4-amidobenzoyl}$, 6′-C$_{4-amidobenzoyl}$), 134.6 (1C, C-4′$_{benzamidyl}$), 137.0 (1C, C-4′$_{pyridyl}$), 143.7 (1C, C-4′$_{4-amidobenzoyl}$), 149.0 (1C, C-2′$_{pyridyl}$), 149.7 (1C, C-6′$_{pyridyl}$), 159.05 (1C, C-5′$_{triazole}$), 159.45 (1C, C-3′$_{triazole}$), 166.15 (1C, CONH), 166.93 (1C, C=ONR$_2$). IR (neat): $\tilde{\nu}$ [cm^{-1}] = 3462, 3399, 3345, 1686, 1655, 1634, 1605, 1589, 1518, 1506, 1485, 1404, 1354, 1308, 1256, 1188, 1150, 1126, 1101, 1072, 970, 928, 847. HRMS (m/z): [M + H]$^+$ calcd for C$_{21}$H$_{17}$N$_6$O$^+$ 385.1408, found 385.1387. HPLC: t_R = 17.0 min, purity 95.4%.

1-(5-Amino-3-(pyridin-2-yl)-1H-1,2,4-triazol-1-yl)-2-phenyl-ethan-1-one (21r). It was synthesized according to general procedure C from **9a** (80 mg, 496 μmol, 1 equiv) and phenylacetic acid (67.6 mg, 496 μmol, 1 equiv), with EDCI (190 mg, 993 μmol, 2 equiv) and DMAP (121 mg, 993 μmol, 2 equiv) in DMF (3 mL). Stirring at 0 °C was continued for 1 h, followed by 2 h at room temperature. After the washing steps, pure product **21r** was obtained as a colorless solid (7.0 mg, 25 μmol, 5%). TLC: 0.50 (DCM/MeOH = 9:1). ^{1}H NMR (600 MHz, DMSO-d_6) δ 4.43 (s, 2H, CH$_2$), 7.26−7.31 (m, 1H, 4′-H$_{phenyl}$), 7.32−7.40 (m, 4H, 2′-H$_{phenyl}$, 3′-H$_{phenyl}$, 5′-H$_{phenyl}$, 6′-H$_{phenyl}$), 7.49 (ddd, J = 7.6, 4.7, 1.3 Hz, 1H, 5′-H$_{pyridyl}$), 7.66 (br s, 2H, NH$_2$), 7.94 (td, J = 7.7, 1.8 Hz, 1H, 4′-H$_{pyridyl}$), 8.04 (d, J = 7.8 Hz, 1H, 3′-H$_{pyridyl}$), 8.70 (d, J = 4.4 Hz, 1H, 6′-H$_{pyridyl}$). ^{13}C NMR (151 MHz, DMSO-d_6) δ 41.1 (1C, CH$_2$), 122.4 (1C, C-3′$_{pyridyl}$), 124.7 (1C, C-5′$_{pyridyl}$), 127.0 (1C, C-4′$_{phenyl}$), 128.3 (2C, C-3′$_{phenyl}$, C-5′$_{phenyl}$), 130.0 (2C, C-2′$_{phenyl}$, C-6′$_{phenyl}$), 133.5 (1C, C-1′$_{phenyl}$), 137.1 (1C, C-4′$_{pyridyl}$), 148.9 (1C, C-2′$_{pyridyl}$), 149.7 (1C, C-6′$_{pyridyl}$), 157.7 (1C, C-5′$_{triazole}$), 159.2 (1C, C-3′$_{triazole}$), 172.1 (1C, C=O). HRMS (m/z): [M + H]$^+$ calcd for C$_{15}$H$_{14}$N$_5$O$^+$ 280.1193, found 280.1196. HPLC: t_R = 15.6 min, purity 98.8%.

1-(5-Amino-3-(pyridin-2-yl)-1H-1,2,4-triazol-1-yl)-2-(2-iodophenyl)ethan-1-one (21s). It was synthesized according to general procedure C from **9a** (100 mg, 621 μmol, 1 equiv) and 2-(2-iodophenyl)acetic acid (163 mg, 621 μmol, 1 equiv), with EDCI (238 mg, 1.24 mmol, 2 equiv) and DMAP (152 mg, 1.24 mmol, 2 equiv) in DMF (4 mL). Stirring at 0 °C was continued for 1 h, followed by 2 h at room temperature. The crude product was purified by flash column chromatography (DCM/ACN = 9/1 → 1/3) to give **21s** as a colorless solid (152 mg, 375 μmol, 61%); mp = >300 °C. TLC: 0.34 (DCM/MeOH = 9:1). ^{1}H NMR (600 MHz, DMSO-d_6) δ 4.60 (s, 2H, CH$_2$), 7.08 (td, J = 7.6, 1.7 Hz, 1H, 4′-H$_{2\text{-iodophenyl}}$), 7.41 (td, J = 7.4, 1.3 Hz, 1H, 5′-H$_{2\text{-iodophenyl}}$), 7.47−7.52 (m, 2H, 5′-H$_{\text{pyridyl}}$, 6′-H$_{2\text{-iodophenyl}}$), 7.70 (br s, 2H, NH$_2$), 7.89 (dd, J = 7.9, 1.3 Hz, 1H, 3′-H$_{2\text{-iodophenyl}}$), 7.94 (td, J = 7.7, 1.8 Hz, 1H, 4′-H$_{\text{pyridyl}}$), 8.05 (dt, J = 7.9, 1.1 Hz, 1H, 3′-H$_{\text{pyridyl}}$), 8.70 (ddd, J = 4.7, 1.8, 0.9 Hz, 1H, 6′-H$_{\text{pyridyl}}$). ^{13}C NMR (151 MHz, DMSO-d_6) δ 46.5 (1C, CH$_2$), 102.1 (1C, C-2′$_{2\text{-iodophenyl}}$), 122.5 (1C, C-3′$_{\text{pyridyl}}$), 124.8 (1C, C-5′$_{\text{pyridyl}}$), 128.4 (1C, C-5′$_{2\text{-iodophenyl}}$), 129.3 (1C, C-4′$_{2\text{-iodophenyl}}$), 131.9 (1C, C-6′$_{2\text{-iodophenyl}}$), 137.1 (1C, C-4′$_{\text{pyridyl}}$), 137.4 (1C, C-1′$_{2\text{-iodophenyl}}$), 138.8 (1C, C-3′$_{2\text{-iodophenyl}}$), 148.9 (1C, C-2′$_{\text{pyridyl}}$), 149.8 (1C, C-6′$_{\text{pyridyl}}$), 157.5 (1C, C-5′$_{\text{triazole}}$), 159.4 (1C, C-3′$_{\text{triazole}}$), 170.8 (1C, C=O). IR (neat): $\tilde{\nu}$ [cm^{-1}] = 3456, 2980, 1713, 1634, 1528, 1398, 1368, 1348, 1287, 1263, 1246, 1173, 1152, 1099, 1080, 1049, 995, 970. HRMS (m/z): [M + H]$^{+}$ calcd for C$_{15}$H$_{13}$IN$_5$O^{+} 406.0159, found 406.0141. HPLC: t_R = 17.6 min, purity 99.9%.

N-(2-(5-Amino-3-(pyridin-2-yl)-1H-1,2,4-triazol-1-yl)-2-oxoethyl)benzamide (21t). It was synthesized according to general procedure C from **9a** (150 mg, 931 μmol, 1 equiv) and hippuric acid (167 mg, 931 μmol, 1 equiv), with EDCI (232 mg, 1.21 mmol, 1.3 equiv) and DMAP (148 mg, 1.21 mmol, 1.3 equiv) in DMF (3 mL). The reaction mixture was stirred at room temperature for 3 h. After the washing steps, pure product **21t** was obtained as a colorless solid (198 mg, 613 μmol, 66%); mp = 278 °C. TLC: 0.62 (DCM/MeOH = 85:15). ^{1}H NMR (400 MHz, DMSO-d_6) δ 4.74 (d, J = 5.7 Hz, 2H, CH$_2$), 7.47−7.55 (m, 3H, 3′-H$_{\text{phenyl}}$, 5′-H$_{\text{phenyl}}$, 5′-H$_{\text{pyridyl}}$), 7.58 (tt, J = 7.3, 2.4 Hz, 1H, 4′-H$_{\text{phenyl}}$), 7.71 (br s, 2H, NH$_2$), 7.91−7.98 (m, 3H, 2′-H$_{\text{phenyl}}$, 6′-H$_{\text{phenyl}}$, 4′-H$_{\text{pyridyl}}$), 8.05 (dt, J = 7.9, 1.1 Hz, 1H, 3′-H$_{\text{pyridyl}}$), 8.70 (ddd, J = 4.8, 1.8, 1.0 Hz, 1H, 6′-H$_{\text{pyridyl}}$), 9.06 (t, J = 5.7 Hz, 1H, NH). ^{13}C NMR (101 MHz, DMSO-d_6) δ 42.7 (1C, CH$_2$), 122.5 (1C, C-3′$_{\text{pyridyl}}$), 124.8 (1C, C-5′$_{\text{pyridyl}}$), 127.3 (2C, C-2′$_{\text{phenyl}}$, 6′-C-6′$_{\text{phenyl}}$), 128.4 (2C, C-3′$_{\text{phenyl}}$, C-5′$_{\text{phenyl}}$), 131.6 (1C, C-4′$_{\text{phenyl}}$), 133.5 (1C, C-1′$_{\text{phenyl}}$), 137.1 (1C, C-4′$_{\text{pyridyl}}$), 148.8 (1C, C-2′$_{\text{pyridyl}}$), 149.7 (1C, C-6′$_{\text{pyridyl}}$), 157.6 (1C, C-5′$_{\text{triazole}}$), 159.8 (1C, 3′-C$_{\text{triazole}}$), 166.9 (1C, CONH), 169.9 (1C, CH$_2$CO). IR (neat): $\tilde{\nu}$ [cm^{-1}] = 3453, 3302, 3055, 1736, 1636, 1528, 1485, 1462, 1385, 1354, 1312, 1285, 1250, 1177, 1153, 1084, 999, 976, 802, 760, 744, 714, 691, 625, 610. HRMS (m/z): [M + H]$^{+}$ calcd for C$_{16}$H$_{15}$N$_6$O$_2$$^{+}$ 323.1251, found 323.1246. HPLC: t_R = 12.7 min, purity 99.6%.

(E)-1-(5-Amino-3-(pyridin-2-yl)-1H-1,2,4-triazol-1-yl)-3-phenyl-prop-2-en-1-one (21u). It was synthesized according to general procedure C from **9a** (100 mg, 621 μmol, 1 equiv) and cinnamic acid (91.9 mg, 621 μmol, 1 equiv), with EDCI (238 mg, 1.24 mmol, 2 equiv) and DMAP (152 mg, 1.24 mmol, 2 equiv) in DMF (4 mL). The reaction mixture was gradually heated from 0 °C to room temperature over 18 h. After the washing steps, pure product **21u** was obtained as a yellow solid (136 mg, 465 μmol, 75%); mp = 215 °C. TLC: 0.50 (DCM/MeOH = 9:1). ^{1}H NMR (600 MHz, DMSO-d_6) δ 7.48−7.50 (m, 1H, 5′-H$_{\text{pyridyl}}$), 7.50−7.53 (m, 3H, 3′-H$_{\text{phenyl}}$, 4′-H$_{\text{phenyl}}$, 5′-H$_{\text{phenyl}}$), 7.75 (d, J = 16.0 Hz, 2H, PhCH=CH), 7.78 (br s, 2H, NH$_2$), 7.82−7.87 (m, 2H, 2′-H$_{\text{phenyl}}$, 6′-H$_{\text{phenyl}}$), 7.94 (td, J = 7.7, 1.8 Hz, 1H, 4′-H$_{\text{pyridyl}}$), 7.99 (d, J = 16.0 Hz, 1H, PhCH=CH), 8.09 (d, J = 7.8 Hz, 1H, 3′-H$_{\text{pyridyl}}$), 8.70 (d, J = 4.5 Hz, 1H, 6′-H$_{\text{pyridyl}}$). ^{13}C NMR (151 MHz, DMSO-d_6) δ 116.7 (1C, PhCH=CH), 122.6 (1C, C-3′$_{\text{pyridyl}}$), 124.8 (1C, C-5′$_{\text{pyridyl}}$), 128.9 (2C, C-2′$_{\text{phenyl}}$, C-6′$_{\text{phenyl}}$), 129.2 (2C, 3′$_{\text{phenyl}}$, C-5′$_{\text{phenyl}}$), 131.4 (1C, C-4′$_{\text{phenyl}}$), 133.9 (1C, C-1′$_{\text{phenyl}}$), 137.0 (1C, C-4′$_{\text{pyridyl}}$), 147.1 (1C, PhCH=CH), 148.9 (1C, C-2′$_{\text{pyridyl}}$), 149.7 (1C, C-6′$_{\text{pyridyl}}$), 158.1 (1C, C-5′$_{\text{triazole}}$), 159.3 (1C, C-3′$_{\text{triazole}}$), 165.0 (1C, C=O). IR (neat): $\tilde{\nu}$ [cm^{-1}] = 3449, 3028, 1682, 1634, 1612, 1574, 1530, 1485, 1404, 1366, 1342, 1287, 1246, 1173, 1152, 1032, 1022, 999, 968, 860, 800. HRMS (m/z): [M + H]$^{+}$

calcd for C$_{16}$H$_{14}$N$_5$O^{+} 292.1193, found 2921192. HPLC: t_R = 17.3 min, purity 99.4%.

(S)-(5-Amino-3-(pyridin-2-yl)-1H-1,2,4-triazol-1-yl)(1,2,3,4-tetra-hydronaphthalen-1-yl)methanone (21v). It was synthesized according to general procedure C from **9a** (100 mg, 621 μmol, 1 equiv) and 1,2,3,4-tetrahydro-2-naphthoic acid (109 mg, 621 μmol, 1 equiv), with EDCI (238 mg, 1.24 mmol, 2 equiv) and DMAP (152 mg, 1.24 mmol, 2 equiv) in DMF (4 mL). Stirring at 0 °C was continued for 1 h, followed by 2 h at room temperature. After the washing steps, pure product **21v** was obtained as a yellow solid (148 mg, 463 μmol, 75%); mp = 157−158 °C. TLC: 0.61 (DCM/MeOH = 9:1). ^{1}H NMR (600 MHz, DMSO-d_6) δ 1.73−1.81 (m, 1H, 3′-H$_{\text{tetrahydronaphthyl}}$), 1.86−1.94 (m, 1H, 3′-H$_{\text{tetrahydronaphthyl}}$), 2.07−2.13 (m, 1H, 2′-H$_{\text{tetrahydronaphthyl}}$), 2.17−2.25 (m, 1H, 2′-H$_{\text{tetrahydronaphthyl}}$), 2.74−2.86 (m, 2H, 4′-H$_{\text{tetrahydronaphthyl}}$), 5.07 (t, J = 6.4 Hz, 1H, 1′-H$_{\text{tetrahydronaphthyl}}$), 7.07−7.12 (m, 2H, 7′-H$_{\text{tetrahydronaphthyl}}$, 8′-H$_{\text{tetrahydronaphthyl}}$), 7.14−7.19 (m, 2H, 5′-H$_{\text{tetrahydronaphthyl}}$, 6′-H$_{\text{tetrahydronaphthyl}}$), 7.49 (ddd, J = 7.6, 4.7, 1.2 Hz, 1H, 5′-H$_{\text{pyridyl}}$), 7.72 (br s, 2H, NH$_2$), 7.94 (td, J = 7.7, 1.8 Hz, 1H, 4′-H$_{\text{pyridyl}}$), 8.05 (dt, J = 7.8, 1.0 Hz, 1H, 3′-H$_{\text{pyridyl}}$), 8.69 (ddd, J = 4.7, 1.7, 0.7 Hz, 1H, 6′-H$_{\text{pyridyl}}$). ^{13}C NMR (151 MHz, DMSO-d_6) δ 20.0 (1C, C-3′$_{\text{tetrahydronaphthyl}}$), 26.3 (1C, C-2′$_{\text{tetrahydronaphthyl}}$), 28.6 (1C, C-4′$_{\text{tetrahydronaphthyl}}$), 43.2 (1C, C-1′$_{\text{tetrahydronaphthyl}}$), 122.6 (1C, C-3′$_{\text{pyridyl}}$), 124.8 (1C, C-5′$_{\text{pyridyl}}$), 125.8 (1C, C-7′$_{\text{tetrahydronaphthyl}}$), 126.8 (1C, C-6′$_{\text{tetrahydronaphthyl}}$), 129.2 (1C, C-5′$_{\text{tetrahydronaphthyl}}$), 129.3 (1C, C-8′$_{\text{tetrahydronaphthyl}}$), 133.1 (1C, C-8a′$_{\text{tetrahydronaphthyl}}$), 137.1 (1C, C-4′$_{\text{pyridyl}}$), 137.5 (1C, C-4a′$_{\text{tetrahydronaphthyl}}$), 148.9 (1C, C-2′$_{\text{pyridyl}}$), 149.7 (1C, C-6′$_{\text{pyridyl}}$), 157.9 (1C, C-5′$_{\text{triazole}}$), 159.5 (1C, C-3′$_{\text{triazole}}$), 175.7 (1C, C=O). IR (neat): $\tilde{\nu}$ [cm^{-1}] = 3447, 3426, 2932, 2866, 2835, 1713, 1628, 1533, 1464, 1447, 1391, 1368, 1352, 1271, 1256, 1169, 1150, 1090, 993, 968, 920, 876, 802. HRMS (m/z): [M + H]$^{+}$ calcd for C$_{18}$H$_{18}$N$_5$O^{+} 320.1506, found 3201517. HPLC: t_R = 17.8 min, purity 97.5%.

X-ray Diffraction. Data sets for compound **21m** were collected with a D8 Venture Dual Source 100 CMOS diffractometer. Programs used: data collection: APEX3 V2016.1−0 (Bruker AXS Inc., 2016); cell refinement: SAINT V8.37A (Bruker AXS Inc., 2015); data reduction: SAINT V8.37A (Bruker AXS Inc., 2015); absorption correction, SADABS V2014/7 (Bruker AXS Inc., 2014); structure solution *SHELXT-2015*;[65] structure refinement *SHELXL-2015*[65] and graphics, *XP* (Version 5.1, Bruker AXS Inc., Madison, Wisconsin, 1998). *R*-values are given for observed reflections, and wR^2 values are given for all reflections.

FXIIa Inhibition Assay. The inhibitory activity of synthesized compounds toward the human coagulation factor XIIa was measured by quantifying the hydrolysis rate of the fluorogenic substrate as reported previously.[41,43] Briefly, the enzymatic activity was measured in buffer (10 mM Tris-Cl, 150 mM NaCl, 10 mM MgCl$_2$·6H$_2$O, 1 mM CaCl$_2$·2H$_2$O, 0.1% w/v BSA, 0.01% v/v Triton-X100, pH = 7.4) using clear flat-bottom, black polystyrene 96 well plates. The enzyme (human β-FXIIa, HFXIIAB, >95% purity; Molecular Innovations, 2.5 nM: final concentration) and the fluorogenic substrate Boc-Gln-Gly-Arg-AMC (Pepta Nova, 25 μM: final concentration, K_m = 167 μM) were employed. Dilutions of test compounds ranging from 0.5 nM to 132 μM (final concentrations) in DMSO were prepared. The fluorogenic substrate solution was added into the wells followed by the addition of 2 μL of test compound solution, and the reaction was triggered by the addition of the enzyme solution (final testing volume: 152 μL). In the case of blank (substrate + buffer) and control (substrate + enzyme) wells, 2 μL of DMSO was added instead of the test compound solution. Fluorescence intensity was measured with Microplate Reader Mithras LB 940 (Berthold Technologies, excitation at 355 nm, emission at 460 nm) for a period of 1 h with a read every minute. The reactions were performed at 25 °C. To derive 1 h IC$_{50}$ values, end-point RFU (single fluorescence reading after 1 h) was used. Sigmoidal curves were prepared in the GraphPad Prism software, and IC$_{50}$ values were derived from the fitted curves.

The time-dependent inhibition experiment of FXIIa was performed similarly to the FXIIa inhibition assay. The enzyme (FXIIa, 2.5 nM) was added to a solution of fluorogenic substrate (Boc-Gln-Gly-Arg-AMC, 25 μM) and an inhibitor (ranged 0.5 nM−132 μM, 10

concentrations) in an assay buffer, and fluorescence (excitation at 355 nm, emission at 460 nm) was read immediately in the kinetic mode (readout every 87 s) for up to 180 min. The IC_{50} values were calculated for each time point in the GraphPad Prism software and plotted against the measurement time.

Thrombin Inhibition Assay. The inhibitory activity of synthesized compounds toward the coagulation factor IIa (human α-thrombin (active) protein, ABIN2127880, >95% purity; antibodies-online, 0.25 nM: final concentration) was determined analogously to the described procedure for FXIIa. The fluorogenic substrate Boc-Val-Pro-Arg-AMC (Pepta Nova, 25 μM: final concentration, K_m = 18 μM) was utilized.

FXa Inhibition Assay. The inhibitory activity of synthesized compounds toward the coagulation factor Xa (human factor Xa, HFXA, >95% purity; Molecular Innovations, 2.5 nM: final concentration) was determined analogously to the described procedure for FXIIa. The fluorogenic substrate Boc-Ile-Glu-Gly-Arg-AMC (Pepta Nova, 25 μM: final concentration) was utilized.

Trypsin Inhibition Assay. The inhibitory activity of synthesized compounds toward trypsin (porcine trypsin; Merck, 3.5 nM: final concentration) was determined analogously to the described procedure for FXIIa. The fluorogenic substrate Z-Gly-Gly-Arg-AMC (Sigma-Aldrich, 25 μM: final concentration) was utilized.

Urokinase Inhibition Assay. The inhibitory activity of synthesized compounds toward urokinase (human urokinase; Medac GmbH, 1.68 nM: final concentration) was determined similarly to the described procedure for FXIIa, but 50 mM Tris HCl buffer (pH 8.0), containing 154 mM NaCl, was utilized. The fluorogenic substrate Tos-Gly-Pro-Arg-AMC × TFA (synthesized in house, 143 μM: final concentration, K_m = 75 μM) was utilized.

Plasmin Inhibition Assay. The inhibitory activity of synthesized compounds toward plasmin (human plasmin; Merck, 0.35 nM: final concentration) was determined similarly to the described procedure for FXIIa, but 50 mM Tris HCl buffer (pH 8.0), containing 154 mM NaCl, was utilized. The fluorogenic substrate Mes-dArg-Phe-Arg-AMC × 2 TFA (synthesized in house,[66] 100 μM: final concentration, K_m = 29 μM) was utilized.

FXIa Inhibition Assay. The inhibitory activity of synthesized compounds toward FXIa (human FXIa; Molecular Innovations, 0.897 nM: final concentration) was determined similarly to the described procedure for FXIIa, but 50 mM Tris HCl buffer (pH 8.0), containing 154 mM NaCl, was utilized. The fluorogenic substrate Mes-dArg-Pro-Arg-AMC × 2 TFA (synthesized in house,[67] 143 μM: final concentration, K_m = 77 μM) was utilized.

Plasma Kallikrein Inhibition Assay. The inhibitory activity of synthesized compounds toward plasma kallikrein (human plasma kallikrein; Enzyme Research South Bend, 0.112 nM: final concentration) was determined similarly to the described procedure for FXIIa, but 50 mM Tris HCl buffer (pH 8.0), containing 154 mM NaCl, was utilized. The fluorogenic substrate Mes-dArg-Pro-Arg-AMC × 2 TFA (synthesized in house,[67] 100 μM: final concentration, K_m = 40 μM) was utilized.

In Vitro Blood Coagulation Assays (aPTT and PT). All measurements were performed using citrated (3.8%) human whole blood (University Hospital Münster) on a semiautomated coagulometer (Thrombotimer-2, Behnk Elektronik, Germany) according to the manufacturer instructions. For aPTT measurements, whole blood (100 μL) was placed into the incubation cuvettes of the instrument and incubated for 2 min at 37 °C. Then, the test compound solution (10 μL) or solvent (DMSO, 10 μL) was added with a pipette. After 1 min of incubation, 100 μL of prewarmed (37 °C) aPTT reagent (Convergent Technologies, Germany) was added and incubated for additional 2 min. The cuvettes were transferred to a measuring position, the coagulation was initiated by the addition of 100 μL of a CaCl$_2$ solution (25 mM, prewarmed at 37 °C, Convergent Technologies, Germany), and the clotting time was recorded. For PT assays, whole blood (100 μL) was incubated for 2 min at 37 °C. Then, the test compound solution (10 μL) or solvent (DMSO, 10 μL) was added with a pipette. After 3 min of incubation, the cuvettes were transferred to a measuring position, the coagulation was initiated

by the addition of 100 μL of the PT assay reagent already containing CaCl$_2$ (prewarmed at 37 °C, Convergent Technologies, Germany), and the clotting time was recorded.

Microscale Parallel Synthesis. A 96-well plate (clear, polystyrene, flat bottom) was charged with 95 carboxylic acids (620 mmol/L in dry DMSO-d_6, 30 μL, 1 equiv, one acid in each well) and 95 micro magnetic stirring bars. DMAP (930 mmol/L in dry DMSO-d_6, 30 μL, 1.5 equiv), EDCI (930 mmol/L in dry DMSO-d_6, 30 μL, 1.5 equiv), and aminotriazole **9a** (620 mmol/L in dry DMSO-d_6, 30 μL, 1 equiv) were sequentially pipetted into each well. The plate was covered with a lid, then sealed with parafilm, and placed on the magnetic stirrer. After 3 h of incubation at room temperature, the lid was opened and 20 μL aliquot from each microscale reaction was withdrawn, diluted with DMSO (980 μL, dry), and immediately frozen at −20 °C* (samples for MTS). The residual 100 μL of the reaction solution was diluted with DMSO-d_6 (600 μL, dry) and directly submitted for ^{1}H NMR analysis to measure the reaction conversion rate. *: several samples (S19−S28, S34, and Table S1 in the Supporting Information) were found to be moisture-sensitive and were stored in a desiccator (with CaCl$_2$) under a N$_2$ atmosphere without freezing.

Determination of Microscale Reaction Conversions by ^{1}H NMR. The NMR spectra of microscale parallel synthesis samples were recorded at 25 °C using an Agilent DD2 400 MHz NMR spectrometer and analyzed with the MestReNova software (version 12.0.3−21384, Mestrelab Research S.L.). The purest proton resonance signals of the reaction product (S1−S95) and starting material (aminotriazole **9a** or a carboxylic acid) were identified, integrated, and normalized. The averaged normalized integrals of product (Int$_P$) protons and of the starting material (Int$_{Sm}$) protons were used to calculate the reactions' conversion (C, %) using the following formula: C [%] = (Int$_P$/(Int$_P$ + Int$_{Sm}$)) × 100. When no pure signals of either starting material (**9a** or carboxylic acid) could be identified, the signals of DMAP (Int$_R$) were used instead with the consideration of the used reaction equivalents (eq$_R$) using the following equation: C [%] = (Int$_P$ × eq$_R$/Int$_R$) × 100.

Microscale Reaction Product Screening in the Enzyme Inhibition Assay. After the reaction conversion determination (by ^{1}H NMR), frozen samples of the microscale parallel synthesis were defrosted at room temperature and 50 μL aliquot was withdrawn from each sample and diluted with the calculated amount of dry DMSO to set the reaction product concentration to 76 μmol/L. For this, the actual product concentration c_P [mmol/L] in the microscale reaction was calculated using theoretical product concentration (1.55 mmol/L) and the actual reaction conversion rate of each sample C [%] applying the following formula: c_P [mmol/L] = 1.55 mmol/L × C [%]/100. Resultant equimolar samples (90 acylated 1,2,4-triazol-5-amines) were appropriately diluted to be directly screened at 1 μM and 100 nM in the enzyme inhibition assays (FXIIa and thrombin) using the fluorogenic substrates. The results of these measurements (triplicate) were expressed as the percentage of inhibition at 1 μM and 100 nM for each sample.

Analysis of Covalent FXIIa-Inhibitor Complexes by SEC/ESI-MS. *Materials.* Formic acid was obtained from Th. Geyer (Renningen, DE); sodium hydroxide and ammonium acetate were obtained from Merck (Darmstadt, DE); and isopropanol, acetic acid, and ammonia solution were obtained from VWR International (Radnor, PA). All chemicals were of analytical grade. Human plasma β-FXIIa was purchased from Molecular Innovations (Novi, MI). Aqueous solutions were prepared using an Aquatron A4000D water still (Stuart, Staffordshire, GB). All pH values were adjusted using a FiveEasy pH meter from Mettler Toledo (Greifensee, DE). *Equipment:* The herein used HPLC system from Shimadzu (Kyoto, JP) was equipped with a system controller (CBM-20A), a degasser (DGU-14A), two pumps (LC-10ADvp), an autosampler (SIL-HTA), and a column oven (CTO-10Avp). Mass spectrometric detection was carried out using a micrOTOF time-of-flight mass spectrometer from Bruker Daltonics (Bremen, DE) equipped with an electrospray ionization interface. Mass calibration was performed prior to the measurement using a solution of 0.2% formic acid and 5 mM sodium

hydroxide in a mixture of purified water and isopropanol (1:1, v/v), which was directly introduced into the mass spectrometer using a syringe pump. The system was controlled using micrOTOF control (Version 3.0) and HyStar (Version 3.2), and post-processing was carried out using DataAnalysis (Version 5.3). Size-exclusion chromatography (SEC) was performed using a MAbPac SEC-1 analytical column (150 mm × 4 mm, 5 μm particle size, 300 Å pore size) from Thermo Fisher Scientific (Bremen, DE).

Sample Preparation. The protein stock solution (37.67 μM) was diluted by adding 90 μL of purified water. An aliquot of 46.3 μL was mixed with 3.7 μL of inhibitor solution (1 mM in DMSO) to prepare the enzyme−inhibitor solution (molar ratio of 1:20), which was then analyzed via SEC/ESI-MS.

Enzyme−Inhibitor Covalent Complex Stability Measurement (Desalination Procedure). The prepared enzyme−inhibitor solution (50 μL) was diluted with 450 μL of purified water. The mixture was transferred into the vial equipped with Amicon Ultra 0.5 mL Centrifugal Filters (Ultracel − 3K) (Merck Millipore) and centrifuged at 14000 rpm for 30 min. The residue was again diluted with purified water to 500 μL volume, and the centrifugation process was repeated. Last, the residue was diluted to the initial volume of 50 μL with purified water and analyzed by SEC/ESI-MS.

SEC/ESI-MS Analysis. For chromatographic analysis of the sample solutions, isocratic elution was carried out using an aqueous ammonium acetate solution (10 mM, pH 6.8) as the mobile phase for 15 min. The flow rate was 150 μL/min, the column oven temperature was set to 30 °C, and the injection volume was 10 μL. The LC outlet was directly coupled to the ESI source of the mass spectrometer. The enzyme−inhibitor complexes were analyzed in the positive ion mode using the following ESI-MS parameters. The mass range was set to m/z 1000−5000, nebulizer gas (nitrogen) was 1.2 bar, dry gas (nitrogen) was 9.0 L/min, the dry gas temperature was 200 °C, hexapole RF was 600 V, pre pulse storage time was 30 μs, and transfer time was 100 μs. Deconvoluted mass spectra were obtained by averaging frames from 6.8 min to 7.6 min retention time and deconvolution using the charge states 9+ to 11+ of the respective protein species.

Binding Mode Study by Molecular Modeling. Structures of small molecules were prepared using the LigPrep module of the Schrodinger suite (Schrödinger Release 2019−4: Schrödinger, LLC, New York, NY, 2019) employing the OPLS3e force field. The experimental structures of studied proteins were obtained from the RCSB database (PDB IDs: 6B77/FXIIa, 6CYM/thrombin). Structures were processed with the protein preparation wizard of Schrodinger Maestro suite 2019−4 (Schrödinger Release 2019−4) to optimize the hydrogen-bonding network, followed by constrained minimization (heavy-atom RMSD converge of 0.3 Å) to remove crystallographic artifacts. Covalent docking was carried out using the Schrödinger Covalent Docking procedure with Nucleophilic Addition to a Double Bond protocol. In both cases, active serine residues (195/FXIIa and 219/thrombin) were selected as attachment points and centers for Glide Grid. Input and output files are available upon request.

Cell Lines. The human breast cancer cell line MDA-MB-231 was grown in Dulbecco's modified Eagle's Medium (DMEM) (Sigma-Aldrich, St. Louis) with 10% (v/v) FCS, 1% L-glutamine, 100 U/mL penicillin, 100 μg/mL streptomycin, and 1% sodium pyruvate. Cells were incubated at 37 °C in a humidified atmosphere containing 5% CO_2. Cells were detached at 90% confluence using a solution of ethylenediamine tetraacetic acid (EDTA, 0.2 g/L EDTA × 4 Na) for 10 min at 37 °C. All reagents were from Thermo Fisher Scientific Inc. (Waltham, MA). Cell identity was evaluated using an STR profile analysis.

Preparation of Platelets. Platelet-rich-plasma was obtained from the Institute for Experimental Hematology and Transfusion Medicine, University of Bonn, Medical Centre, in accordance with the declaration of Helsinki. Isolated human platelets (Plts) in buffer were prepared from platelet-rich-plasma as described[54] by centrifugation (670 g, 10 min, 22 °C) and resuspension (400 × 10^6 Plts/mL) in recalcified (1 mM) platelet buffer (10 mM HEPES, 137 mM NaCl,

2.6 mM KCl, 1 mM $MgCl_2$, 13.8 mM $NaHCO_3$, 0.36 mM NaH_2PO_4, 5.5 mM D-glucose), which results in a remaining plasma protein content of about 1%. Prior to activation, platelets were preincubated with the indicated inhibitors or left untreated for control.

Light Transmission Aggregometry. The measurement of tumor-cell-induced platelet aggregation was performed by light transmission aggregometry using an APACT-4004 aggregometer (Haemochrom Diagnostica, Essen, Germany). Platelets were prepared and coincubated with the indicated inhibitors as described. Platelet aggregation was induced by either $1 × 10^4$ tumor cells/mL or 20.5 μM TRAP-6 or 0.2 U thrombin. The measurement was performed at 37 °C in adequate cuvettes, stirred continuously at 1000 rpm. Aggregate formation was measured by light transmission, with buffer set as 100% and platelets in the buffer as 0% reference values.

ATP Release Assay. Platelets were coincubated with inhibitors for 20 min or phosphate-buffered saline (PBS). MDA-MB-231 cells were detached with EDTA and resuspended in PBS. Platelets (400 × 10^6 Plts/mL) were activated with $1 × 10^4$ tumor cells/mL for 30 min, with 20.5 μM TRAP6 for 10 min or 0.2 U thrombin for 10 min. Platelets' ATP secretion from dense granules was assessed by luminescence measurements using a luciferin-based ATP-Determination Kit (Thermo Fisher Scientific, Waltham) and a FLUOstar Optima plate reader (BMG Labtech, Ortenberg, Germany).

Thrombin Generation Assay. *Reagents.* The following regents were uses: relipidated recombinant TF (Instrumentation Laboratory, Bedford, MA); and Thrombodynamics-4D kits consisting of a corn trypsin inhibitor with the fluorogenic substrate Z-Gly-Gly-Arg-AMC, calcium acetate, and phospholipids in the form of a lyophilized suspension of phospholipid vesicles (HemaCore Labs, Moscow, Russia).

Plasma Preparation. Blood was taken from apparently healthy individuals after obtaining an informed consent. We used Vacuette 3.2% citrate tubes (Greiner BioOne, Kremsmunster, Austria) with straight 21G x 1 1/2 needles. The first tube after the venipuncture was discarded. Blood was immediately processed by two sequential centrifugations: 15 min at 1 600g and 5 min at 10 000g at room temperature. Platelet-free plasma (PFP) was mixed from $n = 3$ donors (1:1:1) and was aliquoted and snap-frozen in liquid nitrogen, stored at −80 °C.

Experimental Design. Frozen samples of plasma were thawed in a water bath at 37 °C for 15 min and then incubated for 15 min at room temperature. Thawed plasma (110 μL) was added to the dried corn trypsin inhibitor (final concentration 0.2 mg/mL) with a dried substrate (final concentration 400 μM), and 5 μL of phospholipids (prepared according to manufacturer's instructions, final concentration 4 μM) was added. Plasma was spiked with 4 μL of **21a**, **21i**, **21m**, dabigatran (**1**), or DMSO or diluted from the stock solution with buffer (20 mM HEPES, 140 mM NaCl, pH 7.2−7.4). The final **21a**, **21i** and **21m** concentration was 100 μM and that of dabigatran was 1 μM, and the DMSO concentration in plasma did not exceed 1% (except for "buffer" sample, which was spiked only with 5 μL of buffer). The sample was incubated for 15 min at 37 °C and then supplemented with dried calcium acetate (final concentration 20 mM). Clotting was activated using 5 μL of TF diluted in distilled water (stored at −80 °C, final concentration 5 pM) poured directly into the plasma, and the sample (120 mL) was placed in a plastic cuvette.

Thrombodynamics-T2T analyzer (HemaCore Labs LLC, Moscow, Russia) allows detecting a fluorescence signal from AMC generated during clot formation as well as light scattering from the fibrin clot (Thrombodynamics-4D Analyzer; HemaCore Labs, as described[68]). The fluorogenic substrate added to the plasma was cleaved by thrombin and produced a fluorescent AMC molecule. Its generation rate was proportional to the thrombin concentration. The plasma sample was illuminated in turn by red (625 nm) and ultraviolet (365 nm) light-emitting diodes. The fibrin clot formation was detected by red light scattering, and the fluorescence of AMC was excited by ultraviolet emission (440 nm). Scattered light and fluorescence passed through a multiband filter and were detected by a digital camera every 30 s for 90 min.

Parameters of fibrin clot growth and thrombin generation were calculated from a series of images as described before.[69] The light scattering of fibrin clots and thrombin concentrations were plotted as functions of time, and the following parameters were calculated: clotting time (the time to reach one-half maximum light scattering, $T_{1/2}$), the amplitude of the thrombin peak (A_{max}), the time to peak (T_{max}), and endogenous thrombin potential (ETP, the area under the curve). For each compound were done $n = 3$ measurements. Six curves of one representative experiment for each compound are shown in Figure 14. Mean values and standard deviation of calculated parameters are shown in Table 3.

Cytotoxicity. To examine the cytotoxicity, 10 mM solutions of each test compound were prepared in DMSO. Human liver cancer cells (HepG2, HB-8065) (ATCC, Manassas, VA) were cultivated in Dulbecco's modified Eagle's medium (DMEM) supplemented with 10 mM N-2-hydroxyethylpiperazine-N′-2-ethane-sulfonic acid (HEPES buffer), 100 U/mL penicillin, 100 μg/mL streptomycin, 2 mM L-glutamine, and 10% (v/v) fetal calf serum (FCS) using standardized culture conditions (37 °C, 5% CO_2, saturated humidified atmosphere). The human astrocytoma cell line (CCF-STTG-1) (ATCC, Manassas, VA) was cultivated in Roswell Park Memorial Institute medium (RPMI 1640) supplemented with 100 U/mL penicillin, 100 μg/mL streptomycin, 2 mM L-glutamine, and 10% (v/v) FCS. For the subcultivation, both cell types were trypsinated when reaching a microscopic confluence of 80%. Media were changed two times in 7 days. Cytotoxic effects of the tested compounds were evaluated with the Alamar blue assay. The assay was performed according to previous studies.[70−72] Briefly, the cells were seeded in 96-well plates of a suspension of 25 000 cells/well for HepG2 and 10 000 cells/well for CCF. Cells were incubated for 24 h after the medium was replaced by serum-free medium and cultivated for another 24 h. Afterward, the cells were treated with **21i**, **21m**, and **21q** in a concentration range of 0.05−300 μM (HepG2) and 0.5−300 μM (CCF) and incubated for 48 h. After compound exposure, the dye solution of resazurin was added to the cells, followed by incubation for 1.5 h at 37 °C. The fluorescence of reduced resazurin (resorufin) was measured at $\lambda = 590$ nm with a microplate reader (Infinite M200 pro, Tecan, Männendorf, Switzerland). Cytotoxicity tests were repeated three times from three independent passages ($n \geq 9$). The data are shown as the mean ± standard deviation (SD). As a positive control, T-2 toxin, which was previously isolated by the working group of Prof. Humpf,[70] was used at a concentration of 10 μM. The statistical analysis of the data was performed using one-way analysis of variance (ANOVA) and Tukey's post-hoc test; * statistically significant ($p \leq 0.05$), ** statistically highly significant ($p \leq 0.01$).

Inhibition of MAGL (Monoacylglycerol Lipase). The effect of selected compounds on the activity of the endocannabinoid-degrading enzyme monoacylglycerol lipase (MAGL) was evaluated as previously described using human recombinant MAGL.[73,74] Briefly, the substrate 1,3-dihydroxypropan-2-yl 4-pyren-1-ylbutanoate was solubilized with Triton X-100 (0.2 %). The enzyme reaction was terminated after 45 min by the addition of a mixture of acetonitrile/methanol (1:1, v/v) supplemented with the internal standard 6-pyren-1-ylhexanoic acid. Blank incubations in the absence of the enzyme were carried out in parallel. MAGL inhibition was determined by measuring the amount of 4-pyren-1-ylbutanoic acid released by the enzyme in the absence and the presence of a test compound (corrected by the blank value) by reversed-phase HPLC with fluorescence detection. Under the conditions applied, for the reference MAGL inhibitor CAY10499, an IC_{50} value of 0.48 μM was measured.

Inhibition of FAAH (Fatty Acid Amide Hydrolase). Inhibition of FAAH by selected compounds was measured in a similar manner as described recently.[73] The substrate N-(2-hydroxyethyl)-4-pyren-1-ylbutanamide[75] was dissolved in methanol (2.5 mg/mL). An aliquot of this solution was thoroughly dried under a stream of nitrogen. The residue was dissolved in such an amount of DMSO that a 5 mM substrate solution was obtained. The enzyme solution was prepared by diluting 50 μL of the rat brain homogenate obtained as described recently[4] with 350 μL of potassium phosphate buffer (0.1 M, pH 7.4)

containing EDTA (1 mM). Then, 10 volume parts of this dilution were mixed with 86 volume parts of 0.2% Triton X-100 in phosphate-buffered saline (prepared from tablets from Sigma-Aldrich, P4417: one tablet dissolved in 200 mL of deionized water yields 0.01 M phosphate buffer, 0.0027 M potassium chloride, and 0.137 M sodium chloride, pH 7.4, at 25 °C). The assay was started by adding 2 μL of the substrate solution in DMSO (5 mM) to 2 μL of a DMSO solution of the inhibitor or to 2 μL of DMSO in the case of the controls. The mixture was preincubated for 5 min at 37 °C. Then, the enzymatic reaction was started by adding 96 μL of the prepared enzyme solution in Triton X-100/phosphate-buffered saline. In the final incubation volume of 100 μL, the pyrenylbutanamide substrate concentration was 100 μM. After incubation at 37 °C for 60 min, the enzyme reaction was terminated by the addition of 200 μL of acetonitrile/methanol (1:1, v/v) supplemented with the internal standard 6-pyren-1-ylhexanoic acid (0.025 μg/200 μL). After being cooled in an ice bath for 10 min, the samples were centrifuged at 12 000g at 4 °C for 5 min. Blank incubations in the absence of the enzyme were carried out in parallel. FAAH inhibition was determined by measuring the amount of 4-pyren-1-ylbutanoic acid released by the enzyme in the absence and the presence of a test compound (corrected by the blank value) by reversed-phase HPLC with fluorescence detection as described recently.[75] Under the conditions applied, for the reference FAAH inhibitor URB597, an IC_{50} value of 0.043 μM was measured.

ASSOCIATED CONTENT

Supporting Information

The Supporting Information is available free of charge at https://pubs.acs.org/doi/10.1021/acs.jmedchem.0c01635.

> ^{1}H and ^{13}C NMR spectra of all synthesized compounds; experimental procedures and analytical data for the compounds **9a−c**, **18a−c**, **15**, and **19a−c**; conversion rates in microscale parallel synthesis and inhibitory activity screening of 1,2,4-triazol-5-amines **S1−S95**; extended cytotoxicity data for **21i**, **21m**, and **21q**; X-ray crystal structure analysis of **21m** (PDF)

> Molecular formula strings (CSV)

> CCDC-1997967 for **21m** contains the crystallographic data; data can be obtained free of charge from the Cambridge Crystallographic Data Centre via www.ccdc.cam.ac.uk/data_request/cif; coordinates for the inhibitors **21i** docked in FXIIa (PDB)

> Coordinates for the inhibitor **21m** docked in FIIa (PDB)

AUTHOR INFORMATION

Corresponding Author

Dmitrii V. Kalinin − *Institute of Pharmaceutical and Medicinal Chemistry, University of Münster, 48149 Münster, Germany;* orcid.org/0000-0003-2717-5364; Phone: +49-251-8333372; Email: d_kali01@uni-muenster.de

Authors

Marvin Korff − *Institute of Pharmaceutical and Medicinal Chemistry, University of Münster, 48149 Münster, Germany*

Lukas Imberg − *Institute of Pharmaceutical and Medicinal Chemistry, University of Münster, 48149 Münster, Germany*

Jonas M. Will − *Institute of Inorganic and Analytical Chemistry, University of Münster, 48149 Münster, Germany*

Nico Bückreiß − *Pharmaceutical Institute, University of Bonn, 53121 Bonn, Germany*

Svetlana A. Kalinina − *Institute of Food Chemistry, University of Münster, 48149 Münster, Germany;* orcid.org/0000-0001-7564-8213

Benjamin M. Wenzel − *Department of Pharmacy, Institute of Pharmaceutical Chemistry, Philipps University Marburg, 35032 Marburg, Germany*

Gregor A. Kastner − *Institute of Pharmaceutical and Medicinal Chemistry, University of Münster, 48149 Münster, Germany*

Constantin G. Daniliuc − *Institute for Organic Chemistry, University of Münster, 48149 Münster, Germany;* orcid.org/0000-0002-6709-3673

Maximilian Barth − *Institute of Pharmaceutical and Medicinal Chemistry, University of Münster, 48149 Münster, Germany*

Ruzanna A. Ovsepyan − *Laboratory of Translational Medicine, Dmitriy Rogachev National Medical Research Center of Pediatric Hematology, Oncology, and Immunology, 117997 Moscow, Russia; Center for Theoretical Problems of Physicochemical Pharmacology, Russian Academy of Sciences, 119991 Moscow, Russia*

Kirill R. Butov − *Laboratory of Translational Medicine, Dmitriy Rogachev National Medical Research Center of Pediatric Hematology, Oncology, and Immunology, 117997 Moscow, Russia; Center for Theoretical Problems of Physicochemical Pharmacology, Russian Academy of Sciences, 119991 Moscow, Russia;* orcid.org/0000-0002-4664-6953

Hans-Ulrich Humpf − *Institute of Food Chemistry, University of Münster, 48149 Münster, Germany;* orcid.org/0000-0003-3296-3058

Matthias Lehr − *Institute of Pharmaceutical and Medicinal Chemistry, University of Münster, 48149 Münster, Germany*

Mikhail A. Panteleev − *Laboratory of Translational Medicine, Dmitriy Rogachev National Medical Research Center of Pediatric Hematology, Oncology, and Immunology, 117997 Moscow, Russia; Faculty of Physics, Lomonosov Moscow State University, 119991 Moscow, Russia; Center for Theoretical Problems of Physicochemical Pharmacology, Russian Academy of Sciences, 119991 Moscow, Russia; Faculty of Biological and Medical Physics, Moscow Institute of Physics and Technology, 141700 Dolgoprudnyi, Russia*

Antti Poso − *School of Pharmacy, Faculty of Health Sciences, University of Eastern Finland, 70211 Kuopio, Finland; Department of Internal Medicine VIII, University Hospital Tübingen, 72076 Tübingen, Germany;* orcid.org/0000-0003-4196-4204

Uwe Karst − *Institute of Inorganic and Analytical Chemistry, University of Münster, 48149 Münster, Germany;* orcid.org/0000-0002-1774-6787

Torsten Steinmetzer − *Department of Pharmacy, Institute of Pharmaceutical Chemistry, Philipps University Marburg, 35032 Marburg, Germany;* orcid.org/0000-0001-6523-4754

Gerd Bendas − *Pharmaceutical Institute, University of Bonn, 53121 Bonn, Germany*

Complete contact information is available at:
https://pubs.acs.org/10.1021/acs.jmedchem.0c01635

Author Contributions

The manuscript was written through contributions of all authors. All authors have given approval to the final version of the manuscript.

Notes

The authors declare no competing financial interest.

ABBREVIATIONS

ACN, acetonitrile; ADP, adenosine diphosphate; AMC, 7-Amino-4-methylcoumarin; aPTT, activated partial thromboplastin time; DCM, dichloromethane; DMAP, 4-dimethylaminopyridine; DOACs, direct oral anticoagulants; ESI-MS, electrospray ionization mass spectrometry; ETP, endogenous thrombin potential; FAAH, fatty acid amide hydrolase; MAGL, monoacylglycerol lipase; MTS, medium-throughput screening; PARs, protease-activated receptors; PK, plasma kallikrein; PT, prothrombin time; SAR, structure−activity relationship; SEC, size-exclusion chromatography; TGA, thrombin generation assay; THF, tetrahydrofuran; TF, tissue factor; TOF, time-of-flight; TRAP-6, thrombin receptor activating peptide-6; uPA, urokinase-type plasminogen activator (urokinase)

REFERENCES

(1) Lamichhane, M.; Salehi, N.; Ahmadjee, A.; Abela, G. S. Chapter 2 - Pathology of Arterial Thrombosis: Characteristics and Thrombus Types. In *Cardiovascular Thrombus*; Topaz, O., Ed.; Academic Press, 2018; pp 15−30.

(2) Beckman, M. G.; Hooper, W. C.; Critchley, S. E.; Ortel, T. L. Venous thromboembolism: a public health concern. *Am. J. Prev. Med.* **2010**, *38*, S495−S501.

(3) Wendelboe, A. M.; Raskob, G. E. Global burden of thrombosis: epidemiologic aspects. *Circ. Res.* **2016**, *118*, 1340−1347.

(4) Al-Horani, R. A.; Desai, U. R. Factor XIa inhibitors: A review of the patent literature. *Expert Opin. Ther. Pat.* **2016**, *26*, 323−345.

(5) Steinmetzer, T.; Pilgram, O.; Wenzel, B. M.; Wiedemeyer, S. J. A. Fibrinolysis inhibitors: potential drugs for the treatment and prevention of bleeding. *J. Med. Chem.* **2020**, *63*, 1445−1472.

(6) Ahmed, I.; Majeed, A.; Powell, R. Heparin induced thrombocytopenia: diagnosis and management update. *Postgrad. Med. J.* **2007**, *83*, 575−582.

(7) Eikelboom, J. W.; Hankey, G. J. Low molecular weight heparins and heparinoids. *Med. J. Aust.* **2002**, *177*, 379−383.

(8) Winter, Y.; Dodel, R.; Korchounov, A.; Grond, M.; Oertel, W. H.; Back, T. Clinical and pharmacological properties of new oral anticoagulants for the prevention of cerebral thromboembolism: Factor Xa and thrombin inhibitors. *World J. Neurosci.* **2012**, *02*, 7−14.

(9) Connolly, S. J.; Ezekowitz, M. D.; Yusuf, S.; Eikelboom, J.; Oldgren, J.; Parekh, A.; Pogue, J.; Reilly, P. A.; Themeles, E.; Varrone, J.; Wang, S.; Alings, M.; Xavier, D.; Zhu, J.; Diaz, R.; Lewis, B. S.; Darius, H.; Diener, H. C.; Joyner, C. D.; Wallentin, L.; RE-LY Steering Committee and Investigators. Dabigatran versus warfarin in patients with atrial fibrillation. *N. Engl. J. Med.* **2009**, *361*, 1139−1151.

(10) Ruff, C. T.; Giugliano, R. P.; Braunwald, E.; Hoffman, E. B.; Deenadayalu, N.; Ezekowitz, M. D.; Camm, A. J.; Weitz, J. I.; Lewis, B. S.; Parkhomenko, A.; Yamashita, T.; Antman, E. M. Comparison of the efficacy and safety of new oral anticoagulants with warfarin in patients with atrial fibrillation: a meta-analysis of randomised trials. *Lancet* **2014**, *383*, 955−962.

(11) Hohnloser, S. H.; Basic, E.; Nabauer, M. Comparative risk of major bleeding with new oral anticoagulants (NOACs) and phenprocoumon in patients with atrial fibrillation: a post-marketing surveillance study. *Clin. Res. Cardiol.* **2017**, *106*, 618−628.

(12) Baeriswyl, V.; Calzavarini, S.; Chen, S.; Zorzi, A.; Bologna, L.; Angelillo-Scherrer, A.; Heinis, C. A synthetic factor XIIa inhibitor blocks selectively intrinsic coagulation initiation. *ACS Chem. Biol.* **2015**, *10*, 1861−1870.

(13) Naudin, C.; Burillo, E.; Blankenberg, S.; Butler, L.; Renne, T. Factor XII contact activation. *Semin. Thromb. Hemostasis* **2017**, *43*, 814−826.

(14) Renne, T.; Pozgajova, M.; Gruner, S.; Schuh, K.; Pauer, H. U.; Burfeind, P.; Gailani, D.; Nieswandt, B. Defective thrombus formation in mice lacking coagulation factor XII. *J. Exp. Med.* **2005**, *202*, 271−281.

(15) Kenne, E.; Renne, T. Factor XII: a drug target for safe interference with thrombosis and inflammation. *Drug Discovery Today* **2014**, *19*, 1459−1464.

(16) Kenne, E.; Nickel, K. F.; Long, A. T.; Fuchs, T. A.; Stavrou, E. X.; Stahl, F. R.; Renne, T. Factor XII: a novel target for safe

prevention of thrombosis and inflammation. *J. Intern. Med.* **2015**, *278*, 571−585.

(17) Davoine, C.; Bouckaert, C.; Fillet, M.; Pochet, L. Factor XII/XIIa inhibitors: their discovery, development, and potential indications. *Eur. J. Med. Chem.* **2020**, *208*, No. 112753.

(18) Tillman, B.; Gailani, D. Inhibition of factors XI and XII for prevention of thrombosis induced by artificial surfaces. *Semin. Thromb. Hemostasis* **2018**, *44*, 060−069.

(19) Larsson, M.; Rayzman, V.; Nolte, M. W.; Nickel, K. F.; Bjorkqvist, J.; Jamsa, A.; Hardy, M. P.; Fries, M.; Schmidbauer, S.; Hedenqvist, P.; Broome, M.; Pragst, I.; Dickneite, G.; Wilson, M. J.; Nash, A. D.; Panousis, C.; Renne, T. A factor XIIa inhibitory antibody provides thromboprotection in extracorporeal circulation without increasing bleeding risk. *Sci. Transl. Med.* **2014**, *6*, 222ra17.

(20) Yau, J. W.; Liao, P.; Fredenburgh, J. C.; Stafford, A. R.; Revenko, A. S.; Monia, B. P.; Weitz, J. I. Selective depletion of factor XI or factor XII with antisense oligonucleotides attenuates catheter thrombosis in rabbits. *Blood* **2014**, *123*, 2102−2107.

(21) Yau, J. W.; Stafford, A. R.; Liao, P.; Fredenburgh, J. C.; Roberts, R.; Brash, J. L.; Weitz, J. I. Corn trypsin inhibitor coating attenuates the prothrombotic properties of catheters in vitro and in vivo. *Acta Biomater.* **2012**, *8*, 4092−4100.

(22) Eikelboom, J. W.; Brueckmann, M.; van de Werf, F. Dabigatran versus warfarin in patients with mechanical heart valves: reply. *J. Thromb. Haemostasis* **2014**, *12*, 426.

(23) Yau, J. W.; Stafford, A. R.; Liao, P.; Fredenburgh, J. C.; Roberts, R.; Weitz, J. I. Mechanism of catheter thrombosis: comparison of the antithrombotic activities of fondaparinux, enoxaparin, and heparin in vitro and in vivo. *Blood* **2011**, *118*, 6667−6674.

(24) Björkqvist, J.; de Maat, S.; Lewandrowski, U.; Di Gennaro, A.; Oschatz, C.; Schonig, K.; Nothen, M. M.; Drouet, C.; Braley, H.; Nolte, M. W.; Sickmann, A.; Panousis, C.; Maas, C.; Renne, T. Defective glycosylation of coagulation factor XII underlies hereditary angioedema type III. *J. Clin. Invest.* **2015**, *125*, 3132−3146.

(25) Raghunathan, V.; Zilberman-Rudenko, J.; Olson, S. R.; Lupu, F.; McCarty, O. J. T.; Shatzel, J. J. The contact pathway and sepsis. *Res. Pract. Thromb. Haemostasis* **2019**, *3*, 331−339.

(26) Göbel, K.; Pankratz, S.; Asaridou, C. M.; Herrmann, A. M.; Bittner, S.; Merker, M.; Ruck, T.; Glumm, S.; Langhauser, F.; Kraft, P.; Krug, T. F.; Breuer, J.; Herold, M.; Gross, C. C.; Beckmann, D.; Korb-Pap, A.; Schuhmann, M. K.; Kuerten, S.; Mitroulis, I.; Ruppert, C.; Nolte, M. W.; Panousis, C.; Klotz, L.; Kehrel, B.; Korn, T.; Langer, H. F.; Pap, T.; Nieswandt, V.; Wiendl, H.; Chavakis, T.; Kleinschnitz, C.; Meuth, S. G. Blood coagulation factor XII drives adaptive immunity during neuroinflammation via CD87-mediated modulation of dendritic cells. *Nat. Commun.* **2016**, *7*, No. 11626.

(27) Chen, Z. L.; Revenko, A. S.; Singh, P.; MacLeod, A. R.; Norris, E. H.; Strickland, S. Depletion of coagulation factor XII ameliorates brain pathology and cognitive impairment in Alzheimer disease mice. *Blood* **2017**, *129*, 2547−2556.

(28) Dementiev, A.; Silva, A.; Yee, C.; Li, Z.; Flavin, M. T.; Sham, H.; Partridge, J. R. Structures of human plasma beta-factor XIIa cocrystallized with potent inhibitors. *Blood Adv.* **2018**, *2*, 549−558.

(29) Matthews, J. H.; Krishnan, R.; Costanzo, M. J.; Maryanoff, B. E.; Tulinsky, A. Crystal structures of thrombin with thiazole-containing inhibitors: probes of the S1' binding site. *Biophys. J.* **1996**, *71*, 2830−2839.

(30) Sheth, R. A.; Niekamp, A.; Quencer, K. B.; Shamoun, F.; Knuttinen, M. G.; Naidu, S.; Oklu, R. Thrombosis in cancer patients: etiology, incidence, and management. *Cardiovasc. Diagn. Ther.* **2017**, *7*, S178−S185.

(31) Levitan, N.; Dowlati, A.; Remick, S. C.; Tahsildar, H. I.; Sivinski, L. D.; Beyth, R.; Rimm, A. A. Rates of initial and recurrent thromboembolic disease among patients with malignancy versus those without malignancy. Risk analysis using Medicare claims data. *Medicine* **1999**, *78*, 285−291.

(32) Han, X.; Guo, B.; Li, Y.; Zhu, B. Tissue factor in tumor microenvironment: a systematic review. *J. Hematol. Oncol.* **2014**, *7*, No. 54.

(33) Campello, E.; Henderson, M. W.; Noubouossie, D. F.; Simioni, P.; Key, N. S. Contact system activation and cancer: new insights in the pathophysiology of cancer-associated thrombosis. *Thromb. Haemostasis* **2018**, *118*, 251−265.

(34) Geddings, J. E.; Mackman, N. New players in haemostasis and thrombosis. *Thromb. Haemostasis* **2014**, *111*, 570−574.

(35) Puy, C.; Tucker, E. I.; Wong, Z. C.; Gailani, D.; Smith, S. A.; Choi, S. H.; Morrissey, J. H.; Gruber, A.; McCarty, O. J. Factor XII promotes blood coagulation independent of factor XI in the presence of long-chain polyphosphates. *J. Thromb. Haemostasis* **2013**, *11*, 1341−1352.

(36) Swystun, L. L.; Mukherjee, S.; Liaw, P. C. Breast cancer chemotherapy induces the release of cell-free DNA, a novel procoagulant stimulus. *J. Thromb. Haemostasis* **2011**, *9*, 2313−2321.

(37) Rousseau, A.; Larsen, A. K.; Van Dreden, P.; Sabbah, M.; Elalamy, I.; Gerotziafas, G. T. Differential contribution of tissue factor and Factor XII to thrombin generation triggered by breast and pancreatic cancer cells. *Int. J. Oncol.* **2017**, *51*, 1747−1756.

(38) Nickel, K. F.; Ronquist, G.; Langer, F.; Labberton, L.; Fuchs, T. A.; Bokemeyer, C.; Sauter, G.; Graefen, M.; Mackman, N.; Stavrou, E. X.; Ronquist, G.; Renne, T. The polyphosphate-factor XII pathway drives coagulation in prostate cancer-associated thrombosis. *Blood* **2015**, *126*, 1379−1389.

(39) Worm, M.; Kohler, E. C.; Panda, R.; Long, A.; Butler, L. M.; Stavrou, E. X.; Nickel, K. F.; Fuchs, T. A.; Renne, T. The factor XIIa blocking antibody 3F7: a safe anticoagulant with anti-inflammatory activities. *Ann. Transl. Med.* **2015**, *3*, 247.

(40) Campos, I. T.; Souza, T. A.; Torquato, R. J.; De Marco, R.; Tanaka-Azevedo, A. M.; Tanaka, A. S.; Barbosa, J. A. The kazal-type inhibitors infestins 1 and 4 differ in specificity but are similar in three-dimensional structure. *Acta Crystallogr., Sect. D: Biol. Crystallogr.* **2012**, *68*, 695−702.

(41) Middendorp, S. J.; Wilbs, J.; Quarroz, C.; Calzavarini, S.; Angelillo-Scherrer, A.; Heinis, C. Peptide macrocycle inhibitor of coagulation factor XII with subnanomolar affinity and high target selectivity. *J. Med. Chem.* **2017**, *60*, 1151−1158.

(42) Bouckaert, C.; Serra, S.; Rondelet, G.; Dolusic, E.; Wouters, J.; Dogne, J. M.; Frederick, R.; Pochet, L. Synthesis, evaluation and structure-activity relationship of new 3-carboxamide coumarins as FXIIa inhibitors. *Eur. J. Med. Chem.* **2016**, *110*, 181−194.

(43) Chen, J. J. F.; Visco, D. P., Jr. Identifying novel factor XIIa inhibitors with PCA-GA-SVM developed vHTS models. *Eur. J. Med. Chem.* **2017**, *140*, 31−41.

(44) Chernyshev, V. M.; Tarasova, E. V.; Chernysheva, A. V.; Taranushich, V. A. Synthesis of 3-pyridyl-substituted 5-amino-1,2,4-triazoles from aminoguanidine and pyridinecarboxylic acids. *Russ. J. Appl. Chem.* **2011**, *84*, 1890−1896.

(45) Dolzhenko, A. V.; Pastorin, G.; Dolzhenko, A. V.; Chui, W. K. An aqueous medium synthesis and tautomerism study of 3(5)-amino-1,2,4-triazoles. *Tetrahedron Lett.* **2009**, *50*, 2124−2128.

(46) Dolzhenko, A. V.; Kalinin, D. V.; Kalinina, S. A. Synthesis of novel trichloromethyl substituted azolo[1,3,5]triazines. *Heterocycles* **2012**, *85*, 2515−2522.

(47) Romagnoli, R.; Baraldi, P. G.; Salvador, M. K.; Prencipe, F.; Bertolasi, V.; Cancellieri, M.; Brancale, A.; Hamel, E.; Castagliuolo, I.; Consolaro, F.; Porcu, E.; Basso, G.; Viola, G. Synthesis, antimitotic and antivascular activity of 1-(3',4',5'-trimethoxybenzoyl)-3-arylamino-5-amino-1,2,4-triazoles. *J. Med. Chem.* **2014**, *57*, 6795−6808.

(48) Bera, H.; Tan, B. J.; Sun, L.; Dolzhenko, A. V.; Chui, W. K.; Chiu, G. N. A structure-activity relationship study of 1,2,4-triazolo[1,5-a][1,3,5]triazin-5,7-dione and its 5-thioxo analogues on anti-thymidine phosphorylase and associated anti-angiogenic activities. *Eur. J. Med. Chem.* **2013**, *67*, 325−334.

(49) Sivaraja, M.; Pozzi, N.; Rienzo, M.; Lin, K.; Shiau, T. P.; Clemens, D. M.; Igoudin, L.; Zalicki, P.; Chang, S. S.; Estiarte, M. A.; Short, K. M.; Williams, D. C.; Datta, A.; Di Cera, E.; Kita, D. B. Reversible covalent direct thrombin inhibitors. *PLoS One* **2018**, *13*, No. e0201377.

(50) Fischer, P. M. Design of small-molecule active-site inhibitors of the S1A family proteases as procoagulant and anticoagulant drugs. *J. Med. Chem.* **2018**, *61*, 3799−3822.

(51) Zilberman-Rudenko, J.; Reitsma, S. E.; Puy, C.; Rigg, R. A.; Smith, S. A.; Tucker, E. I.; Silasi, R.; Merkulova, A.; McCrae, K. R.; Maas, C.; Urbanus, R. T.; Gailani, D.; Morrissey, J. H.; Gruber, A.; Lupu, F.; Schmaier, A. H.; McCarty, O. J. T. Factor XII activation promotes platelet consumption in the presence of bacterial-type long-chain polyphosphate In vitro and in vivo. *Arterioscler., Thromb., Vasc. Biol.* **2018**, *38*, 1748−1760.

(52) Bendapudi, P. K.; Deceunynck, K.; Koseoglu, S.; Bekendam, R. H.; Mason, S. D.; Kenniston, J.; Flaumenhaft, R. C. *Stimulated Platelets but not Endothelium Generate Thrombin via a Factor XIIa-dependent Mechanism Requiring Phosphatidylserine Exposure*; American Society of Hematology: Washington, DC, 2016.

(53) Lima, L. G.; Monteiro, R. Q. Activation of blood coagulation in cancer: implications for tumour progression. *Biosci. Rep.* **2013**, *33*, No. e00064.

(54) Gockel, L. M.; Ponert, J. M.; Schwarz, S.; Schlesinger, M.; Bendas, G. The low molecular weight heparin tinzaparin attenuates platelet activation in terms of metastatic niche formation by coagulation-dependent and independent pathways. *Molecules* **2018**, *23*, 2753.

(55) Coughlin, S. R. How the protease thrombin talks to cells. *Proc. Natl. Acad. Sci. U.S.A.* **1999**, *96*, 11023−11027.

(56) Duvernay, M. T.; Temple, K. J.; Maeng, J. G.; Blobaum, A. L.; Stauffer, S. R.; Lindsley, C. W.; Hamm, H. E. Contributions of protease-activated receptors PAR1 and PAR4 to thrombin-induced GPIIbIIIa activation in human platelets. *Mol. Pharmacol.* **2017**, *91*, 39−47.

(57) Vassallo, R. R., Jr.; Kieber-Emmons, T.; Cichowski, K.; Brass, L. F. Structure-function relationships in the activation of platelet thrombin receptors by receptor-derived peptides. *J. Biol. Chem.* **1992**, *267*, 6081−6085.

(58) Furugohri, T.; Morishima, Y. Paradoxical enhancement of the intrinsic pathway-induced thrombin generation in human plasma by melagatran, a direct thrombin inhibitor, but not edoxaban, a direct factor Xa inhibitor, or heparin. *Thromb. Res.* **2015**, *136*, 658−662.

(59) Perzborn, E.; Heitmeier, S.; Buetehorn, U.; Laux, V. Direct thrombin inhibitors, but not the direct factor Xa inhibitor rivaroxaban, increase tissue factor-induced hypercoagulability in vitro and in vivo. *J. Thromb. Haemostasis* **2014**, *12*, 1054−1065.

(60) Kamisato, C.; Furugohri, T.; Morishima, Y. A direct thrombin inhibitor suppresses protein C activation and factor Va degradation in human plasma: Possible mechanisms of paradoxical enhancement of thrombin generation. *Thromb. Res.* **2016**, *141*, 77−83.

(61) McKinney, M. K.; Cravatt, B. F. Structure and function of fatty acid amide hydrolase. *Annu. Rev. Biochem.* **2005**, *74*, 411−432.

(62) Labar, G.; Wouters, J.; Lambert, D. M. A review on the monoacylglycerol lipase: at the interface between fat and endocannabinoid signalling. *Curr. Med. Chem.* **2010**, *17*, 2588−2607.

(63) Kathuria, S.; Gaetani, S.; Fegley, D.; Valino, F.; Duranti, A.; Tontini, A.; Mor, M.; Tarzia, G.; La Rana, G.; Calignano, A.; Giustino, A.; Tattoli, M.; Palmery, M.; Cuomo, V.; Piomelli, D. Modulation of anxiety through blockade of anandamide hydrolysis. *Nat. Med.* **2003**, *9*, 76−81.

(64) Muccioli, G. G.; Labar, G.; Lambert, D. M. CAY10499, a novel monoglyceride lipase inhibitor evidenced by an expeditious MGL assay. *ChemBiochem* **2008**, *9*, 2704−2710.

(65) Sheldrick, G. M. SHELXT - integrated space-group and crystal-structure determination. *Acta Crystallogr., Sect. A: Found. Adv.* **2015**, *71*, 3−8.

(66) Hinkes, S.; Wuttke, A.; Saupe, S. M.; Ivanova, T.; Wagner, S.; Knorlein, A.; Heine, A.; Klebe, G.; Steinmetzer, T. Optimization of cyclic plasmin inhibitors: from benzamidines to benzylamines. *J. Med. Chem.* **2016**, *59*, 6370−6386.

(67) Meyer, D.; Sielaff, F.; Hammami, M.; Bottcher-Friebertshauser, E.; Garten, W.; Steinmetzer, T. Identification of the first synthetic inhibitors of the type II transmembrane serine protease TMPRSS2

suitable for inhibition of influenza virus activation. *Biochem. J.* **2013**, *452*, 331−343.

(68) Dashkevich, N. M.; Ovanesov, M. V.; Balandina, A. N.; Karamzin, S. S.; Shestakov, P. I.; Soshitova, N. P.; Tokarev, A. A.; Panteleev, M. A.; Ataullakhanov, F. I. Thrombin activity propagates in space during blood coagulation as an excitation wave. *Biophys. J.* **2012**, *103*, 2233−2240.

(69) Kuprash, A. D.; Shibeko, A. M.; Vijay, R.; Nair, S. C.; Srivastava, A.; Ataullakhanov, F. I.; Panteleev, M. A.; Balandina, A. N. Sensitivity and robustness of spatially dependent thrombin generation and fibrin clot propagation. *Biophys. J.* **2018**, *115*, 2461−2473.

(70) Beyer, M.; Ferse, I.; Humpf, H. U. Large-scale production of selected type A trichothecenes: the use of HT-2 toxin and T-2 triol as precursors for the synthesis of d 3-T-2 and d 3-HT-2 toxin. *Mycotoxin Res.* **2009**, *25*, 41−52.

(71) Nociari, M. M.; Shalev, A.; Benias, P.; Russo, C. A novel one-step, highly sensitive fluorometric assay to evaluate cell-mediated cytotoxicity. *J. Immunol. Methods* **1998**, *213*, 157−167.

(72) Kalinina, S. A.; Kalinin, D. V.; Hovelmann, Y.; Daniliuc, C. G.; Muck-Lichtenfeld, C.; Cramer, B.; Humpf, H. U. Auranthine, a benzodiazepinone from penicillium aurantiogriseum: refined structure, absolute configuration, and cytotoxicity. *J. Nat. Prod.* **2018**, *81*, 2177−2186.

(73) Holtfrerich, A.; Hanekamp, W.; Lehr, M. (4-Phenoxyphenyl)-tetrazolecarboxamides and related compounds as dual inhibitors of fatty acid amide hydrolase (FAAH) and monoacylglycerol lipase (MAGL). *Eur. J. Med. Chem.* **2013**, *63*, 64−75.

(74) Terwege, T.; Hanekamp, W.; Garzinsky, D.; Konig, S.; Koch, O.; Lehr, M. omega-Imidazolyl- and omega-tetrazolylalkylcarbamates as inhibitors of fatty acid amide hydrolase: biological activity and in vitro metabolic stability. *ChemMedChem* **2016**, *11*, 429−443.

(75) Forster, L.; Schulze Elfringhoff, A.; Lehr, M. High-performance liquid chromatographic assay with fluorescence detection for the evaluation of inhibitors against fatty acid amide hydrolase. *Anal. Bioanal. Chem.* **2009**, *394*, 1679−1685.